AD-A047 816 AIR FORCE INST OF TECH WRIGHT-PATTERSON AFB OHIO F/G 17/9
TORNADO IDENTIFICATION FROM ANALYSES OF DIGITAL RADAR DATA.(U)
DEC 76 D W PITTMAN
UNCLASSIFIED AFIT-CI-78-9 NL

1 OF 2
AD
AD047816

78-9

TORNADO IDENTIFICATION FROM ANALYSES OF DIGITAL RADAR DATA

A Thesis

by

DONALD WAYNE PITTMAN
Captain, USAF

Submitted to the Graduate College of
Texas A&M University
in partial fulfillment of the requirement for the degree of

MASTER OF SCIENCE

December 1976

Major Subject: Meteorology

93 pages

UNCLASSIFIED

SECURITY CLASSIFICATION OF THIS PAGE (When Data Entered)

REPORT DOCUMENTATION PAGE	READ INSTRUCTIONS BEFORE COMPLETING FORM
(14) 1. REPORT NUMBER AFIT—CI-78-9 ✓	2. GOVT ACCESSION NO. / 3. RECIPIENT'S CATALOG NUMBER
(6) 4. TITLE (and Subtitle) Tornado Identification From Analyses of Digital Radar Data,	5. TYPE OF REPORT & PERIOD COVERED (9) Master's Thesis
	6. PERFORMING ORG. REPORT NUMBER
7. AUTHOR(s) (10) Captain Donald W. Pittman	8. CONTRACT OR GRANT NUMBER(s)
9. PERFORMING ORGANIZATION NAME AND ADDRESS AFIT Student at Texas A&M University, College Station, Texas ✓	10. PROGRAM ELEMENT, PROJECT, TASK AREA & WORK UNIT NUMBERS
11. CONTROLLING OFFICE NAME AND ADDRESS AFIT/CI WPAFB OH 45433	12. REPORT DATE (11) Dec [redacted] 76
	13. NUMBER OF PAGES ~~93~~ Pages (12) 104p.
14. MONITORING AGENCY NAME & ADDRESS(if different from Controlling Office)	15. SECURITY CLASS. (of this report) Unclassified
	15a. DECLASSIFICATION/DOWNGRADING SCHEDULE

16. DISTRIBUTION STATEMENT (of this Report)

Approved for Public Release; Distribution Unlimited

17. DISTRIBUTION STATEMENT (of the abstract entered in Block 20, if different from Report)

18. SUPPLEMENTARY NOTES

APPROVED FOR PUBLIC RELEASE AFR 190-17.

JERRAL F. GUESS, Captain, USAF
Director of Information, AFIT

19. KEY WORDS (Continue on reverse side if necessary and identify by block number)

20. ABSTRACT (Continue on reverse side if necessary and identify by block number)

Ø12200

DD FORM 1 JAN 73 1473 EDITION OF 1 NOV 65 IS OBSOLETE

UNCLASSIFIED

SECURITY CLASSIFICATION OF THIS PAGE (When Data Entered)

INSTRUCTIONS FOR PREPARATION OF REPORT DOCUMENTATION PAGE

RESPONSIBILITY. The controlling DoD office will be responsible for completion of the Report Documentation Page, DD Form 1473, in all technical reports prepared by or for DoD organizations.

CLASSIFICATION. Since this Report Documentation Page, DD Form 1473, is used in preparing announcements, bibliographies, and data banks, it should be unclassified if possible. If a classification is required, identify the classified items on the page by the appropriate symbol.

COMPLETION GUIDE

General. Make Blocks 1, 4, 5, 6, 7, 11, 13, 15, and 16 agree with the corresponding information on the report cover. Leave Blocks 2 and 3 blank.

Block 1. Report Number. Enter the unique alphanumeric report number shown on the cover.

Block 2. Government Accession No. Leave Blank. This space is for use by the Defense Documentation Center.

Block 3. Recipient's Catalog Number. Leave blank. This space is for the use of the report recipient to assist in future retrieval of the document.

Block 4. Title and Subtitle. Enter the title in all capital letters exactly as it appears on the publication. Titles should be unclassified whenever possible. Write out the English equivalent for Greek letters and mathematical symbols in the title *(see "Abstracting Scientific and Technical Reports of Defense-sponsored RDT/E," AD-667 000)*. If the report has a subtitle, this subtitle should follow the main title, be separated by a comma or semicolon if appropriate, and be initially capitalized. If a publication has a title in a foreign language, translate the title into English and follow the English translation with the title in the original language. Make every effort to simplify the title before publication.

Block 5. Type of Report and Period Covered. Indicate here whether report is interim, final, etc., and, if applicable, inclusive dates of period covered, such as the life of a contract covered in a final contractor report.

Block 6. Performing Organization Report Number. Only numbers other than the official report number shown in Block 1, such as series numbers for in-house reports or a contractor/grantee number assigned by him, will be placed in this space. If no such numbers are used, leave this space blank.

Block 7. Author(s). Include corresponding information from the report cover. Give the name(s) of the author(s) in conventional order *(for example, John R. Doe or, if author prefers, J. Robert Doe)*. In addition, list the affiliation of an author if it differs from that of the performing organization.

Block 8. Contract or Grant Number(s). For a contractor or grantee report, enter the complete contract or grant number(s) under which the work reported was accomplished. Leave blank in in-house reports.

Block 9. Performing Organization Name and Address. For in-house reports enter the name and address, including office symbol, of the performing activity. For contractor or grantee reports enter the name and address of the contractor or grantee who prepared the report and identify the appropriate corporate division, school, laboratory, etc., of the author. List city, state, and ZIP Code.

Block 10. Program Element, Project, Task Area, and Work Unit Numbers. Enter here the number code from the applicable Department of Defense form, such as the DD Form 1498, "Research and Technology Work Unit Summary" or the DD Form 1634, "Research and Development Planning Summary," which identifies the program element, project, task area, and work unit or equivalent under which the work was authorized.

Block 11. Controlling Office Name and Address. Enter the full, official name and address, including office symbol, of the controlling office. *(Equates to funding/sponsoring agency. For definition see DoD Directive 5200.20, "Distribution Statements on Technical Documents.")*

Block 12. Report Date. Enter here the day, month, and year or month and year as shown on the cover.

Block 13. Number of Pages. Enter the total number of pages.

Block 14. Monitoring Agency Name and Address *(if different from Controlling Office)*. For use when the controlling or funding office does not directly administer a project, contract, or grant, but delegates the administrative responsibility to another organization.

Blocks 15 & 15a. Security Classification of the Report: Declassification/Downgrading Schedule of the Report. Enter in 15 the highest classification of the report. If appropriate, enter in 15a the declassification/downgrading schedule of the report, using the abbreviations for declassification/downgrading schedules listed in paragraph 4-207 of DoD 5200.1-R.

Block 16. Distribution Statement of the Report. Insert here the applicable distribution statement of the report from DoD Directive 5200.20, "Distribution Statements on Technical Documents."

Block 17. Distribution Statement *(of the abstract entered in Block 20, if different from the distribution statement of the report)*. Insert here the applicable distribution statement of the abstract from DoD Directive 5200.20, "Distribution Statements on Technical Documents."

Block 18. Supplementary Notes. Enter information not included elsewhere but useful, such as: Prepared in cooperation with . . . Translation of *(or by)* . . . Presented at conference of . . . To be published in . . .

Block 19. Key Words. Select terms or short phrases that identify the principal subjects covered in the report, and are sufficiently specific and precise to be used as index entries for cataloging, conforming to standard terminology. The DoD "Thesaurus of Engineering and Scientific Terms" *(TEST)*, AD-672 000, can be helpful.

Block 20. Abstract. The abstract should be a brief *(not to exceed 200 words)* factual summary of the most significant information contained in the report. If possible, the abstract of a classified report should be unclassified and the abstract to an unclassified report should consist of publicly- releasable information. If the report contains a significant bibliography or literature survey, mention it here. For information on preparing abstracts see "Abstracting Scientific and Technical Reports of Defense-Sponsored RDT&E," AD-667 000.

★ U.S. GOVERNMENT PRINTING OFFICE : 1973—729-091/1431 3-1

ABSTRACT

Tornado Identification from Analyses of Digital Radar Data

(December 1976)

Donald Wayne Pittman, B.S., St Louis University

Directed by: Dr. George L. Huebner

An investigation was conducted to determine whether tornadoes presented a unique signature in analyses of digital radar data from central Oklahoma during the Spring. The data were collected by the 10-cm WSR-57 radar at the National Severe Storms Laboratory at Norman, Oklahoma. Three types of numerical analyses were used in this study: constant-altitude reflectivity maps (CAZM), total vertically-summed reflectivity maps (TVSZ), and partial vertically-summed reflectivity maps (PVSZ), with greatest emphasis placed on the PVSZ maps. Presentations covering a 100-km square were constructed at either 5 or 10 min intervals.

From the analysis of three case studies during 1974 and 1975, that contained five tornadoes, it was concluded that tornadoes did not produce a singular identifying signature in analyses of digital radar data, but rather produced a combination of features which indicated, with a high probability, the presence of a tornado. Such features were the appearance of a small area of reduced reflectivity known as a Bounded Weak-Echo Region (BWER), a tilt of the core of the storm toward the BWER, and a rapid decrease in the upper-level mass of the storm as indicated by a rapid decrease in the reflectivity of the upper PVSZ. Further investigation is required before any definitive value of probability can be assigned to this identification technique.

ACKNOWLEDGEMENTS

The author's graduate program was sponsored and financed by the Air Force Institute of Technology, United States Air Force.

I wish to thank Dr. G. L. Huebner for acting as Chairman of my advisory committee and for his patience and help, particularly during the period of topic selection and refinement of goals. Appreciation is extended to my other committee members: Dr. V. E. Moyer for his guidance and assistance in the preparation of the final draft, and Dr. G. N. Williams for his assistance in processing the data tapes. To Dr. P. Das, my sincere appreciation for his guidance and assistance during the formulative stages of preparation. Deep appreciation is extended to Dr. K. C. Brundidge for providing the funds necessary to complete the data processing.

To Dr. E. Kessler and his staff at the National Severe Storms Laboratory, particularly D. Burgess, L. Lemon, and W. Bumgarner, my sincere appreciation for guidance and encouragement and for furnishing the necessary data tapes.

To Dr. C. N. Adams and Mrs. P. Pearson of the Texas A&M Data Processing Center, appreciation is extended for their help in solving several computing problems, particularly the unpacking of data from the NSSL data tapes.

Finally, appreciation is also extended to Debbie Gau for her fine typing assistance.

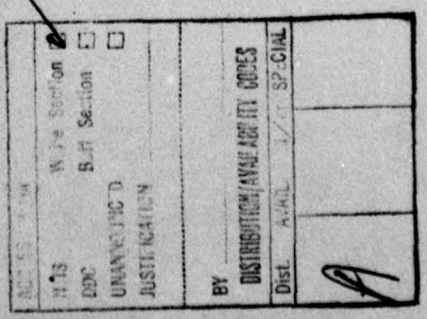

DEDICATION

To Jeff and Bryan

TABLE OF CONTENTS

TABLE OF CONTENTS (continued)

LIST OF TABLES

LIST OF FIGURES

LIST OF FIGURES (continued)

LIST OF FIGURES (continued)

CHAPTER I

INTRODUCTION

Severe local storms are composed of intense thunderstorms that produce heavy rain, structurally-damaging winds, crop-damaging hail, tornadoes, or any combination of the latter three. Each year throughout the world, these types of storms cause millions of dollars of damage and the loss of numerous lives. In 1975 in the United States alone, severe storms were involved in the death of 60 persons, and property damage for a single storm reached a new high of 160 million dollars. It then is no wonder that researchers are continually at work to try to find better methods of detecting and forecasting the occurrence of these storms.

The Need for this Investigation

While better methods of detecting and forecasting severe storms would produce more accurate warnings, their benefit to the populace would be only as great as the response generated. To date, the accuracy of severe storm warnings has been such that populace response has remained minimal [Muench, 1976]. Commercial businesses must weigh the cost of preparation and action during each false alarm against the risk of destruction. Hence, due to the relatively infrequent occurrence of severe storms at a given location, the cost of actions taken, and the inaccuracy of warnings, the response of businesses also has remained

---

The citations on the following pages follow the style of the Journal of Geophysical Research.

minimal. Therefore, in order to improve the response and minimize the loss of life and property, the accuracy of severe local storm warnings must be improved. It is with this fact in mind that this investigation is conducted.

The Scope and Objectives of this Investigation

This investigation examines a new method of detecting the most damaging severe-storm phenomenon, the tornado. Specifically, the objective of this study has been to determine if storms producing a tornado or funnel cloud present a unique signature in analyses of digital radar data. Information recently presented seems to indicate that there is a high correlation between the occurrence of tornadoes in Oklahoma in the Spring and the appearance of a small transient area of reduced reflectivity known as a bounded weak-echo region (BWER) and an acute tilt of the core of maximum reflectivity [Canipe, 1973]. If this information is correct, the meteorologist would be provided with a numerical tool for identifying small areas in which a tornado is occurring.

To evaluate this hypothesis, multi-tilt digital radar data were manipulated by computer to produce several types of numerical displays. These displays were developed for times during which severe weather was forecast to occur, not just during the times a tornado was observed to occur. In this manner an objective evaluation of the correlative points could be conducted. It is not the intent of this investigation to complete a statistical analysis of the accuracy of this observational tool, but rather to contribute case studies toward this goal.

Present Status of the Problem

In general, the task of studying severe storms is a difficult one and progress has been slow. The complexity of severe storms is such that modeling techniques have been ineffective. Hence, the investigator must rely upon nature to produce the dreaded phenomenon in a timely manner at an observable location in order to gain insight into its structure and dynamics.

Invariably, the study of severe storms involves the use of measuring equipment; however, the equipment tends to measure the total effect of many simultaneously-occurring physical processes, thereby leaving the investigator at a loss as to which is causing what.

This does not mean that all instrumentation is of little value, for significant progress has been made in certain areas of severe-storm identification and forecasting, even though the internal processes have not been thoroughly understood. Some of these areas will be examined next.

The Weather Radar

Over the last 20 yr, the most widely-used tool for severe-storm identification has been radar. Even though early studies concentrated on the morphology and travel of radar echoes, researchers did determine that storms producing severe weather exhibited certain unique characteristics. Among the more important were the following: that storms of greater severity often moved with a component to the right of the path of smaller, less intense storms [Battan, 1959]; that storms of greater

severity had higher echo tops [Battan, 1959]; that tornadoes were associated with echoes which were qualitatively very intense and which sometimes displayed a hook or "6"-shaped appendage [Bigler, 1955]; and that tornadoes tended to develop on the right rear side of the intense parent echo and not beneath it [Penn et al., 1955].

The difficulty with these characteristics was that they were qualitative rather than quantitative. Further, although the majority of severe storms tended to follow this set of characteristics, a sizeable number did not. Donaldson [1965] attributed part of this latter difficulty to the geographical variation of the characteristics. He found that storms in New England that produced tornadoes and/or large hail were characterized by echo heights which were significantly greater than the average for that area, yet no such anomaly was onserved in severe storms of the Southwest. Thus, investigators began restricting their efforts to certain geographical locations. Although the number of well-documented storms in a geographical area was relatively small, researchers did have sufficient information to determine that the number of exceptions to any set of identifying characteristics was still significantly greater than zero.

As no single totally-reliable identifier of severe weather had been found, and it did not appear that one was going to be found, researchers began to conduct statistical analyses of various radar parameters to determine which set of characteristics at a given location was most reliable in identifying severe local storms. The results were surprising. Using only the maximum, equivalent, radar-reflectivity factor (Z_e), Boyd and Musil [1970] found that they could identify 90

per cent of all hailstorms in western Nebraska while keeping their false-alarm rate to only 15 per cent. Wilson [1971] found that the best indicator for severe weather in Oklahoma was the size of the contiguous area of severe weather having a radar reflectivity of 3×10^5 mm^6m^{-3}. Brandes [1972] found that Boyd and Musil's technique also worked in Oklahoma, but that the critical value for the maximum Z_e was greater than for Nebraska. One common difficulty among these studies was that each used only the 0-deg elevation scan angle, generally because of the difficulty in collecting and processing multi-tilt data.

Digital Radar Data

To overcome the problem of collection, storage, and processing of multi-tilt data, researchers turned to digitizers, magnetic recorders, and computers. The digitizing units, called Digital Video Integrator Processors, took the returned signal from radar targets, quantified it into discrete levels, and computed an integrated intensity level for a specific area. The result was then stored on magnetic tape by a digital recorder, the data being retrievable by means of a spherical reference system of range, azimuth angle, and antenna tilt.

Digital radar data readily lend themselves to computer manipulation. Greene [1971] developed a numerical method to display values of Z_e on constant-altitude reflectivity maps (CAZM) similar to the constant-altitude plan-position-indicator (CAPPI) presentations of Marshall [1957]. Greene's method converted the stored spherical data to a three-dimensional rectangular presentation by the use of a quadratic interpolation scheme. Such a presentation is desirable for vertical

and horizontal integration and summation techniques.

Greene developed one such analytical tool by converting reflectivities to liquid-water content, M, and then vertically integrating M through the depth of the storm, thus yielding the vertically-integrated liquid-water (VIL) content. He found that tornado-producing systems were characterized by high values of VIL for approximately 1 hr prior to the tornado and by a rapid increase to even greater values during the development of the confirmed tornado. Later, however, other researchers such as Vogel [1973] and Canipe [1973] found that storms other than tornado-producers also were characterized by high values of VIL. In his investigations, Canipe [1972,1973] examined other possible uses of the CAZM, including the horizontal integration of liquid-water (HIL) and the partial vertical integration of liquid-water (PVIL).

The Basis for the Investigation

During his latter investigation, Canipe found nine tornado-producing systems that were characterized by the presence of a small transient area of reduced reflectivity, the BWER. It appeared in the parent cell or a nearby satellite several minutes before tornado formation and dissipated shortly before the tornado visibly disappeared. The region generally appeared first at mid-levels of the storm and developed downward with time. Perhaps even more striking was the fact that no such region developed in ten other cases which produced heavy rain and hail but not tornadoes.

The weak-echo region is not new, its presence having been found by Browning and Ludlam [1962] during their comprehensive study of a

storm near Workingham, England, in July 1959; however, virtually all research into this phenomenon has been conducted in an attempt to understand the dynamics of thunderstorms rather than to identify severe storms. Analyses of storms by Browning and Ludlam, Marwitz and Berry [1971], and Rinehart et al. [1975] in areas of England, western Canada, and the Upper High Plains of the United States, respectively, reveal BWERs that are not associated with tornadoes. Hence, the area of applicability of Canipe's technique must be limited to Oklahoma until further research is conducted in other southern locations. Since Canipe completed his work, further confirmation of the association of BWERs with tornadoes in Oklahoma has come from studies by Bensch [1975], Lemon et al. [1975], and McCarthy et al. [1975]. Also, an analysis of a tornado-less hailstorm by Brandes [1975] revealed no BWER.

The terms "Echo-Free Vault," "Weak-Echo Region," and "Bounded Weak-Echo Region" are used interchangably in the literature with minor technical differences inserted by each author. There are two somewhat different types of BWERs: those of long persistence with a 5-10 km diameter and those of short duration with a diameter of only 1-5 km. A dual-doppler radar study of the smaller-scale phenomena by McCarthy et al. revealed dynamics similar to those discovered in the larger phenomena by Marwitz and Berry, Chisholm [1970], and Foote et al. [1975]: that is, both types of regions contained a strong upward intrusion of warm moist air.

CHAPTER II

DATA

Severe Storm Data

Unless otherwise indicated, actual reports of severe storm occurrences have been extracted from Storm Data, a monthly publication of the Environmental Data Service, National Oceanic and Atmospheric Administration (NOAA). This report provides such information as the location and time of occurrence of the severe-storm event, tornado path width and length, maximum hail size, maximum wind speed, and a brief description of resultant injuries and property damage.

Radar Characteristics

The radar data used in this study were provided by the National Severe Storms Laboratory (NSSL), NOAA. These data were collected by a modified WSR-57 radar system developed and maintained by NSSL at Norman, Oklahoma. Table 1 summarizes the pertinent characteristics of the NSSL WSR-57 system. A detailed description of the design and function of the system used for the processing and recording of radar signals is given by Wilk et al. [1967] and Wilk and Gray [1970]. A block diagram describing the acquisition, processing, and recording of signals received by the NSSL WSR-57 radar is shown in Figure 1. As shown in this diagram, the target echo is detected and the returned data processed generally in the same manner as a conventional radar system. However, after amplification and integration, the signal is quantized into 64

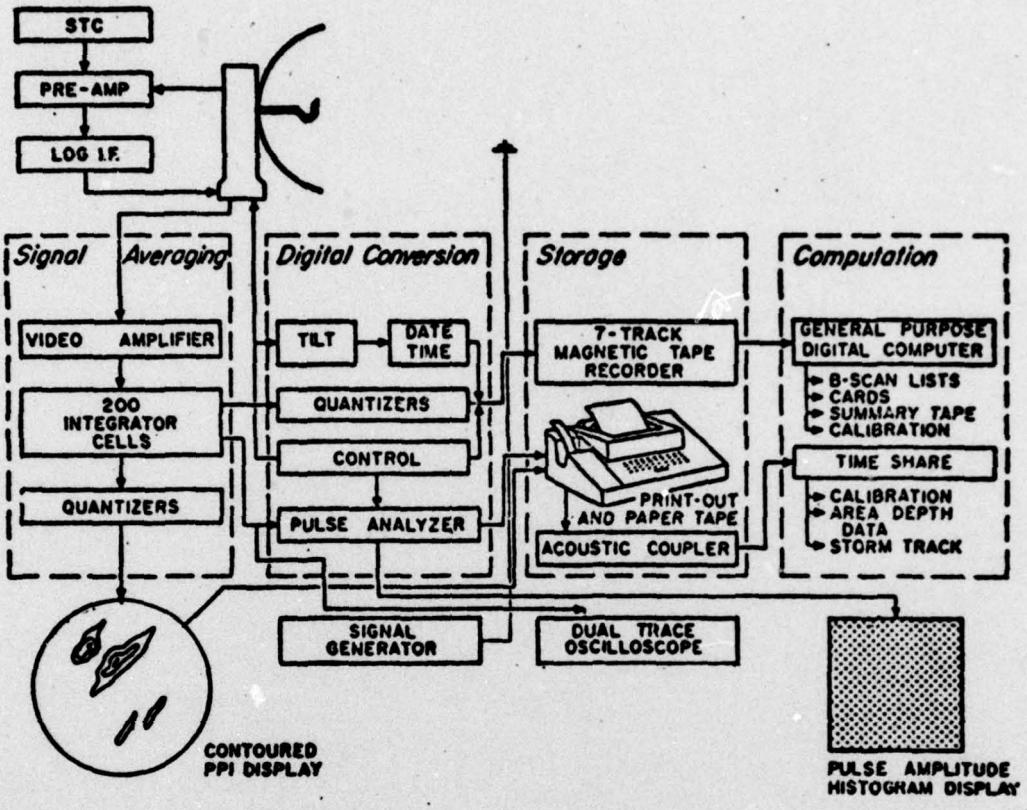

Fig. 1. Block diagram of the NSSL WSR-57 system [after Wilk and Gray, 1970].

discrete intensity levels, the digital conversion process. The intensity thresholds for each level are somewhat arbitrary and vary slightly from day to day. In this form, the data are stored on magnetic tapes. The digital data are collected in 200 intervals of range called gates, each approximately 1 km in length. The precise length of the gate is recorded with each set of data. Two degree azimuth intervals are used for data collection and successive antenna elevation angles, in steps of 1 or 2 deg, up to 20 deg are used. The time given for a particular display is the starting time for the acquisition of the data required to

TABLE 1. Characteristics of the NSSL WSR-57 Radar [after Wilk et al., 1967]

Peak transmitted power	450 kw
Antenna gain	7.079×10^3
Pulse length	1.20×10^3 m
Beam width	2.0 deg
Wavelength	10.4 cm
Pulse repetition frequency	164 sec^{-1}
Minimum detectable signal	-110 dbm

compute the display. The acquisition time, which is a function of the antenna rotation rate, is approximately 4 min.

The Theoretical Basis

The form of the equation used in this study follows the derivation of Probert-Jones [1962] who assumed a more reliable beam-shape in order to reduce the error inherent in a more conventional derivation [Battan, 1959].

If the volume illuminated by the radar beam is filled by the target and there is no attenuation of the radar energy due to precipitation, the average back-scattered power, $\bar{P}_r$, received from a meteorological target at range, r, is given by

$$\bar{P}_r = \frac{CK^2}{r^2} Z_e, \tag{1}$$

where K^2 is the dielectric constant used in scattering theory and Z_e is the equivalent radar reflectivity factor. The radar constant, C, is

determined by the characteristics of the given radar system, viz.,

$$C = \frac{\pi^3 P_t G^2 h \theta^2}{1024 \lambda^2 \ln 2}, \tag{2}$$

where P_t is the peak transmitted power, G the antenna gain, h the pulse length, θ the beam width, and λ the wavelength of the radar. From the values in Table 1, the radar constant for the NSSL WSR-57 has a value of 1.332×10^{14} w m^{-1} or 1.332×10^{-10} w km^2 m^3 mm^{-6}.

For the purposes of this study, the digital radar values have been converted to equivalent radar reflectivity values, Z_e.[1] First, each digital integer is converted to a received power value, $\bar{P}_r$ (in units of negative dbm). This information is provided on the magnetic tape via the header record generated prior to each scan. Next, (1) is solved in terms of Z_e, viz.,

$$Z_e = \frac{\bar{P}_r r^2}{CK^2}. \tag{3}$$

The logarithm of (3) is

$$\log Z_e = \log \bar{P}_r + 2 \log r - \log CK^2. \tag{4}$$

Using a value of 0.9 for K^2 [Battan, 1973] and the value of C obtained earlier, we have

$$\log CK^2 = -9.9. \tag{5}$$

---

[1] For a discussion of radar reflectivity factor, Z, equivalent radar reflectivity factor, Z_e, and dbm, see Battan [1973].

Substitution of this value in (4) yields[2]

$$\log Z_e = \log \bar{P}_r + 2 \log r + 9.9. \quad (6)$$

However, since the received power values are calibrated in terms of dbm instead of watts, (6) is written

$$\log Z_e = 0.1 \bar{P}_r + 2 \log r + 6.9, \quad (7)$$

where

$$\log \bar{P}_r \text{ (watts)} = 0.1 \bar{P} \text{ (dbm)} - 3. \quad (8)$$

Finally, a digital value then may be converted directly to a Z_e value by

$$Z_e(D_i) = 10^{(0.1 \bar{P}_i + 2\log r + 6.9)}, \quad (9)$$

where D_i is a digital value (0 thru 63), $\bar{P}_i$ is the corresponding average received power in dbm as provided in the header record, r is the range to the power return location in km, and Z_e is in units of $mm^6\ m^{-3}$.

It should be noted that threshold calibration values, as opposed to logarithmic mean values between thresholds, have been used in the digital conversions in this study. The actual reflectivity factor values will be somewhere between the calculated values and the next higher threshold setting.

---

[2]The radar actually obtains $\overline{\log P_r}$ rather than $\log \bar{P}_r$. An equation has been obtained by Wilk and Kessler [1970] which corrects (6) slightly. The correction, in general, amounts to less than 1 db.

Data Processing

Beginning with the 1973 storm season, NSSL radically changed its data collection and recording procedures. Range intervals were converted from nautical miles to kilometers, the number of digital intensity levels was increased from 9 to 64, and the magnetic-tape recording format was modified. Of these changes, the latter caused by far the greatest difficulty. As a result of the format modification, all the data no longer could be extracted from the tapes by using standard FORTRAN "READ" statements; in fact, none of it could.

Appendix A contains the record formats for the 1974 and 1975 7-track data tapes that have been used in this study. As indicated in these formats, the first record of each PPI sector scan, called the header record, is recorded by using standard 8-bit bytes, readable in FORTRAN. The follow-on data records, containing two radials of information each, are recorded in 6-bit bytes as only six binary bits are needed to record the digital intensity integers 0 thru 63. These are readable only through bit manipulation via FORTRAN or through an assembler language subroutine. Further, the header record is readable via FORTRAN only when using the 7-track TRTCH=T option, and attempts to read the subsequent 6-bit data records with the TRTCH=T option in effect will produce an abnormal termination of the program. Hence, none of the data can be extracted by using standard FORTRAN "READ" statements.

In order to extract the data from the tapes, a lengthy and costly program was written. Though an assembler language subroutine would execute faster, and hence be cheaper to run, a FORTRAN bit-manipulation

program was chosen so that an analyst without an assembler language background would be able to understand and use the program. The entire fully-commented program used to read the tapes and develop the presentations is listed in Appendix B. Statement numbers 11 thru 83 are used to extract data from the tapes.

Presentations

It is difficult to build a mental picture of the three-dimensional structure of a thunderstorm from reflectivity values collected in a spherical array. If the display is made at a constant antenna tilt, great distortion can occur in the display. For example, if on the 4-deg antenna-tilt display, the near edge of a particular isoline is at a range of 60 km and the far edge of the same isoline is at 80 km, the difference in height of the two edges would be 4577 ft. The difference becomes greater with an increase in antenna elevation angle and range from the radar. The picture is further complicated by the curvature of the earth and the refraction of the radar beam. It is desirable, therefore, to present reflectivity values in a rectangular display (x, y, h), where x and y are the rectangular coordinates on a flat earth and h is a constant height above ground level.

Constant Altitude Reflectivity Maps

Greene [1971] developed a technique to synthesize constant-altitude reflectivity (Z) maps or CAZMs. Vogel [1973] modified Greene's technique and presented an explanation of the procedure in excellent detail. The present study employs this basic technique with minor programming

improvements added by Canipe [1973], Phillips [1975], and this author. Basically, the technique inputs digital radar values into a spherical array while converting the digital integers to reflectivity values, $Z(\theta, r, \phi)$ [Vogel, 1973]. The data then are interpolated linearly to cylindrical coordinates, $Z(\theta, s, h)$. The cylindrical coordinates then are used to fill a rectangular array, $Z(x, y, h)$, by what may be called a quadratic interpolation scheme which selects the nearest nine possible $Z(\theta, s, h)$ values that could be used to approximate each $Z(x, y, h)$ point. This scheme is in reality a finite-difference form of the Taylor series expansion in two dimensions truncated after the second-order terms [Canipe, 1973].

As stated before, this study continues work started by Canipe. In order to provide presentations that are easily comparable to those previously prepared, the same vertical and horizontal resolutions have been retained. For ease of presentation, non-standard units (such as kft) are used throughout. CAZMs for this study are constructed from 5 kft to 50 kft at 5-kft intervals. A grid interval of 2 km, comparable to the previously-used 1 n mi (1.079 n mi) also was chosen. The original CAZMs in this study, which are 25 in. by 25 in. covering an area of 100 km^2, are in a scale of 1 in. equals 4 km. If an entire CAZM were reduced to page size and displayed, the digital values would be too small to be read. Therefore, the CAZMs prepared during this study have not been included in this paper. However, as an example, partial maps for 1810 CST, 23 May 1974, are shown in Figures 2 thru 12. In these figures, reflectivity values are expressed in dbz which is defined as 10 $\log_{10} Z$, where Z is in $mm^6\ m^{-3}$, thus implying a reference

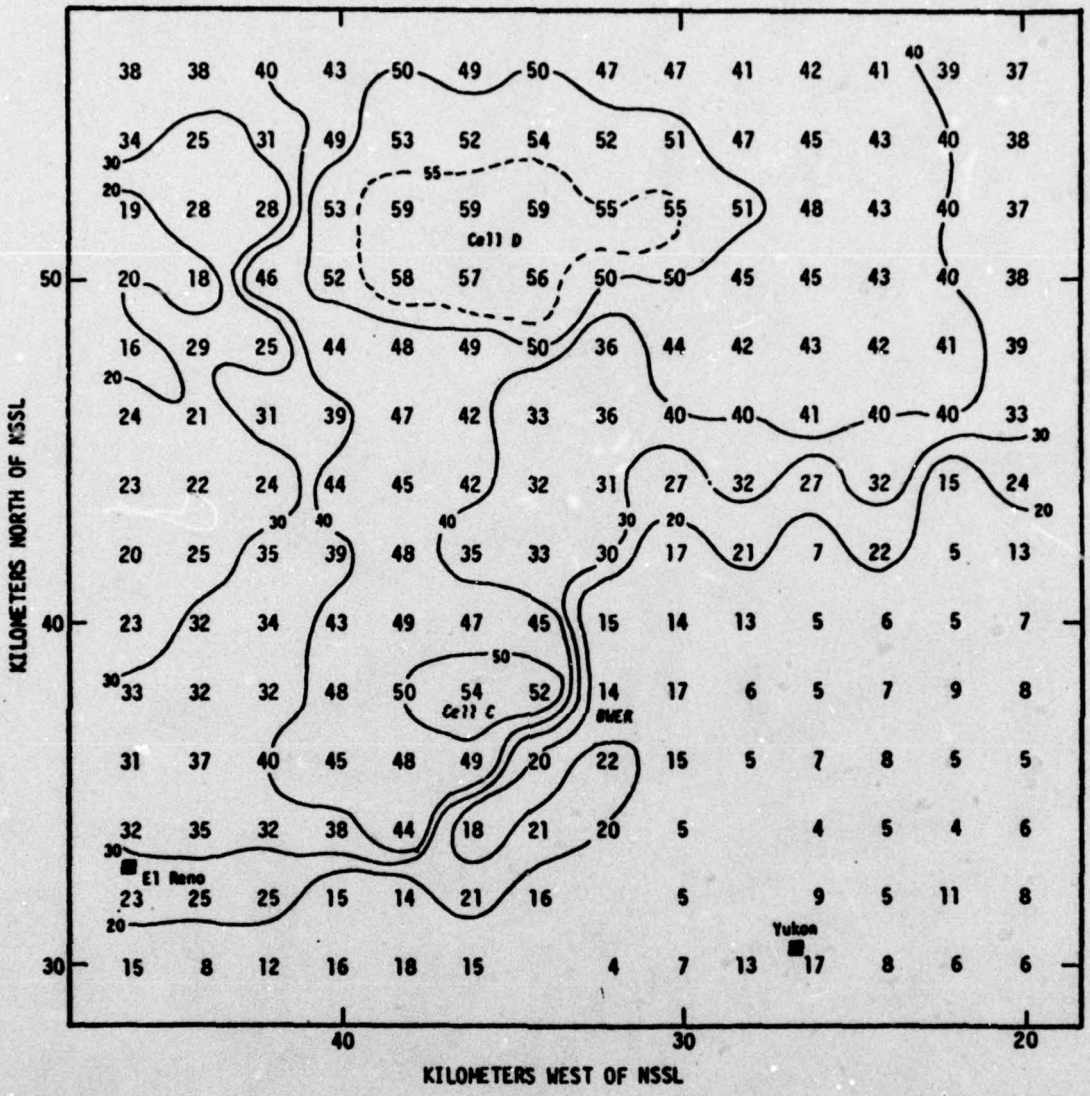

Fig. 2. Reflectivity for 0-deg tilt, 1810 CST, 23 May 1974. Isopleths of reflectivity in dbz.

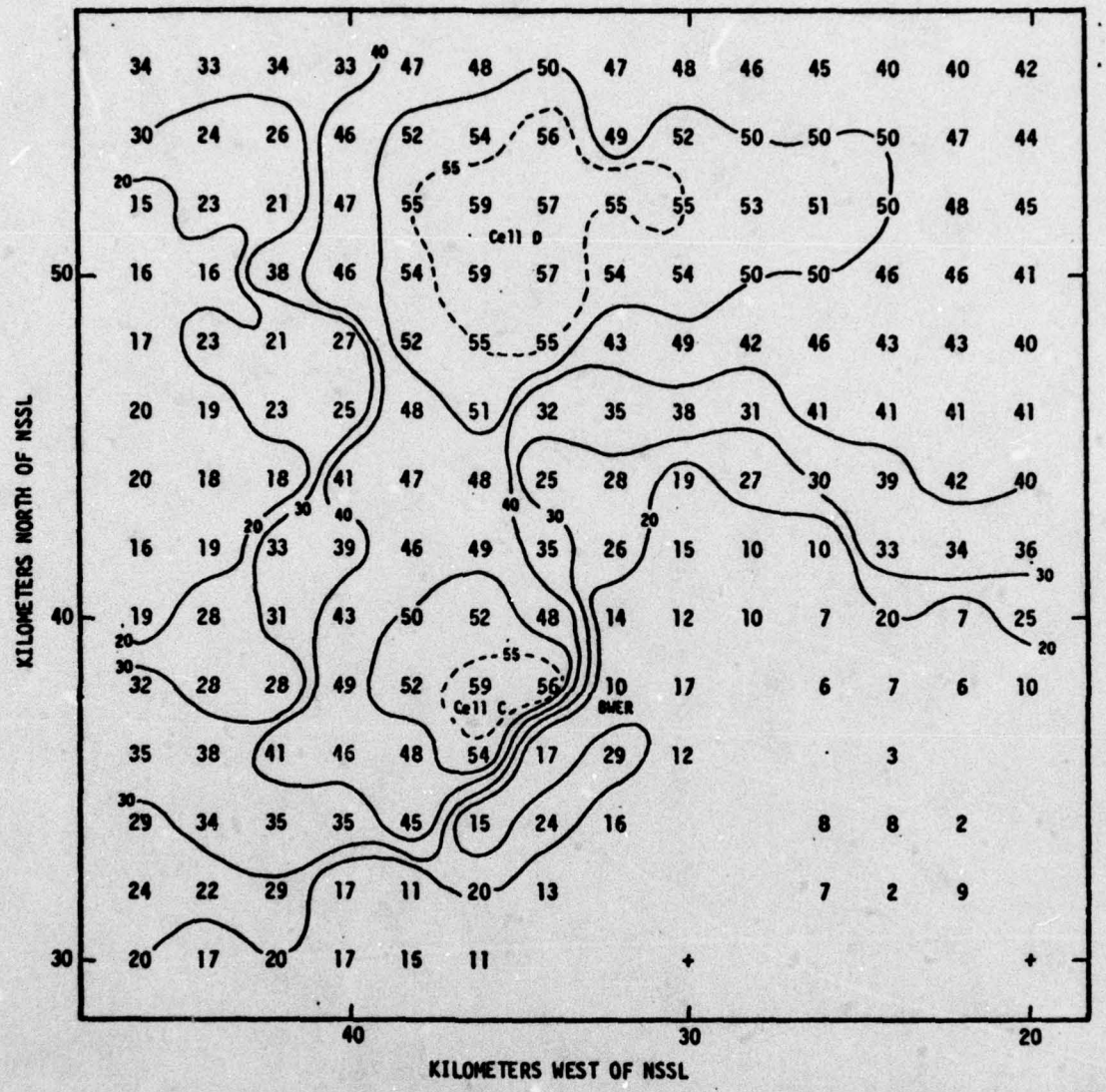

Fig. 3. CAZM for 5 kft, 1810 CST, 23 May 1974.
Isopleths of reflectivity in dbz.

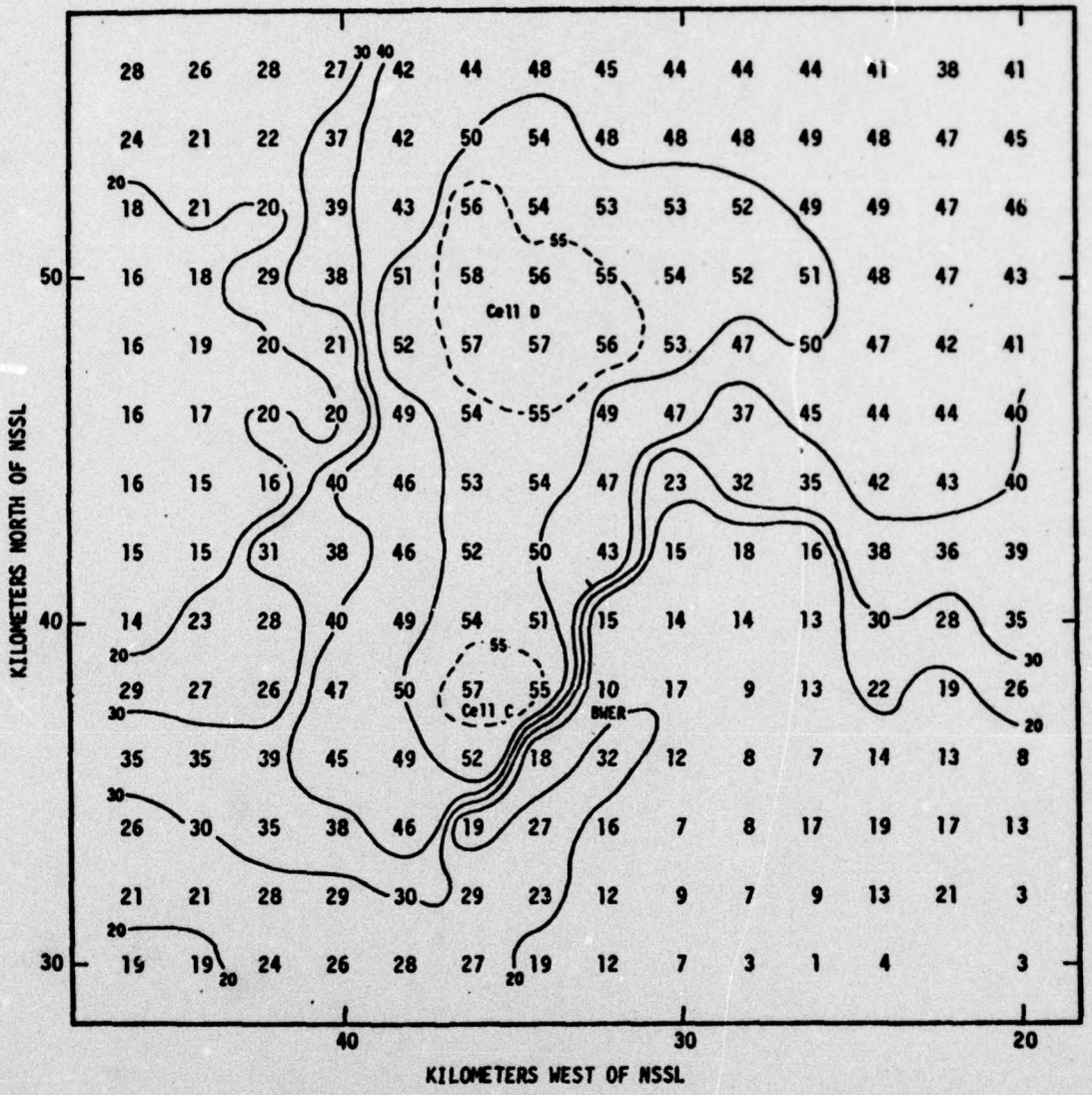

Fig. 4. CAZM for 10 kft, 1810 CST, 23 May 1974.
Isopleths of reflectivity in dbz.

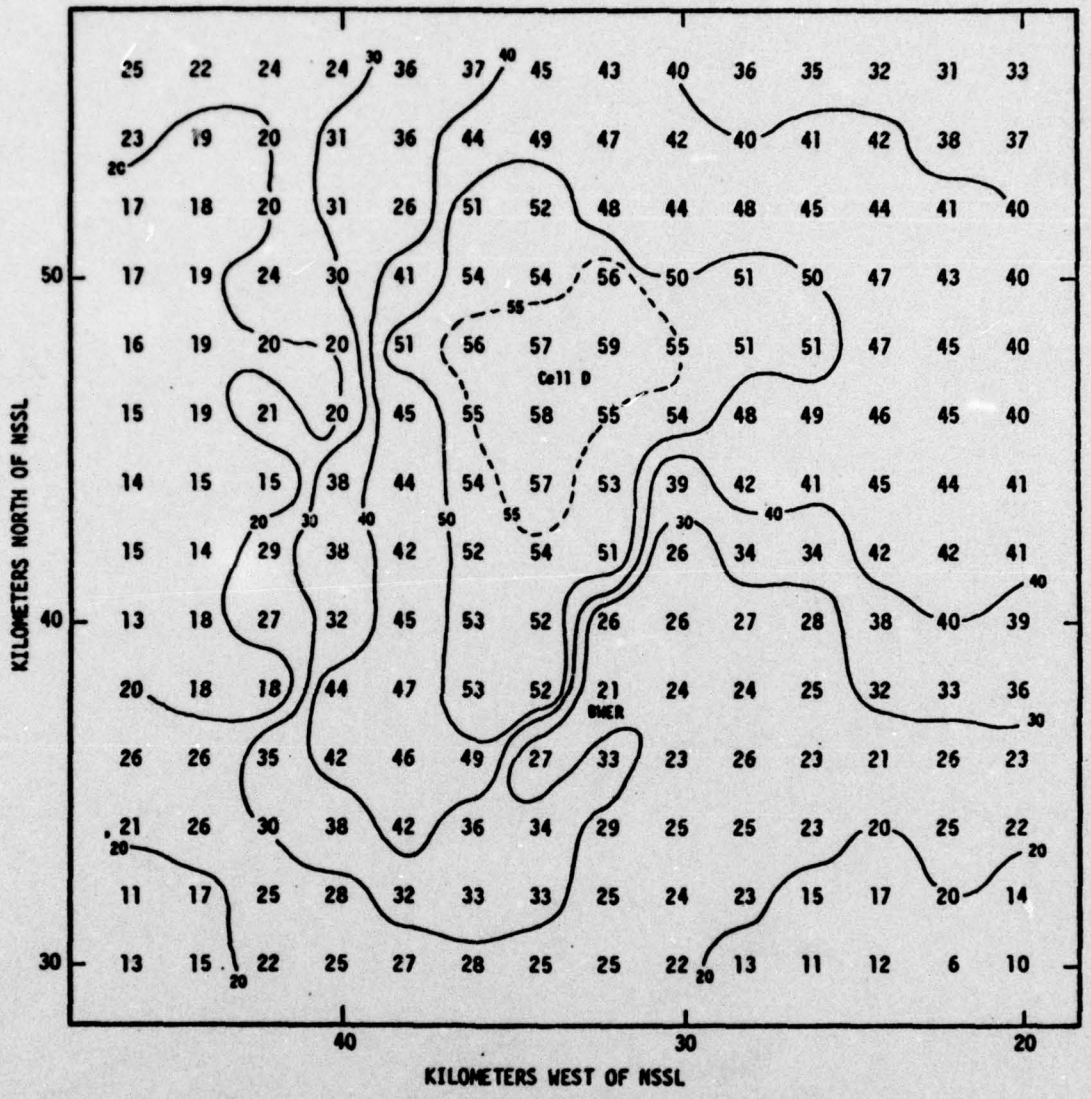

Fig. 5. CAZM for 15 kft, 1810 CST, 23 May 1974. Isopleths of reflectivity in dbz.

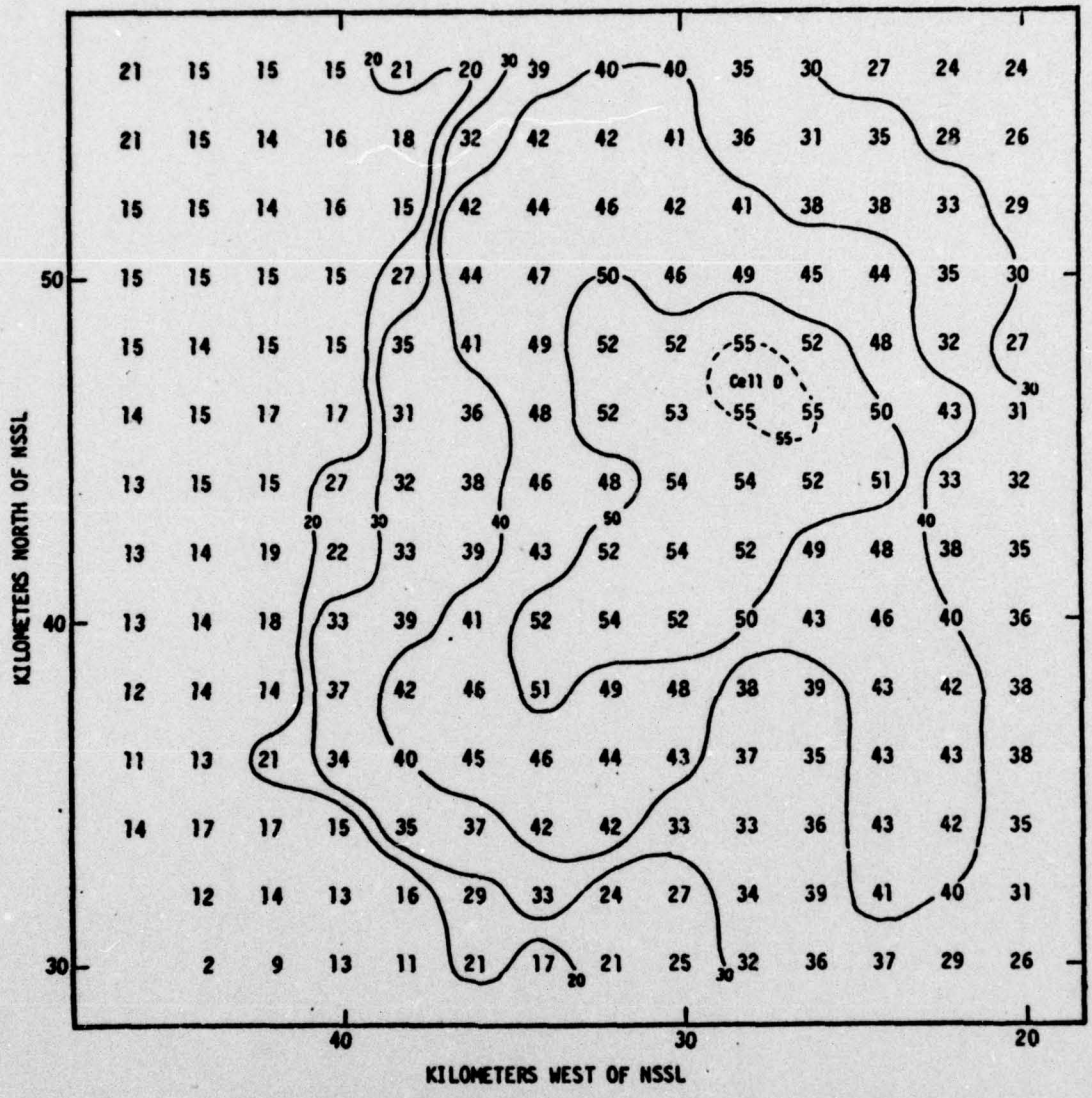

Fig. 6. CAZM for 20 kft, 1810 CST, 23 May 1974. Isopleths of reflectivity in dbz.

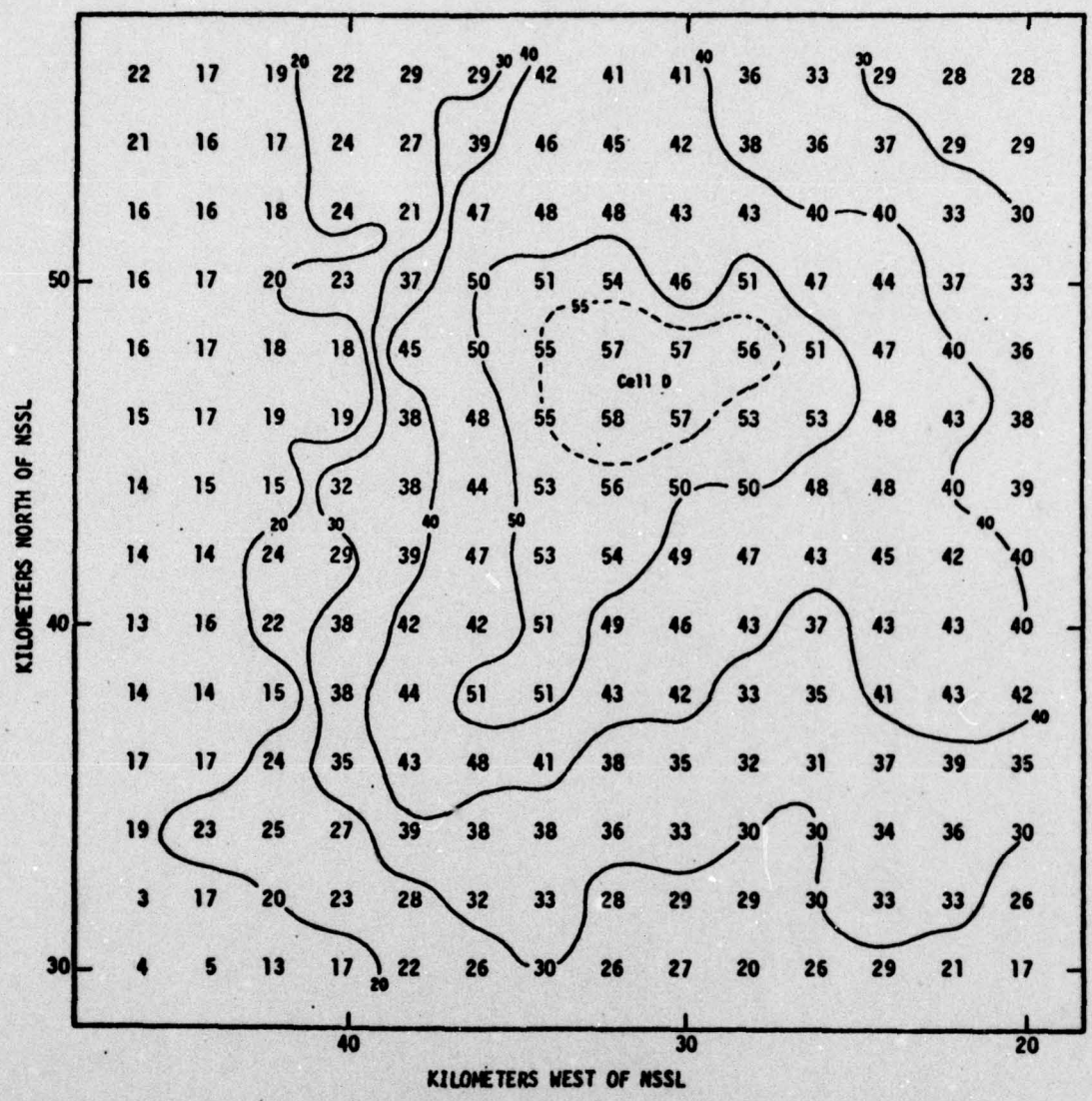

Fig. 7. CAZM for 25 kft, 1810 CST, 23 May 1974. Isopleths of reflectivity in dbz.

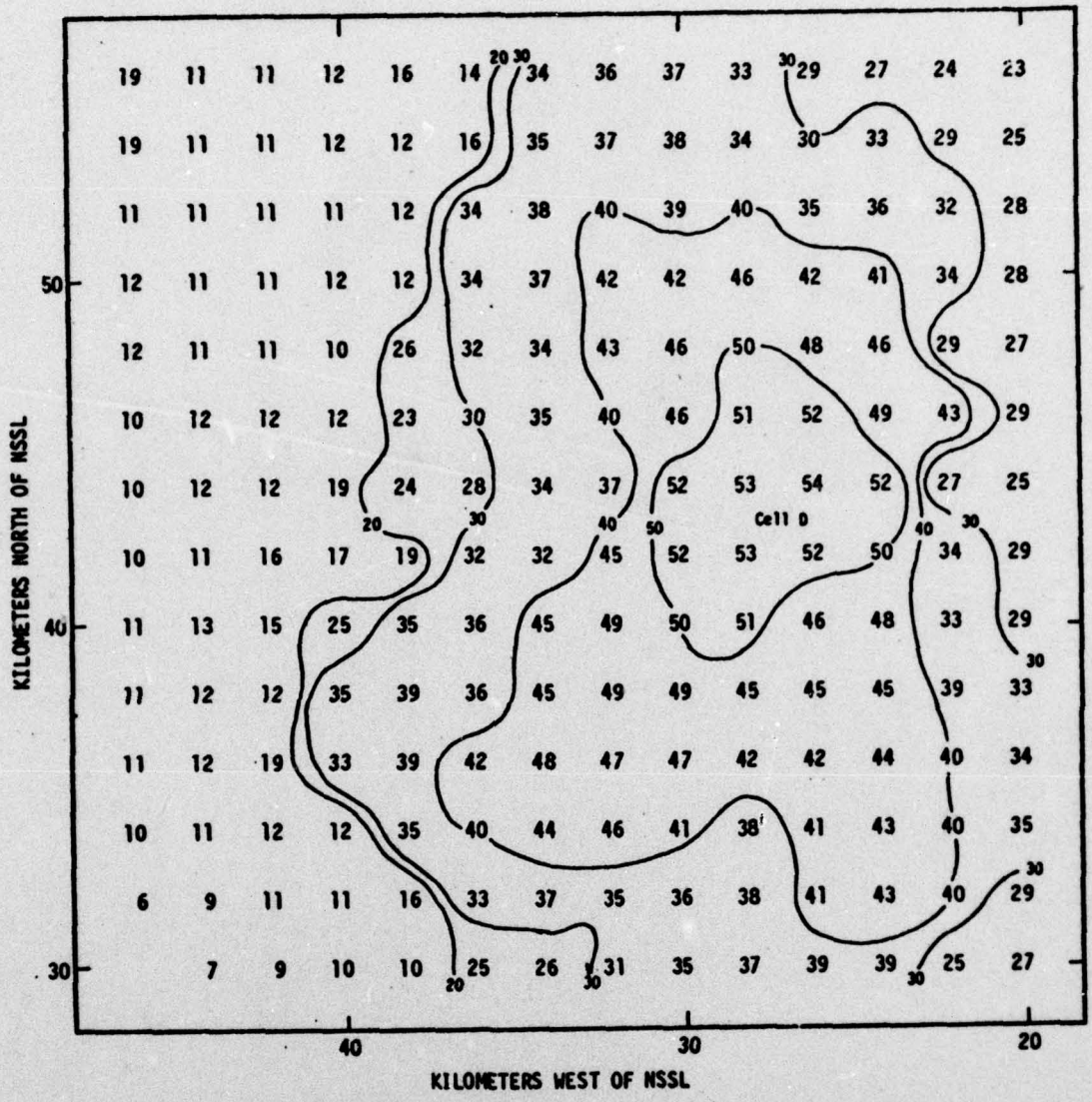

Fig. 8. CAZM for 30 kft, 1810 CST, 23 May 1974. Isopleths of reflectivity in dbz.

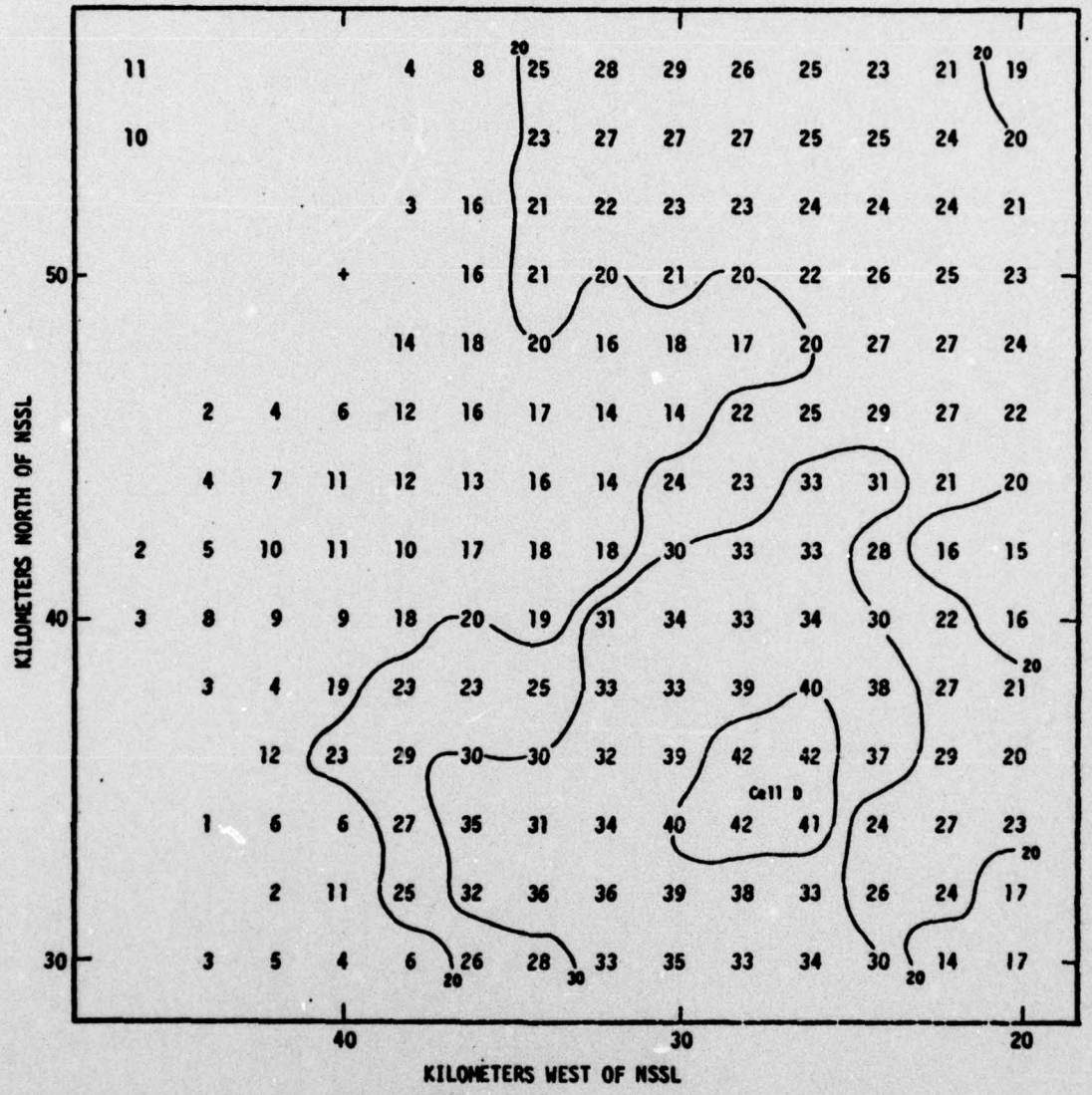

Fig. 9. CAZM for 35 kft, 1810 CST, 23 May 1974. Isopleths of reflectivity in dbz.

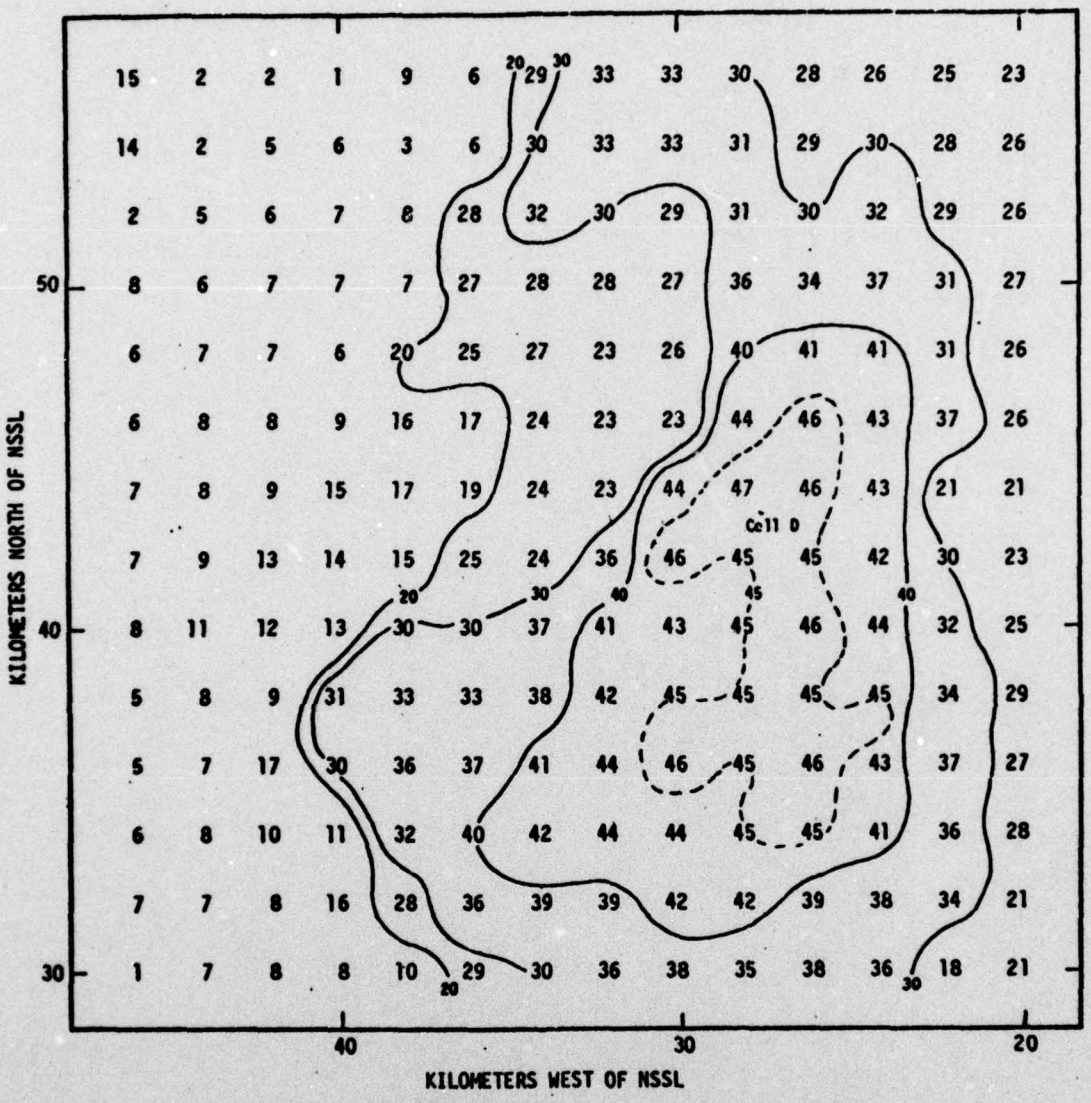

Fig. 10. CAZM for 40 kft, 1810 CST, 23 May 1974. Isopleths of reflectivity in dbz.

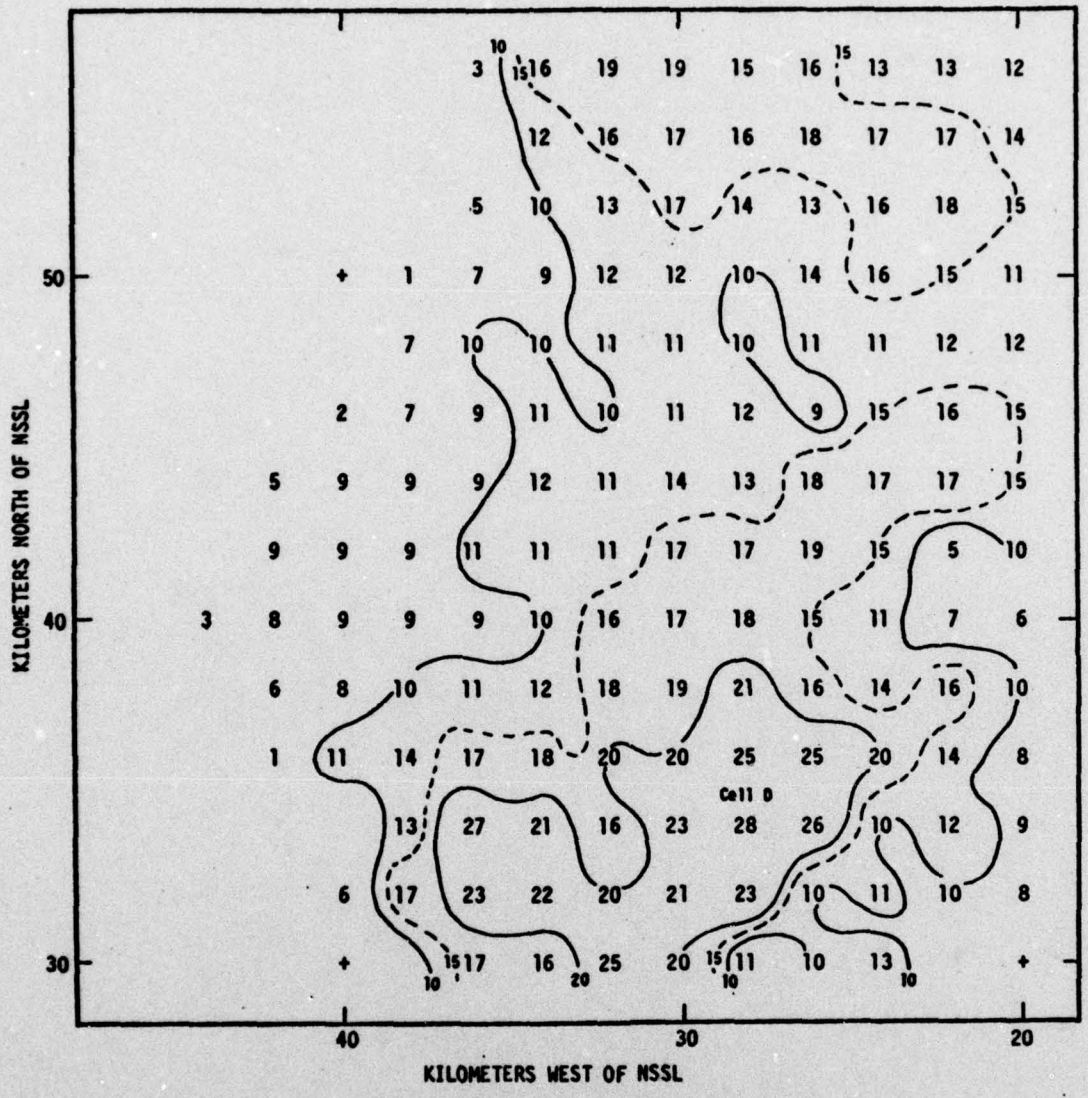

Fig. 11. CAZM for 45 kft, 1810 CST, 23 May 1974. Isopleths of reflectivity in dbz.

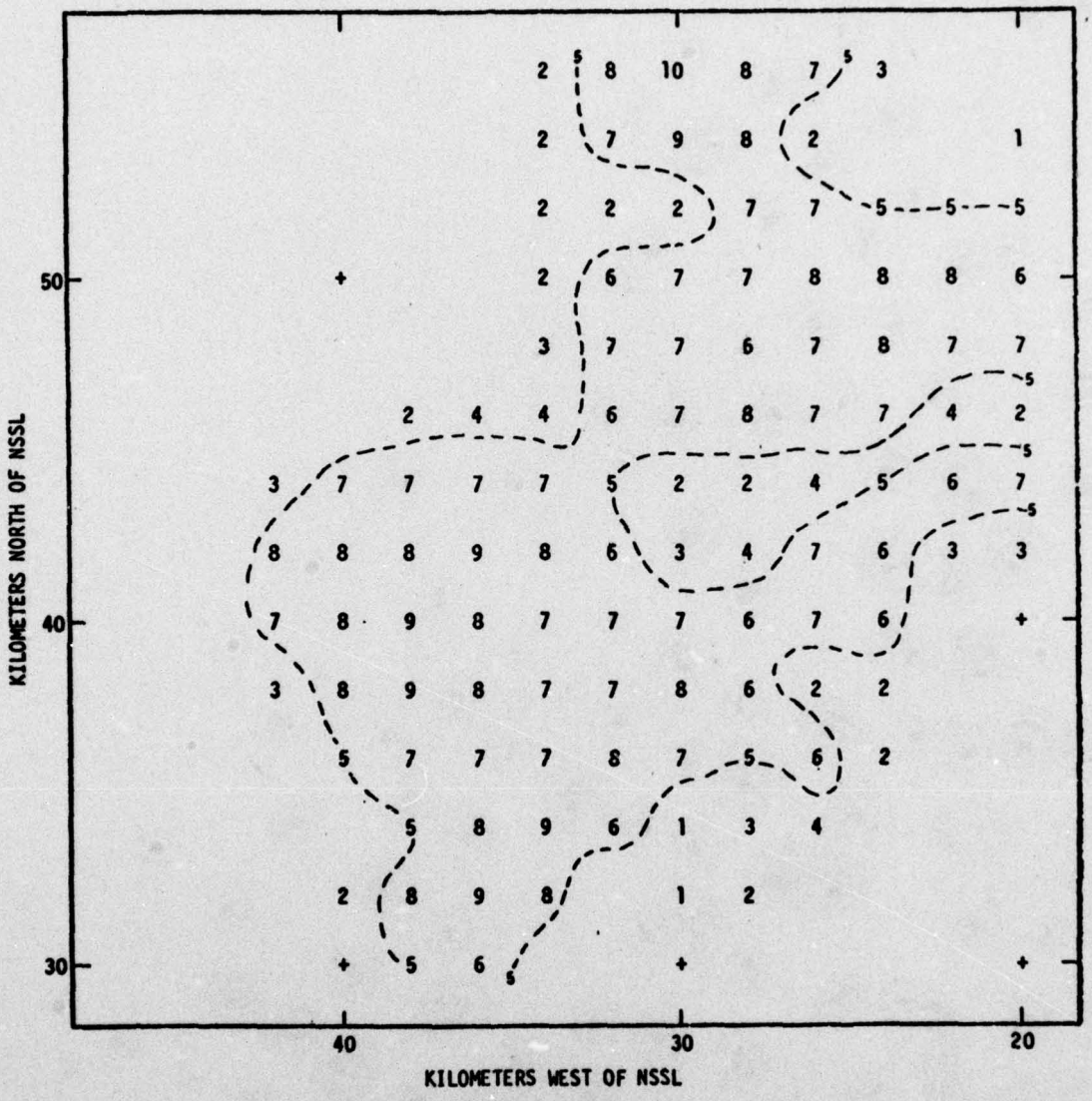

Fig. 12. CAZM for 50 kft, 1810 CST, 23 May 1974. Isopleths of reflectivity in dbz.

level Z as 1 $mm^6 m^{-3}$.

Vertical Summation of Reflectivities

Although CAZMs describe the detailed structure of a storm system, a more rapid, less detailed method of analysis is desirable for operational applications. Greene [1971] developed a technique which integrates the reflectivity factor (in terms of liquid water) through the vertical extent of the storm, thus reducing the analysis to a single two-dimensional display. Greene achieved an integration in depth by averaging adjacent 5000-ft CAZM reflectivities, converting the average reflectivity to liquid water, and then summing the ten resultant liquid water values over a given x,y coordinate. The resultant display, called VIL, was useful in identifying centers of maximum reflectivity intensity and their relative magnitudes.

Canipe [1973], finding that VIL hid many important features of a storm, separated the total VIL into three distinct layers called Partial Integrated Liquid Water (PVIL). The layers correspond roughly to the source region (surface to 15 kft), the active region (15 kft to 35 kft), and the ice region (35 kft to 50 kft). This analytical tool provides information on where development is taking place in the vertical direction and, via an x-y plot of the PVIL centers, the dominant tilt of the cell.

After evaluation, another method of presenting reflectivities was found to be more economical in computer time than Canipe's while retaining all the desired storm-structure features. This technique eliminates the depth-averaging of reflectivities for integration and the constant

algorithm conversion from reflectivity factor to liquid water. Instead, the CAZM reflectivities above a given x,y coordinate are summed through the lower, mid, and upper PVIL layers and the resultant, summed-total reflectivity factor converted to dbz for map presentation. Therefore, lower, mid, and upper Partial Vertical Summed Reflectivity (PVSZ) maps replace the lower, mid, and upper PVIL maps, respectively. Figures 13 thru 15 are PVSZ maps for 1810 CST, 23 May 1974.

In place of the VIL presentation, the ten CAZM reflectivity values (in dbz) over a given x,y point are summed in depth. The product, called Total Vertical Summed Reflectivity (TVSZ), allows the investigator to evaluate Greene's explosive-development theory while reducing computer execution time (and cost). An example of a TVSZ map for 1810 CST, 23 May 1974, is shown in Figure 16.

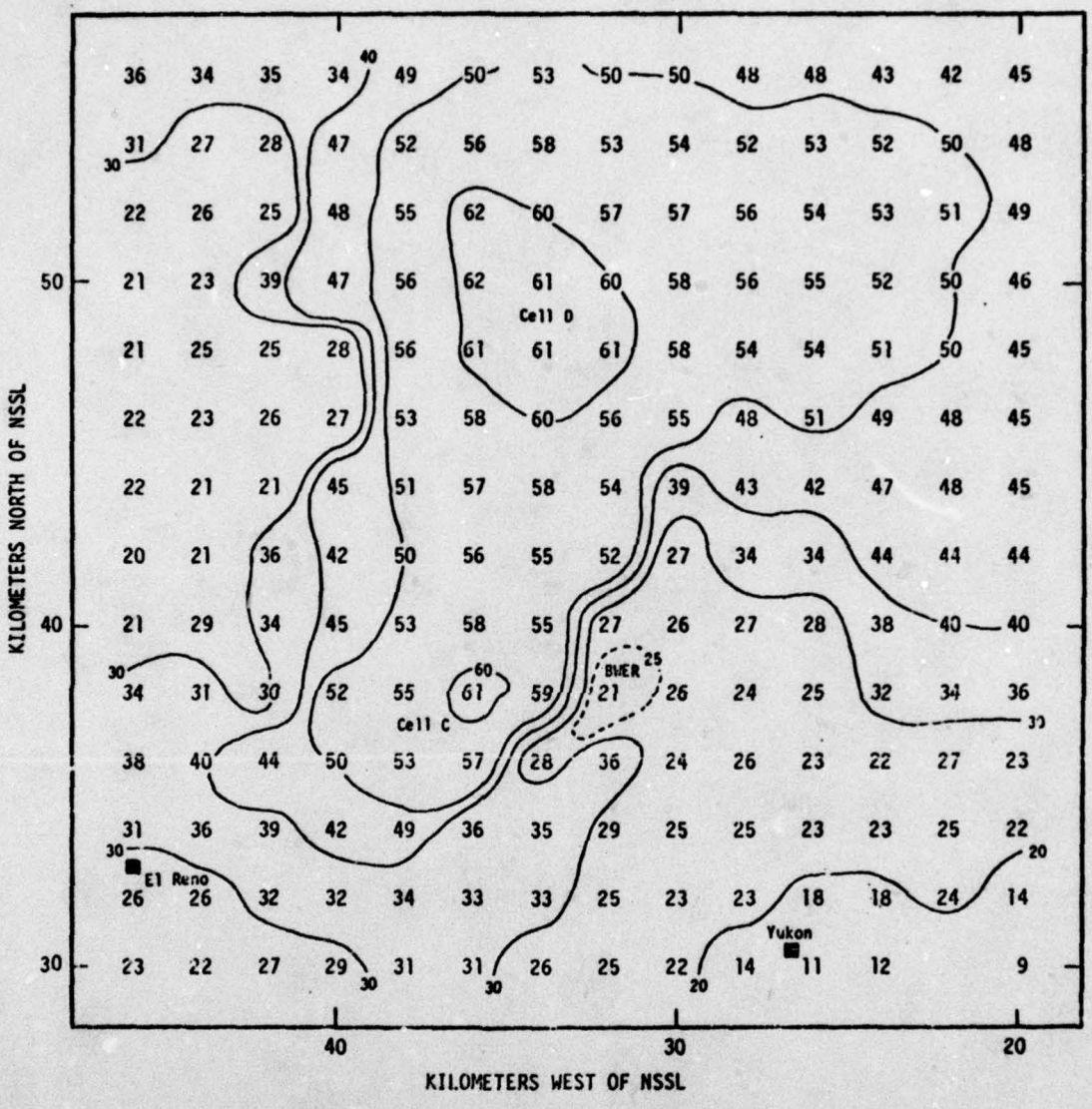

Fig. 13. Lower PYSZ map for 1810 CST, 23 May 1974. Isopleths of reflectivity in dbz.

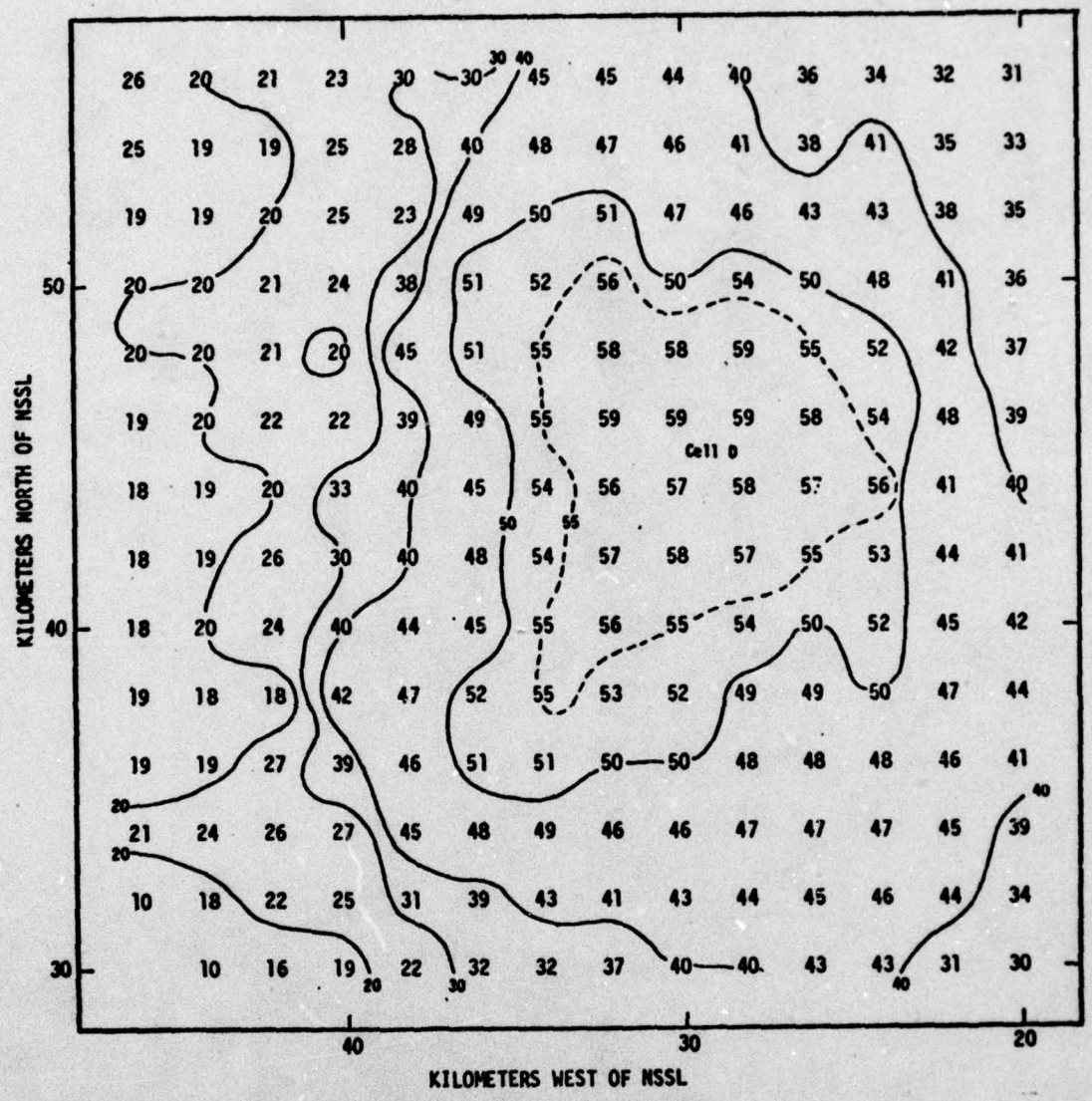

Fig. 14. Middle PVSZ map for 1810 CST, 23 May 1974. Isopleths of reflectivity in dbz.

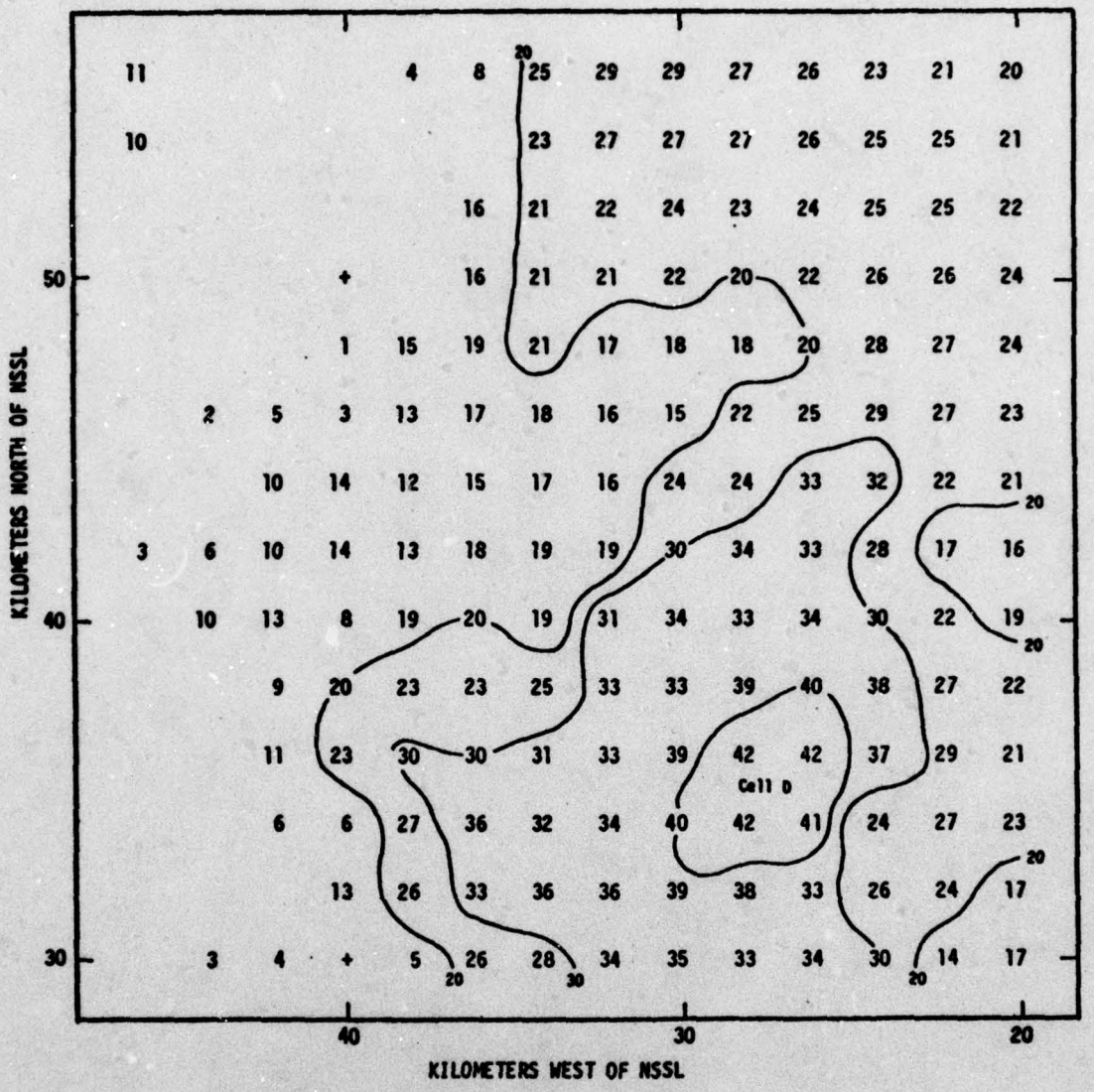

Fig. 15. Upper PVSZ map for 1810 CST, 23 May 1974. Isopleths of reflectivity in dbz.

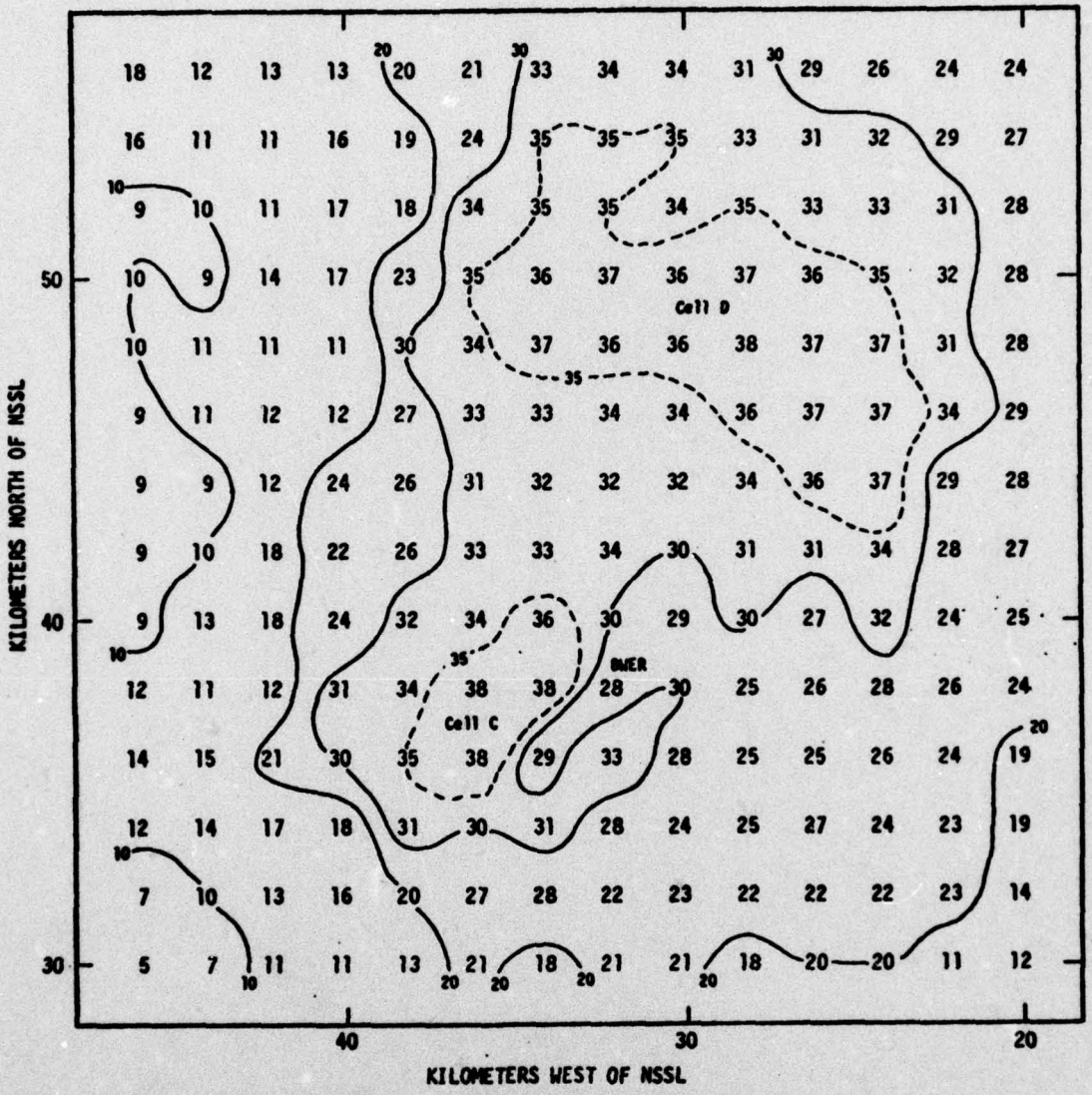

Fig. 16. TVSZ map for 1810 CST, 23 May 1974.
Isopleths of summed reflectivity in dbz/10.

CHAPTER III

CASE STUDIES

The next three sections contain radar case studies for selected storms in central Oklahoma during 1974 and 1975. In each case study, the environmental conditions and severe-storm events are described briefly, followed by a storm structure analysis based on CAZMs, and PVSZ and TVSZ presentations. The significant features to be brought out are the existence and location of BWERs, the tilt of the storm core as revealed by PVSZ analyses, the upper-level mass changes as provided by the Upper PVSZ, and the rapid increases in TVSZ.

Case Study of the Storms on 23 May 1974

Air Mass and Wind Structure

The synoptic conditions in Oklahoma for the evening of 23 May 1974, that were favorable for the formation of severe storms, are presented in Figure 17. A slow-moving cold front had stretched across northern Oklahoma for several days with a series of waves moving rapidly northeastward along the front. On this evening, a wave located in the Texas Panhandle was accelerating the flow of warm, moist Gulf air northward, and thunderstorms developed along the front from southeast Missouri to eastern New Mexico as shown in Figure 18. A mid-level southwesterly jet provided the dry air aloft that produced the atmospheric instability needed for the development of severe activity. The winds aloft for Oklahoma City at 1800 CST, 23 May 1974, presented in Table 2, show this

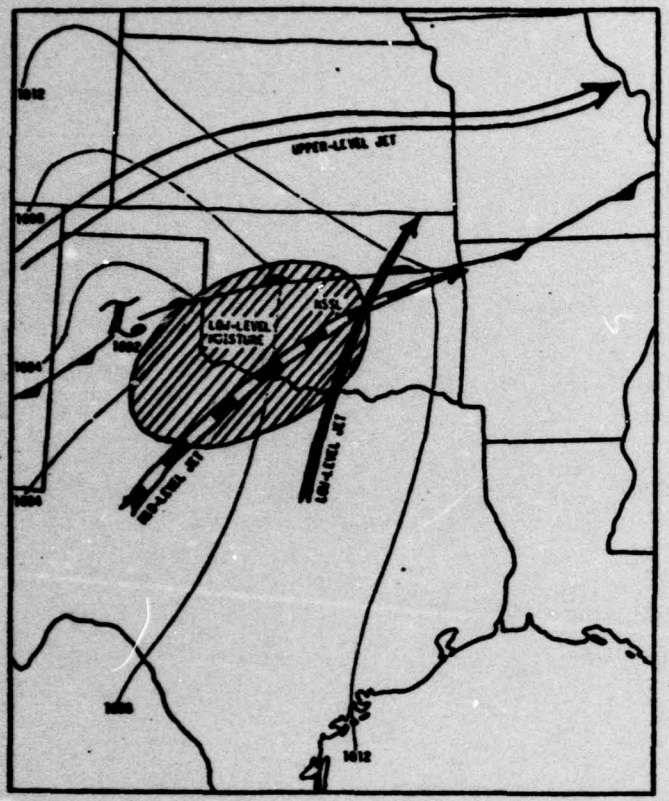

Fig. 17. Synoptic conditions for 1800 CST, 23 May 1974.

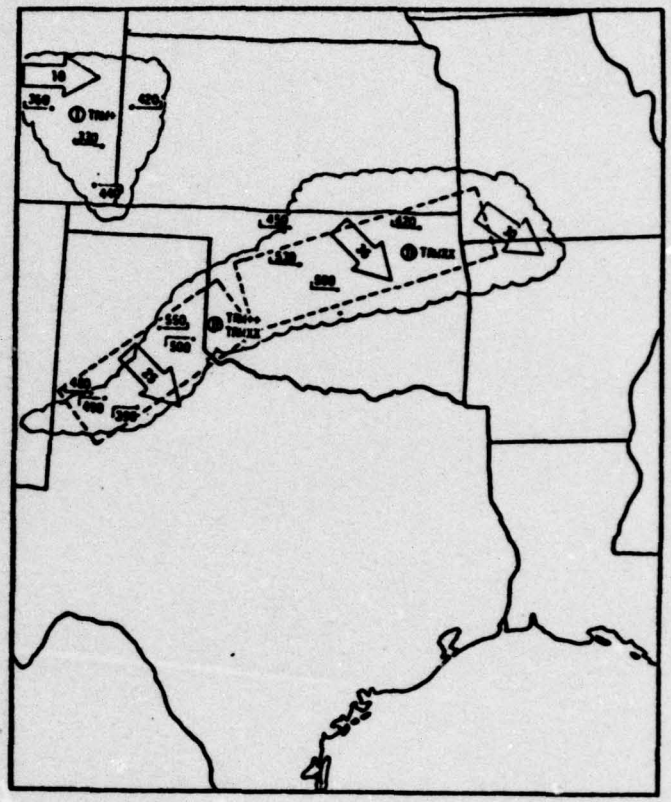

Fig. 18. Radar summary for 1735 CST, 23 May 1974.

TABLE 2. Wind Data for Oklahoma City at 1800 CST, 23 May 1974.

Height (kft)	sfc	2	3	4	5	6	7	8	9
Wind (deg/m sec^{-1})	180/07	175/07	180/08	180/09	190/10	200/10	215/12	225/13	230/14
Height (kft)	10	12	13	14	16	18	20	25	30
Wind (deg/m sec^{-1})	240/14	250/13	255/14	255/14	260/16	265/19	270/21	275/27	275/34
Height (kft)	32	38	44	50		Lower PVSZ average wind = 213/12			
Wind (deg/m sec^{-1})	275/36	285/38	280/34	265/23		Mid PVSZ average wind = 232/31			
						Upper PVSZ average wind = 272/33			

mid-level jet at 9000 ft with a maximum speed of 14 m sec^{-1}.

Severe-Storm Events

Thunderstorms producing various forms of severe weather developed throughout the day along the frontal zone. Golf-ball size hail was reported in early afternoon in north-central Oklahoma. As the system moved southward, a funnel cloud was reported at Kingfisher, 90 km northwest of NSSL, at 1640 CST. A satellite cell southwest of the parent near Kingfisher, continued to develop and produced a tornado which touched down briefly at 1833 CST in the outskirts of Yukon, 40 km northwest of NSSL. Later, a cell to the northwest of Oklahoma City developed to strong intensity and a funnel cloud was reported over Tinker AFB at 1930 CST.

History of the Yukon Storm

During the afternoon, the squall line moved slowly to the southeast with individual cells moving to the east at 15 m sec^{-1}. At 1720 CST, an intense cell (Cell D) developed on the southwest end of an intense

portion of the line. Within 10 min, another less intense cell (Cell A) developed 30 km to the rear of Cell D and the main line of activity. At 1740 CST, Cells A and D began to separate from the line by moving to the right (southeast), and strong satellites developed on the southern extreme of each parent cell. Figure 19, the TVSZ analysis summary, clearly shows the movement of the centers of maximum reflectivity which correspond to each cell in the system. The values of TVSZ, displayed at 5-min intervals, reveal the relative intensity of each cell.

As the cells moved to the southeast, the tilt of Cell D changed from easterly to southeasterly. Figure 20, the PVSZ analysis summary, shows the tilt of Cell D as well as that of the other major cells. The following system is used to depict PVSZ centers in a time series. The symbol, θ, represents the location of the lower PVSZ center, and each succeeding dot is the middle and upper PVSZ centers, respectively. An excellent description of this display method is given by Canipe [1973].

At 1800 CST, a BWER formed east of satellite Cell C. By 1810 CST, the lower CAZMs (Figures 3-5) and the Lower PVSZ (Figure 13) clearly showed a pronounced hook echo just south of the BWER; however, no tornado was reported. The hook existed through 1820 CST but dissipated by 1825 CST as shown in Figure 21. The BWER, however, remained very evident throughout the time period with the minimum reflectivity steadily decreasing from 33 dbz to 6 dbz. Additionally, the tilt of Cell D changed further from southeasterly to southerly, bringing it over the BWER at 1820 CST. By 1825 CST, the gradient of reflectivity over a 4-km distance surrounding the BWER had reached a maximum of 49 dbz

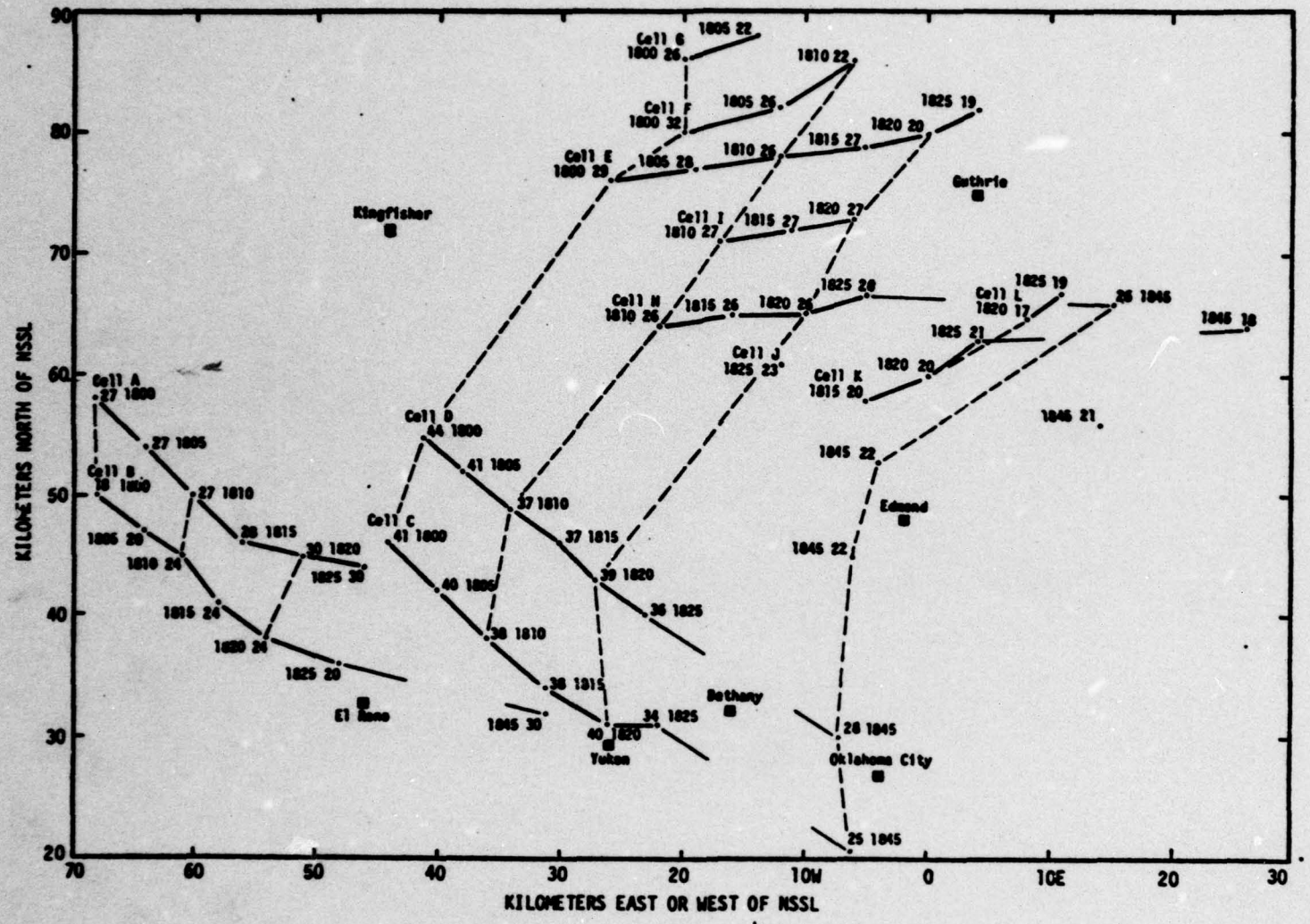

Fig. 19. TVSZ centers for the Yukon storm on 23 May 1974.

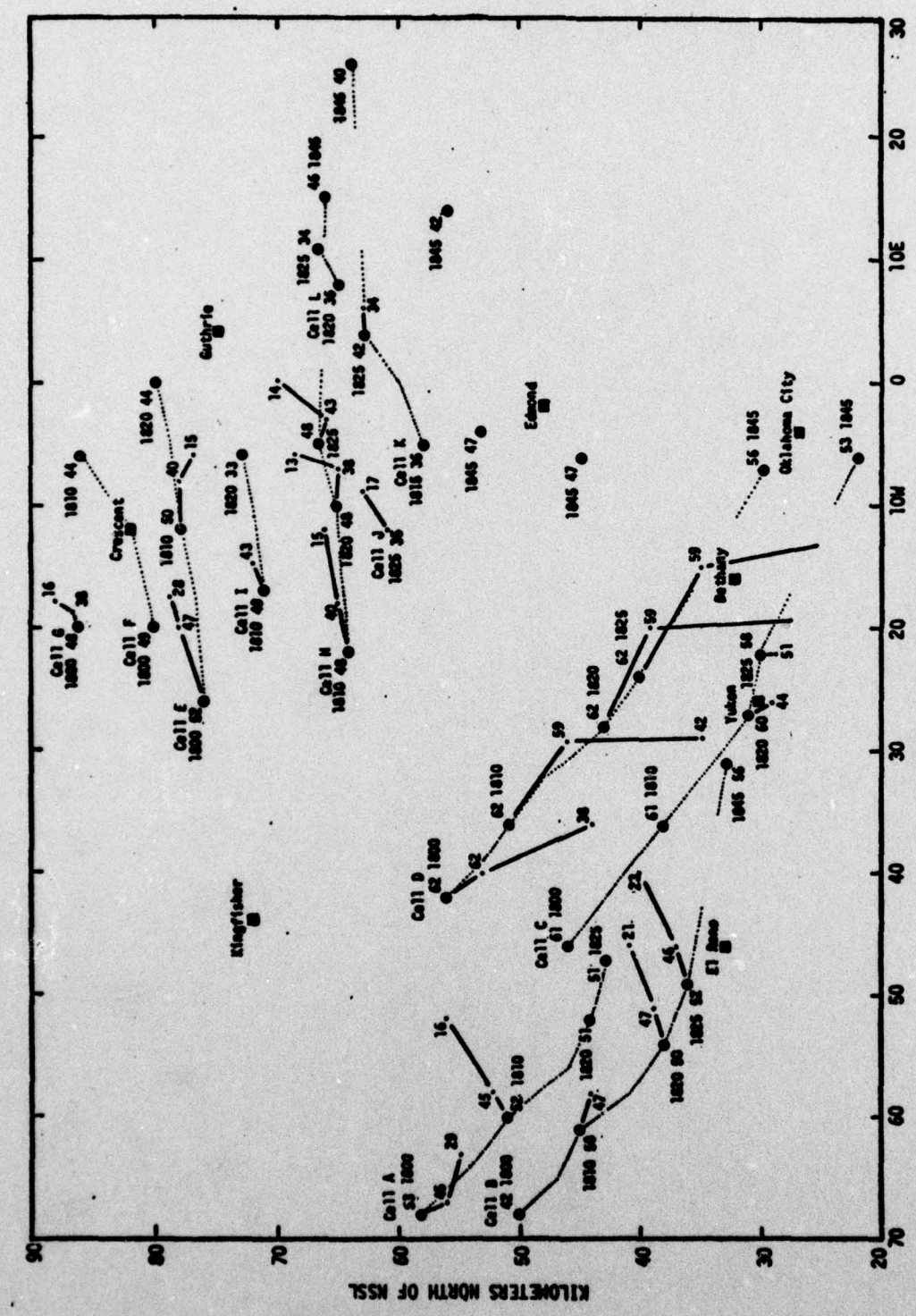

Fig. 20. PVSZ centers for the Yukon storm on 23 May 1974.

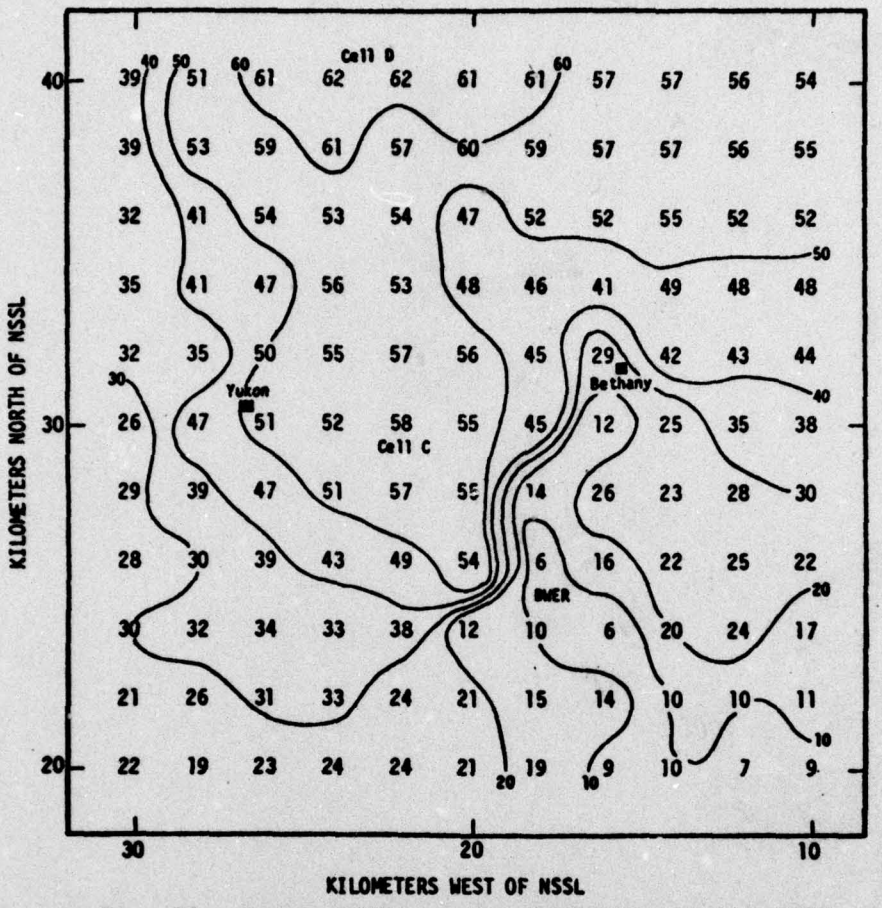

Fig. 21. Lower PVSZ map for 1825 CST, 23 May 1974. Isopleths of reflectivity in dbz.

(55 dbz near Cell C to 6 dbz in the BWER).

For unknown reasons, the collection of multi-tilt data was terminated at 1825 CST, 8 min before the tornado was reported. Collection was not resumed until 1845 CST, and then only below the 4-deg elevation angle. By this time the upper levels of the storm had moved inside the maximum collectable elevation-angle of the radar so that only lower level values of PVSZ are available at 1845 CST. These values, however, do show that a significant decrease in PVSZ occurred in the lower levels between 1825 CST (before the tornado) and 1845 CST (after

the tornado). The development of this system is typical of storms in Oklahoma and follows an evolution almost identical to that of the Minco storm of 26 April 1969 which is described by Canipe [1973].

Evaluation

The evaluation section of each case study compares the significant features of the storm system with those that would be expected from using Canipe's technique for identifying tornadoes. For this case study, the BWER associated with the tornado was present for at least 30 min before the tornado but had dissipated 8 min after the tornado was reported. Hence, the appearance of a BWER is not sufficient evidence to say that a tornado is occurring.

Next, the tilt of Cell D moved over the BWER at 1820 CST, 13 min before the tornado was reported. An evaluation of the duration of this conjuncture is impossible, for by 1825 CST, the upper reaches of both Cells C and D were so close to NSSL as to make measurements of upper-level PVSZ locations (and upper-level mass changes) impossible. For the same reason, the TVSZ values after 1820 CST are of l[illegible] value, as only the lower portions of these cells were sampled by the radar. By combining the above facts, we see that Canipe's identifying characteristics are present 13 min before the reported touch-down of the tornado.

If a BWER is defined simply as an area of reduced reflectivity where the surrounding eight values of reflectivity are greater than the central value (as suggested by Canipe), other BWERs can be found in this storm system. At 1810 CST, a BWER, shown in Figure 22, formed northeast

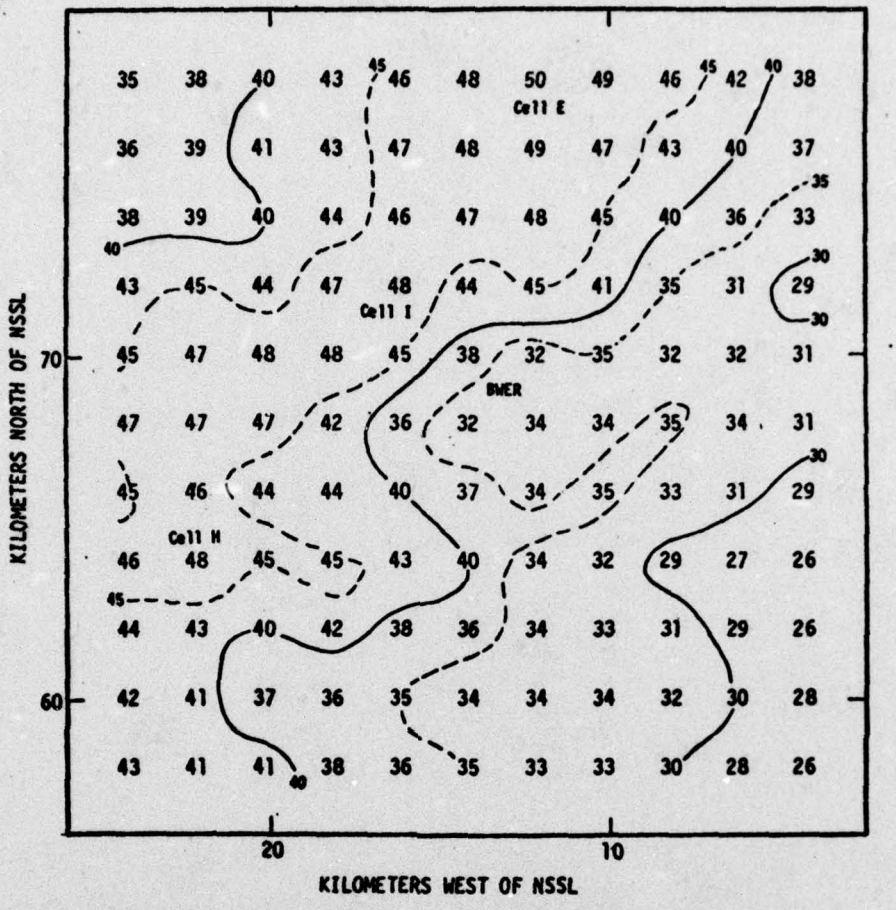

Fig. 22. Lower PVSZ map for 1810 CST, 23 May 1974 for Cell I. Isopleths of reflectivity in dbz.

of Cell H and southeast of Cells I and E (see Figure 19) and a hook-shaped appendage formed south of the BWER. Further, the tilt of Cell E at 1810 CST, though not over the BWER, was to the right of the cell's movement and to the right of the tilt of other cells in the immediate area (see Figure 20); and a significant decrease in Upper PVSZ took place between 1800 CST and 1810 CST (28 dbz to 15 dbz). These characteristics are identical to those required by Canipe [1973] and quite similar to those of the Yukon storm; however, there are some noticeable differences. The core of Cell E, though tilted to the right, was never

closer than 18 km to the BWER and the 4-km reflectivity gradient was a mere 16 dbz (48 dbz to 32 dbz).

Another BWER was visible at 1810 CST, just west of Cell H, and is shown in Figure 23. Again the gradient is small, only 12 dbz (45 dbz to 33 dbz). An out-of-position hook-shaped appendage also is visible yet no tornado was reported.

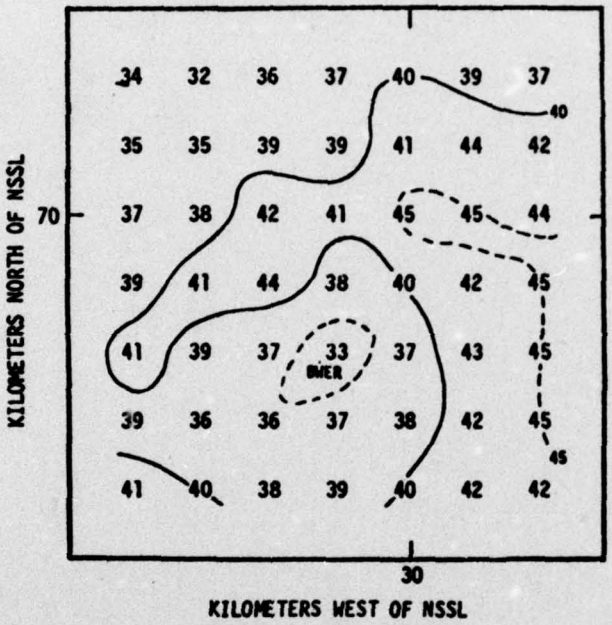

Fig. 23. Lower PVSZ map for 1810 CST, 23 May 1974.
Isopleths of reflectivity in dbz.
Grid interval: 2 km x 2 km.

Case Study of the Storms on 8 June 1974

Air Mass and Wind Structure

The synoptic conditions in Oklahoma for the late afternoon of 8 June 1974 are presented in Figure 24. A cold front, which had remained stationary for several days, was suddenly pushed southeastward by flow around a large cut-off upper low over the Dakotas. Thunderstorms broke out in early afternoon from central Oklahoma northward through Kansas and northern Missouri as shown in Figure 25. A strong low-level jetstream over southeastern Oklahoma was accelerating moist air northward at 20 m sec^{-1}. The winds aloft for Oklahoma City at 1800 CST, 8 June 1974, shown in Table 3, show this jet at 5000 ft with a speed of 18 m sec^{-1}.

TABLE 3. Wind Data for Oklahoma City at 1800 CST, 8 June 1974.

Height (kft)	sfc	2	3	4	5	6	7	8	9
Wind (deg/m sec^{-1})	190/14	190/14	190/14	190/17	200/18	215/16	225/15	235/14	240/14
Height (kft)	10	12	14	16	18	20	25	26	
Wind (deg/m sec^{-1})	245/15	240/20	240/24	240/27	235/30	235/27	230/22	230/22	

Lower PVSZ average wind = 215/16
Mid PVSZ average wind = 235/26

Severe-Storm Events

Cells began developing in the Oklahoma City area shortly after noon and grew to extreme intensity within an hour. At 1342 CST, a tornado touched down on the edge of the Will Rogers Airport and traveled across

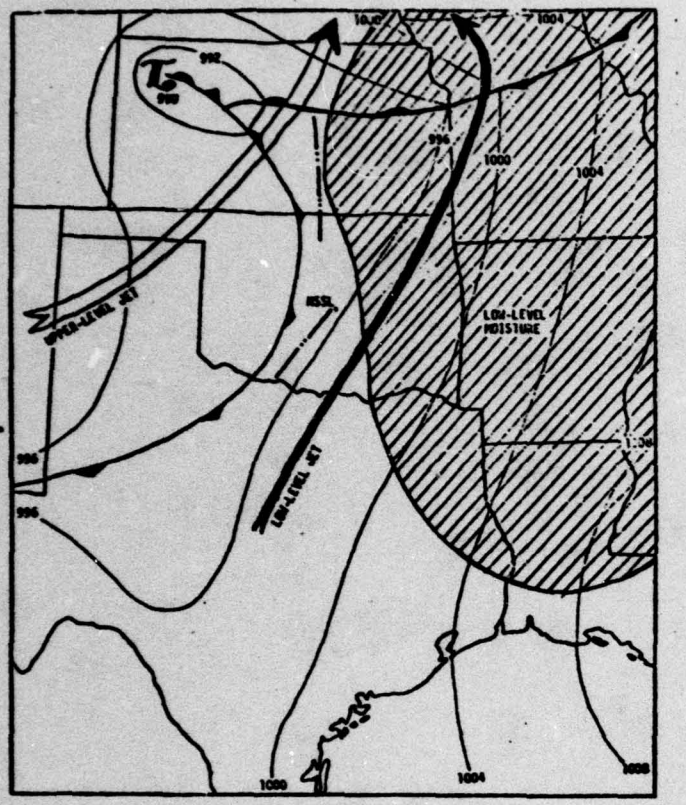

Fig. 24. Synoptic conditions for 1800 CST, 8 June 1974

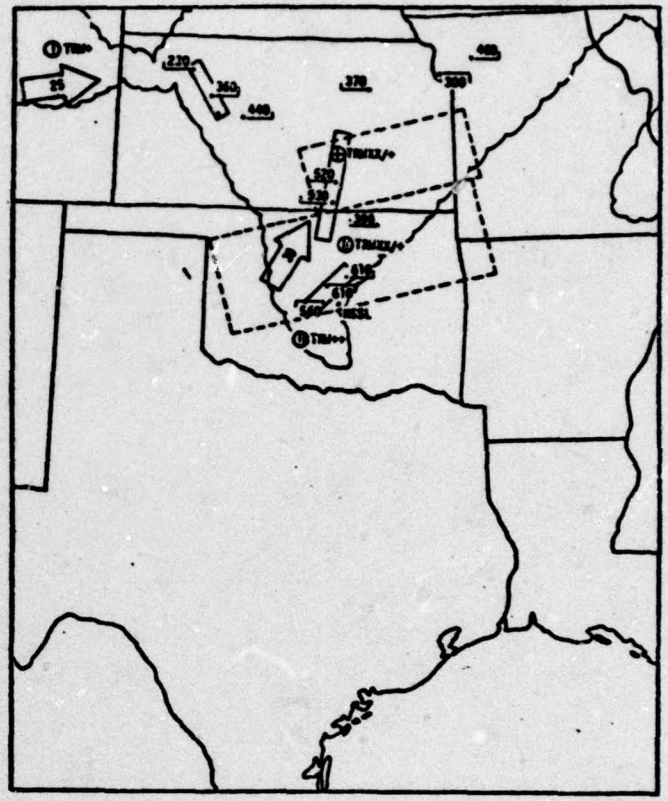

Fig. 25. Radar summary for 1535 CST, 8 June 1974

southwestern Okalhoma City. After lifting over the downtown area, it touched down again at 1411 CST in the northeast suburb of Spencer. Moments later, at 1418 CST, another tornado was reported only 5 km north of Spencer in the community of Jones, Oklahoma.

As the area of initial development moved northeasterly toward Tulsa, new cells formed rapidly on the southwest flank so that a line had formed by 1500 CST. At 1535 CST, a tornado spawned by the southwestern-most cell, touched down in southwest Oklahoma City, 2.5 km southwest of the first one, but it remained on the ground only briefly. At 1555 CST, a tornado was reported at Harrah, 34 km east of Oklahoma City and 39 km northeast of NSSL. (For location of cities, see Figure 28). Moments later, at 1556 CST, a tornado touched down 8 km southwest of Drumright (95 km northeast of NSSL) and stayed intermittently on the ground for 89 min while covering a distance of 85 km. During this time, over 200 homes were destroyed and 14 people were killed. Tornadoes continued to form east of Oklahoma City and south of Tulsa throughout the evening, the twentieth and last being reported at 2224 CST.

History of the Drumright Storm

At 1510 CST, a group of students from the University of Oklahoma spotted a large funnel cloud near Chandler, Oklahoma, 60 km northeast of NSSL. The students watched the funnel for nearly 10 min as it moved to the northeast. Interestingly, the nearest cell to this sighting, some 12 km north, shows none of Canipe's severe storm characteristics.

At 1530 CST, the funnel was sighted again by the State Police,

20 km northeast of its first reported location. At this time, the nearest cell to the funnel, Cell B, developed an appendage on its southernmost edge and a BWER formed south of the cell as shown in Figure 26.

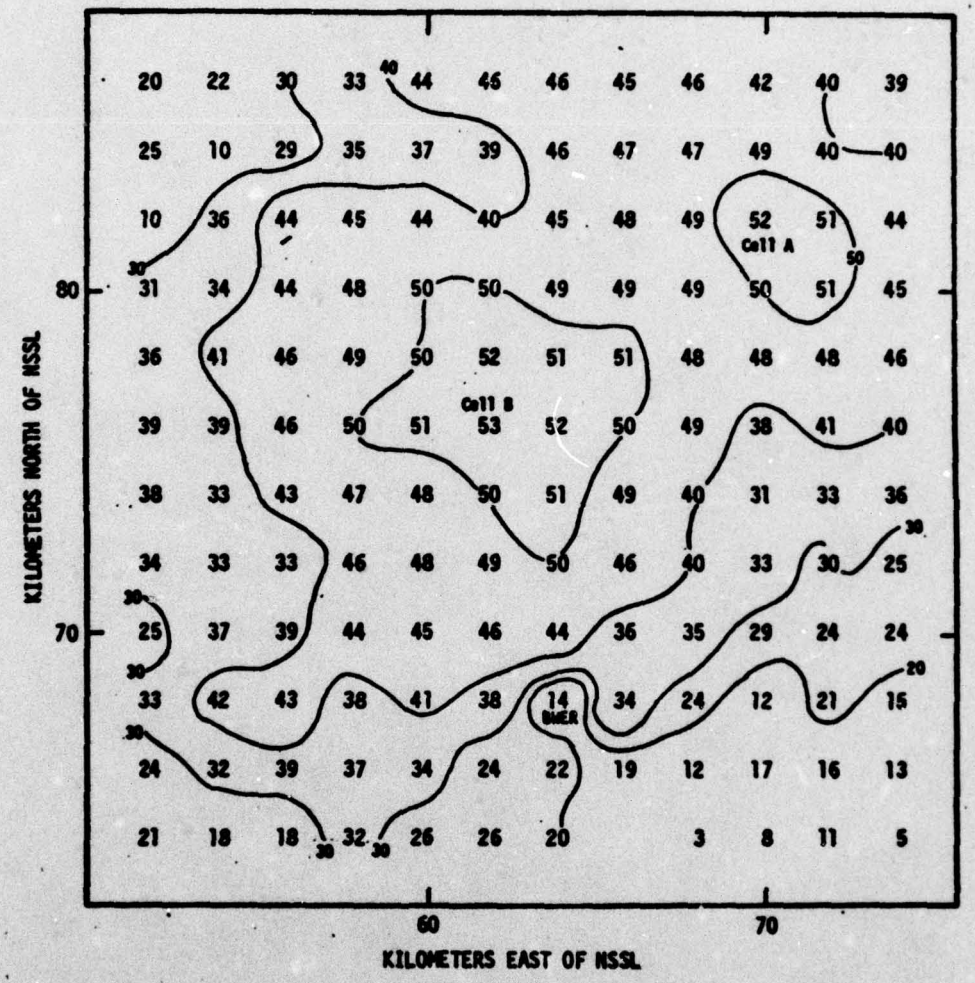

Fig. 26. Lower PVSZ map for 1530 CST, 8 June 1974. Isopleths of reflectivity in dbz.

Figure 27, the PVSZ analysis summary, shows the tilt of Cell B at 1530 CST to be almost vertical. However, the tilt of the cell changed several times during the next few minutes. In a cyclonically-rotating manner, the tilt changed from slightly easterly, to northwesterly, to southerly, and back to easterly by 1600 CST.

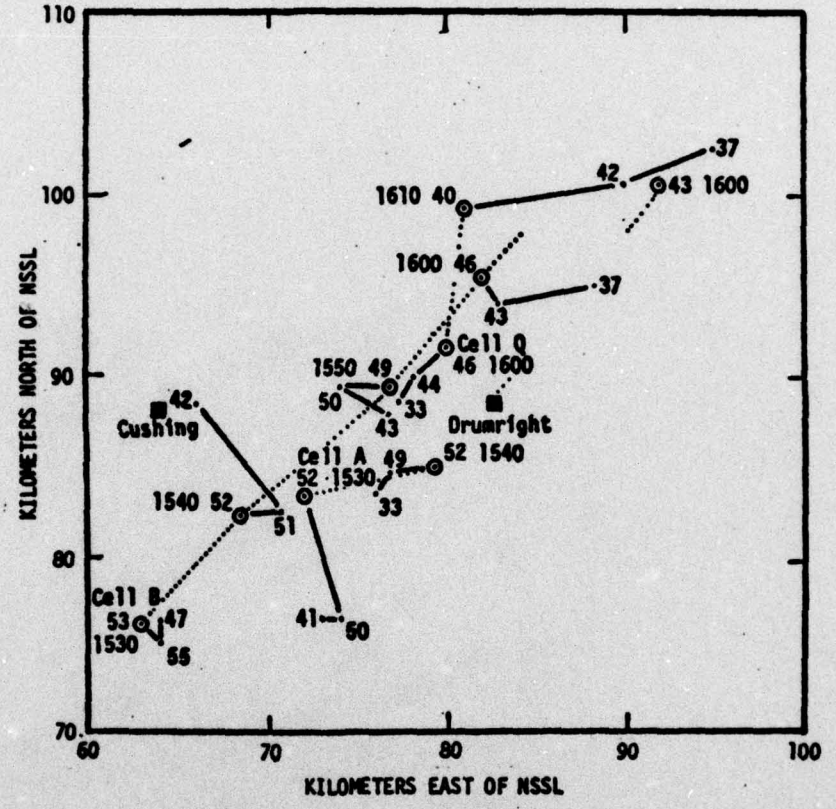

Fig. 27. PVSZ centers for the Drumright storm on 8 June 1974.

Cell B displayed no unusual movement as it progressed northeast at 16 m sec^{-1} along with other cells in the system. Although Figure 28, the TVSZ analysis summary, shows that the TVSZ value of Cell B decreased steadily in magnitude, the BWER and hook echo remained visible in the digital analyses. However, the 4-km reflectivity gradient around the

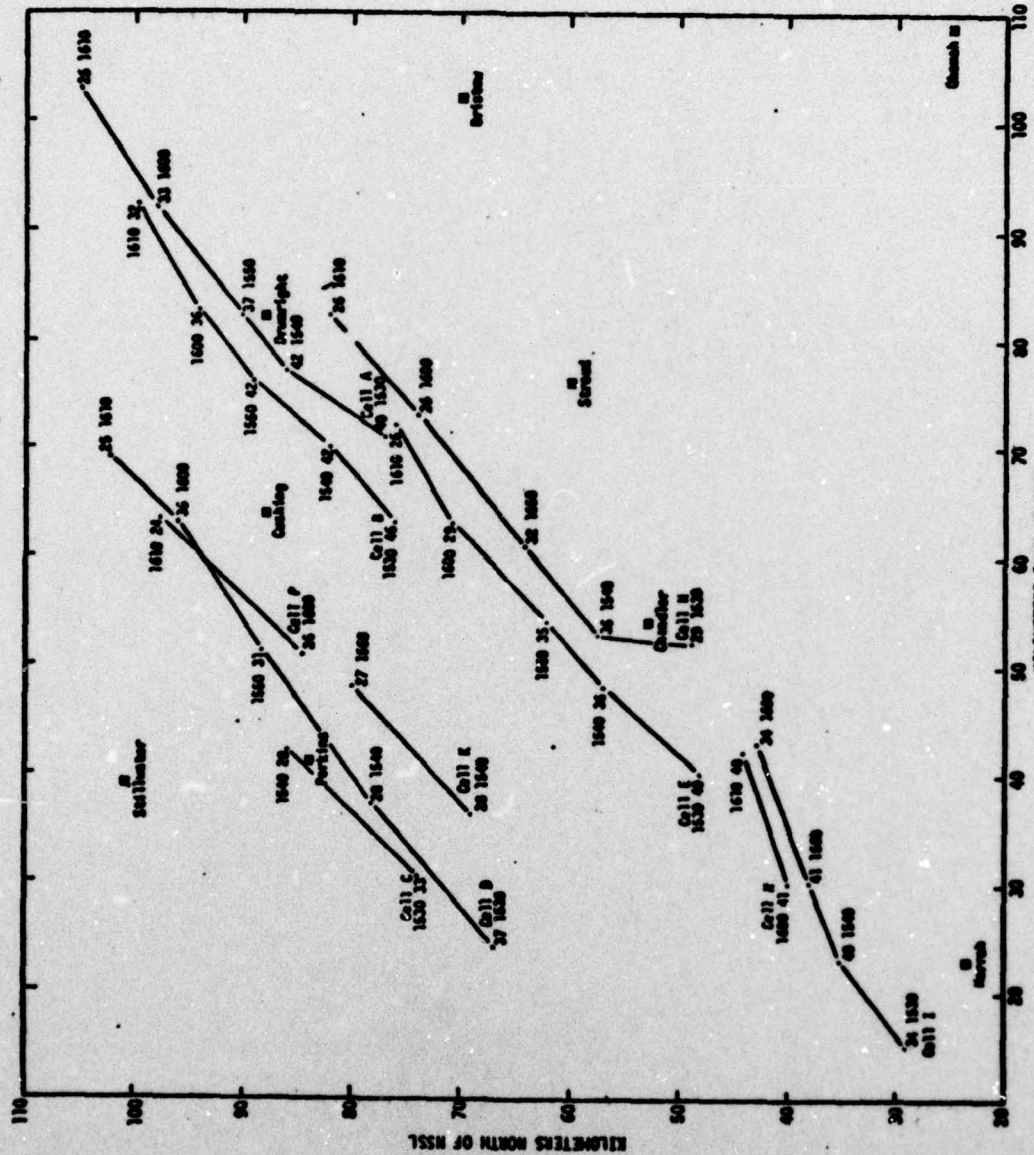

Fig. 28. TVSZ centers for the Drumright storm on 8 June 1974.

BWER decreased from 36 dbz at 1530 CST (see Figure 26) to 24 dbz (41 dbz to 17 dbz) at 1550 CST, as shown in Figure 29.

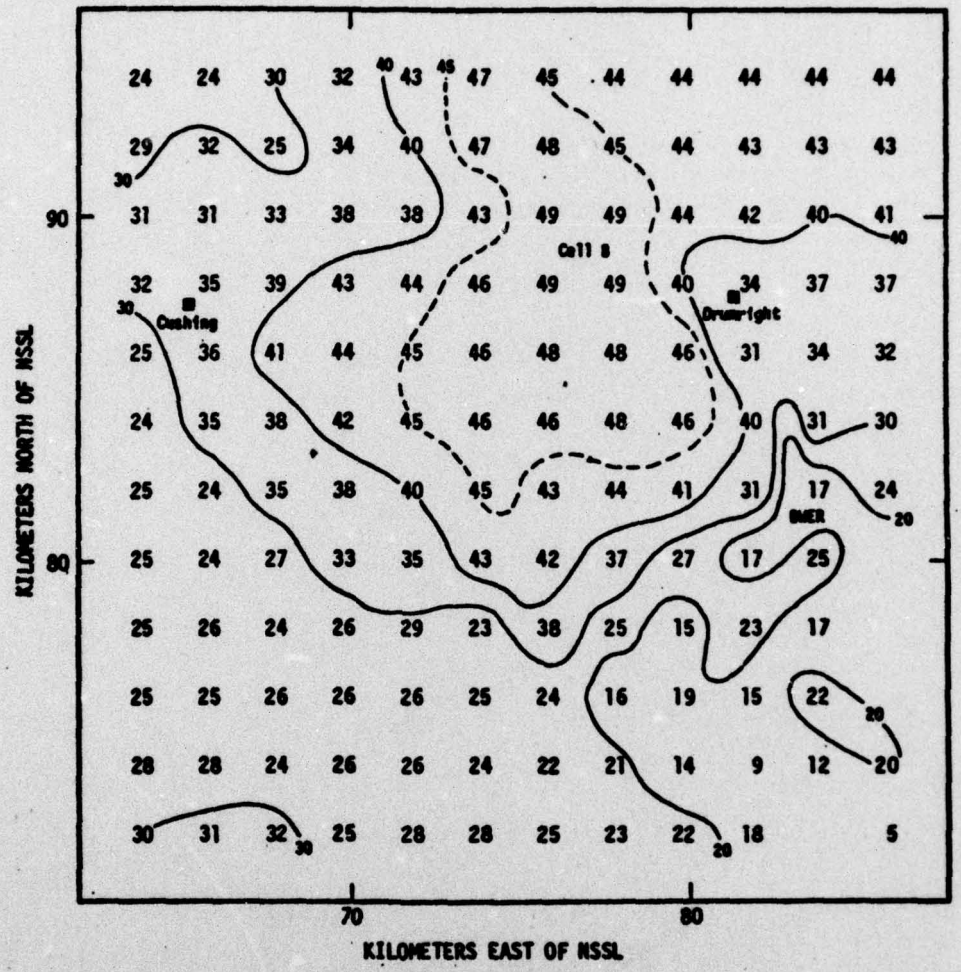

Fig. 29. Lower PVSZ map for 1550 CST, 8 June 1974. Isopleths of reflectivity in dbz.

At 1556 CST, the tornado touched down 8 km southwest of Drumright. The only observable changes in the storm between 1550 CST (before the tornado as shown in Figure 29) and 1600 CST (after the tornado as shown in Figure 30) were a further decrease in the 4-km reflectivity gradient to 22 dbz and the development of a cell, called Cell Q, on the southern

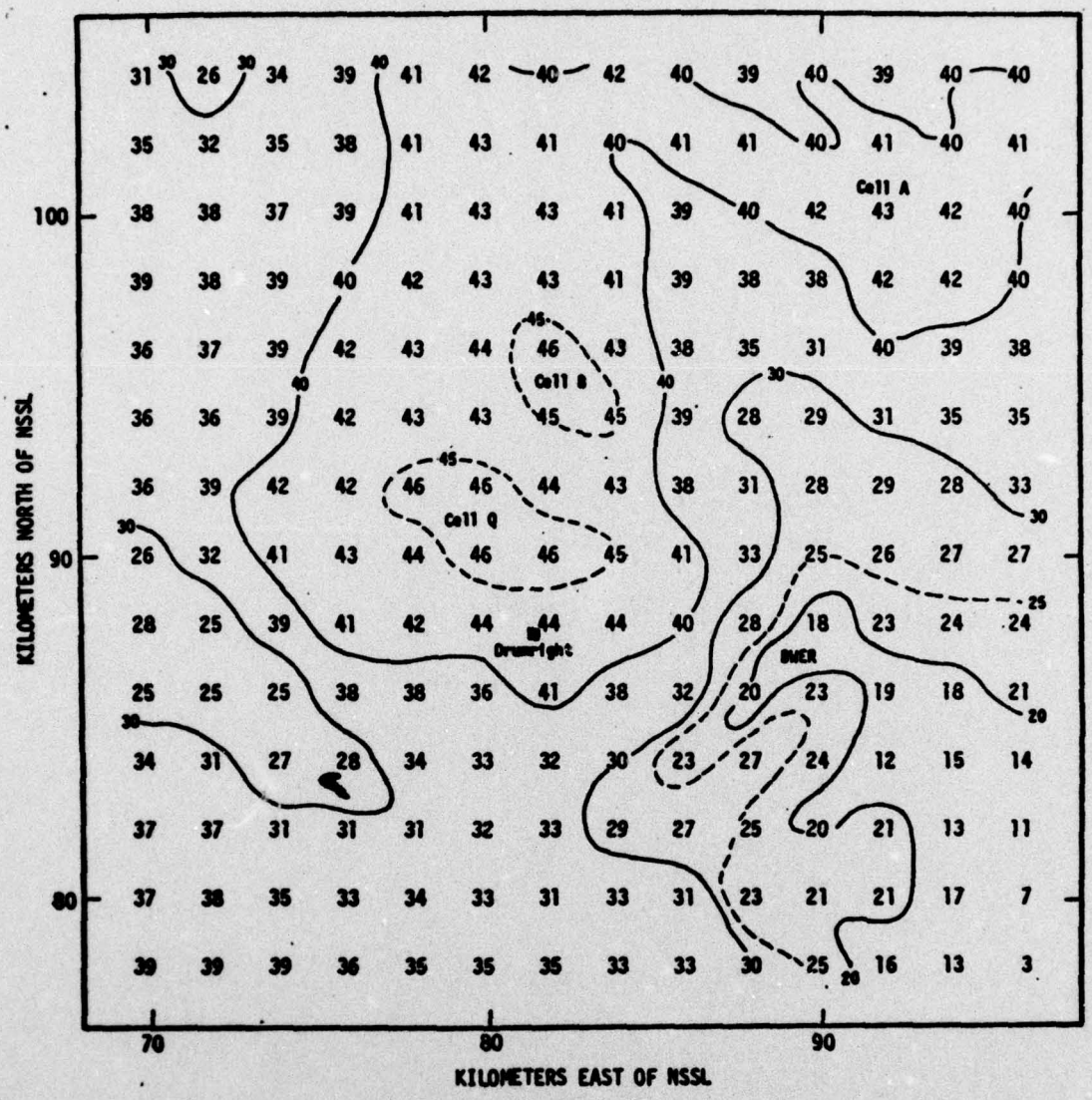

Fig. 30. Lower PVSZ map for 1600 CST, 8 June 1974. Isopleths of reflectivity in dbz.

flank of Cell B. Neither the tilt of Cell B nor that of Cell Q was over the BWER, the nearest being Cell B, tilted 6 km to the north, nor were the tilts of the cells the same, as is shown in Figure 27, Cell B being easterly, Cell Q being southwesterly.

By 1610 CST, the BWER and hook had dissipated; however, another

BWER and hook had formed on the southwestern edge of Cell Q as shown in Figure 31. The tornado remained on the ground and struck the town of Olive at 1620 CST. At this time, a power failure at NSSL caused a disruption in data collection which made a further analysis of this storm system impossible.

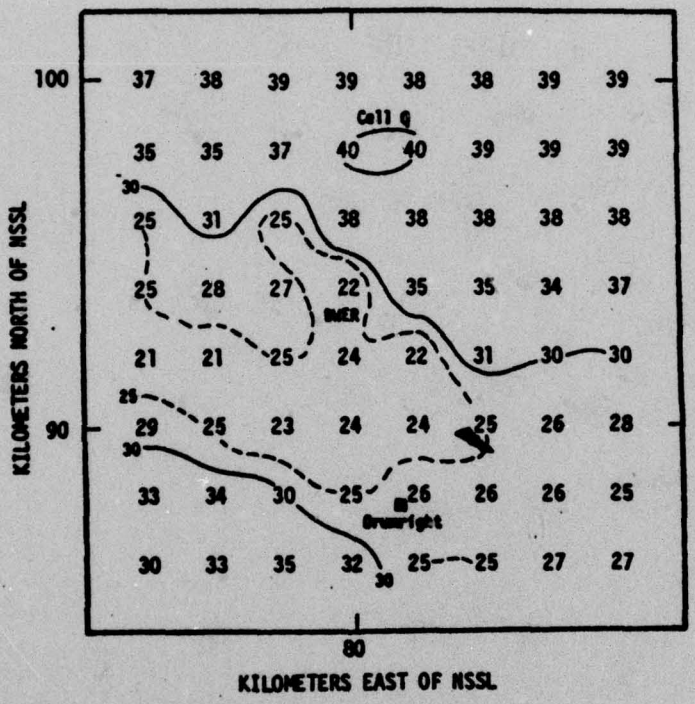

Fig. 31. Lower PVSZ map for 1610 CST, 8 June 1974. Isopleths of reflectivity in dbz.

Evaluation

For this case study, the BWER associated with the tornado was present for at least 25 min before the tornado. Although the BWER had dissipated by 1610 CST, another one had formed so that the characteristic was still present. The tilt of Cell B was never over the BWER but was as close as 6 km at 1600 CST, shortly after the tornado touched down.

Most cells in the central Oklahoma area on this afternoon maintained a rotational wobbling tilt like that of Cell B, rather than a relatively constant tilt as in the Yukon storm case. This wobble was noted by Canipe [1973] in several of his case studies. Tornadic activity was indicated whenever the tilt of the cell became vertical or was in the direction of the BWER. This tilt correlation is excellent in this case, for a large funnel cloud was sighted at 1530 CST when the tilt was vertical, and a tornado was reported at 1600 CST when the tilt was toward the BWER. By 1610 CST, however, Cell B was no longer visible in the lower PVSZ (see Figure 31) and the tilt of Cell Q was away from the newly-formed BWER. Burgess [1976], in his storm damage analysis, does indicate that the tornado was still on the ground at 1610 CST. No explanation of this deviation from Canipe's characteristics is available.

Upper-level mass changes, revealed by upper PVSZ changes (see Figure 27), indicate that a decrease of 5 dbz took place after the funnel was spotted at 1530 CST. Another decrease of 5 dbz occurred as the tornado touched down, just as predicted by Greene [1971] and Canipe [1973]. The TVSZ analysis summary, Figure 28, shows a steady decrease in TVSZ values. This is just the opposite of that expected by Greene. Thus, excluding the TVSZ values, Canipe's characteristics were present for the funnel at 1530 CST and the tornado at 1600 CST, but the characteristics were not present at 1610 CST. Whether this was a brief exception or a precursor of the lifting of the tornado, as it did briefly around 1615 CST [Burgess, 1976], is unknown due to the power failure at NSSL.

Just as in the case of the Yukon storm, other BWERs were present. Figure 32 shows one that formed southeast of Cell E (see Figure 28). The

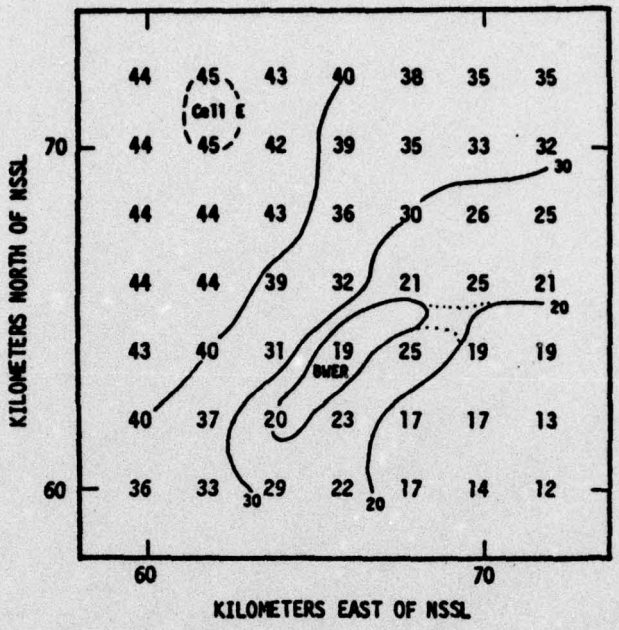

Fig. 32. Lower PVSZ map for 1600 CST, 8 June 1974 for Cell E. Isopleths of reflectivity in dbz.

4-km reflectivity gradient of 21 dbz is just 1 dbz less than the gradient shown in Figure 30. In fact, if the 20 dbz isopleth in Figure 32 is connected by the dots rather the solid line, the hook and BWER look almost identical to those in Figure 30. Further, the tilt of Cell E, which rotates cyclonically as Cell B, is just 6 km north of the BWER at 1600 CST, the time of Figure 32.

The Harrah Storm

The cell producing the Harrah tornado at 1555 CST, moved into full radar view only moments before at 1550 CST. The storm appeared to have none of Canipe's severe-storm characteristics. Figure 33, the lower PVSZ analysis for the area at 1600 CST, shows neither a hook nor a BWER in the conventional position relative to Cell R and the tornado; how-

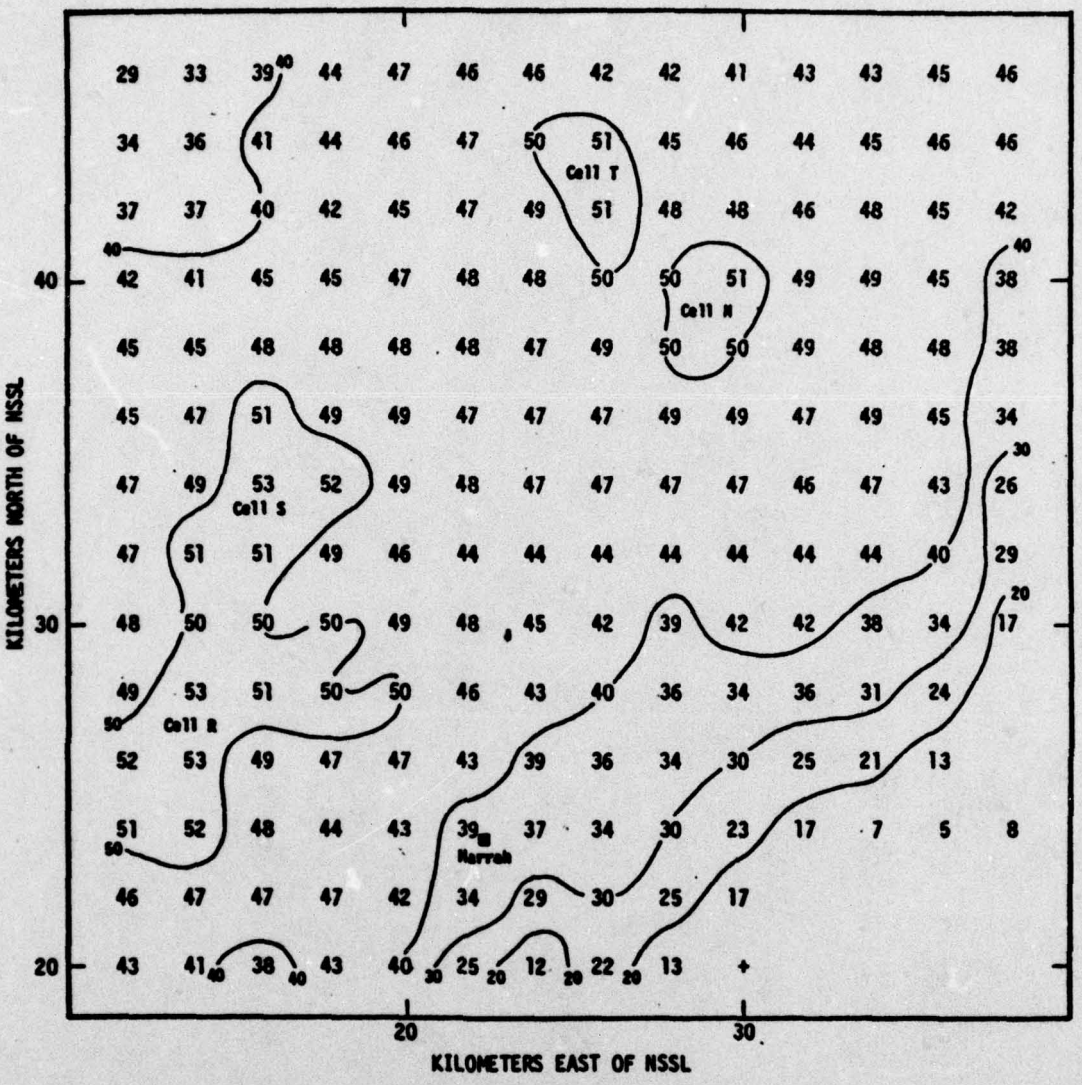

Fig. 33. Lower PVSZ map for 1600 CST, 8 June 1974 for Harrah storm. Isopleths of reflectivity in dbz.

ever, the 20 dbz isopleth near the bottom of the figure may be a portion of a BWER or hook echo, the remainder of which is hidden by the Oklahoma City ground clutter which extends to just south of the map. In any case, the hook-tornado-cell relationship would have to be quite different from that seen in the Yukon and Drumright storms.

Case Study of the Storms on 13 June 1975

Air Mass and Wind Structure

The synoptic conditions in Oklahoma for the early evening of 13 June 1975 are presented in Figure 34. Although no frontal zone was present, a weak trough was pushing into western Oklahoma as a result of an upper level trough moving through the area. Thunderstorms, which broke out ahead of the trough in early afternoon, developed into an area covering most of Oklahoma by early evening as shown in Figure 35. The thunderstorms generally were grouped in pockets of intense activity which moved very slowly to the southeast at 10 m sec^{-1}. A moderate low-level jet to the east of NSSL was carrying moist Gulf air northward while dry air from New Mexico was carried eastward over the entire area by a strong jet at mid-levels. The winds aloft for Oklahoma City at 1800 CST, 13 June 1975, shown in Table 4, show this jet near 10 kft with a speed of approximately 15 m sec^{-1}.

TABLE 4. Wind Data for Oklahoma City at 1800 CST, 13 June 1975.

Height (kft)	sfc	6	10	18	24	30	34	38	44
Wind (deg/m sec^{-1})	180/06	205/11	270/14	290/15	290/14	320/10	335/10	325/17	285/22

Lower PVSZ average wind = 220/10
Mid PVSZ average wind = 310/12
Upper PVSZ average wind = 305/20

Severe Storm Events

Thunderstorms developed in early afternoon with a few cells growing

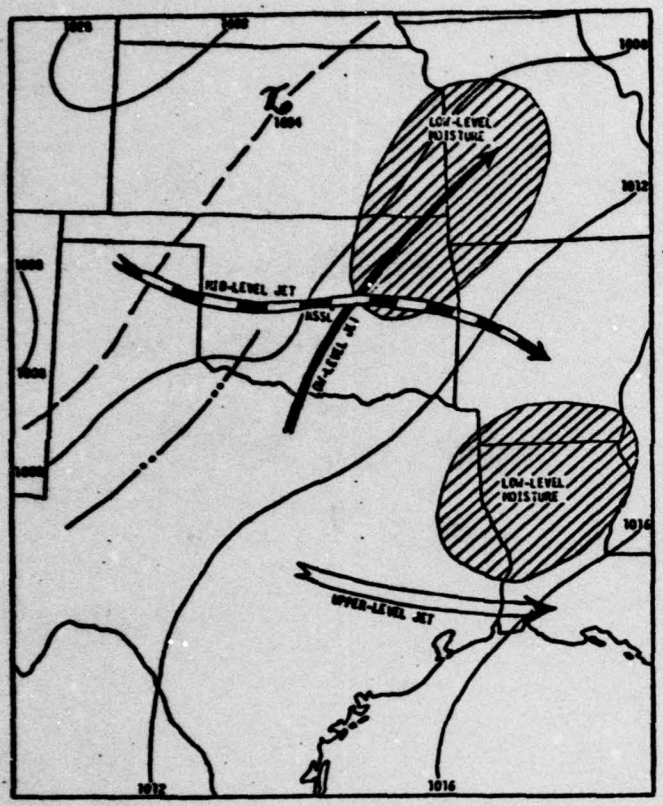

Fig. 34. Synoptic conditions for 1800 CST, 13 June 1975

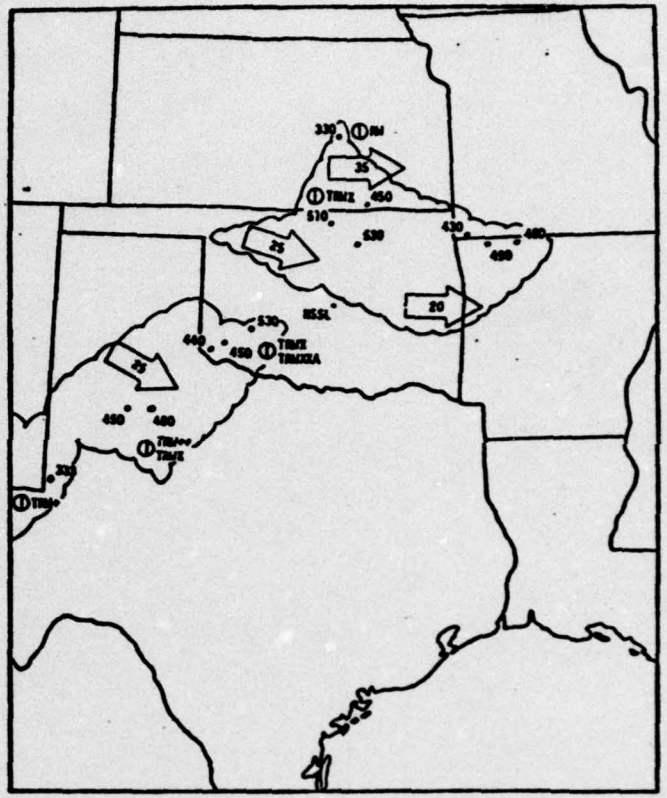

Fig. 35. Radar summary for 1735 CST, 13 June 1975

to severe intensity. At 1430 CST, golfball-size hail was reported at the Stillwater airport, 108 km north-northeast of NSSL. Hail, up to 2 in. in diameter, was reported in north-central Oklahoma near Medford at 1700 CST. The southwestern-most cell in this system continued to develop and a tornado touched down at 1733 CST in northwest Stillwater. It traveled across the city, lifting some 10 min later in the southeastern outskirts. The tornado damaged numerous homes and destroyed 20 trailers in a mobile home park. Only six people were injured and no one was killed.

As the area of development moved southeastward, a tornado, which damaged two homes, was reported near Kendrick (90 km northeast of NSSL) at 1845 CST. At 1712 CST, a cell, trailing the one near Kendrick, spawned a tornado which touched down only 6 km southeast of the first. This storm carried a haybailer about 1/4 mi and destroyed a concrete block garage. Isolated occurrences of hail were reported later in the evening near Tulsa.

History of the Stillwater Storm

The cell spawning the tornado at Stillwater, called Cell A, moved into full radar view at 1630 CST. As the cell moved southeast at 10 m sec^{-1}, as shown in Figure 36, its TVSZ value remained almost constant, as did its tilt to the south, shown in Figure 37, the PVSZ analysis summary for Cell A. At 1730 CST, 3 min before the tornado touched down, a weak BWER and hook echo developed west of Cell A as shown in

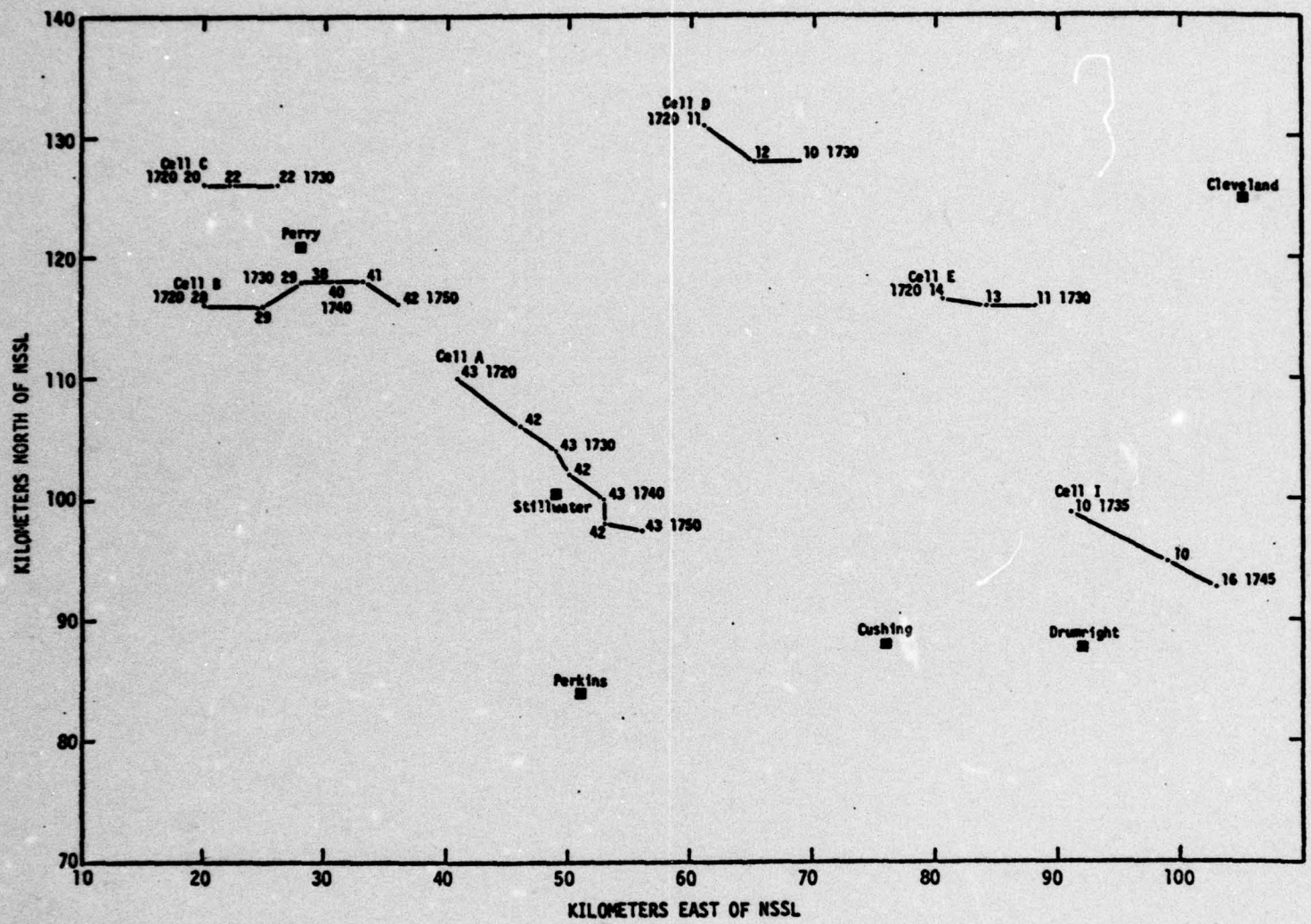

Fig. 36. TVSZ centers for the Stillwater storm on 13 June 1975.

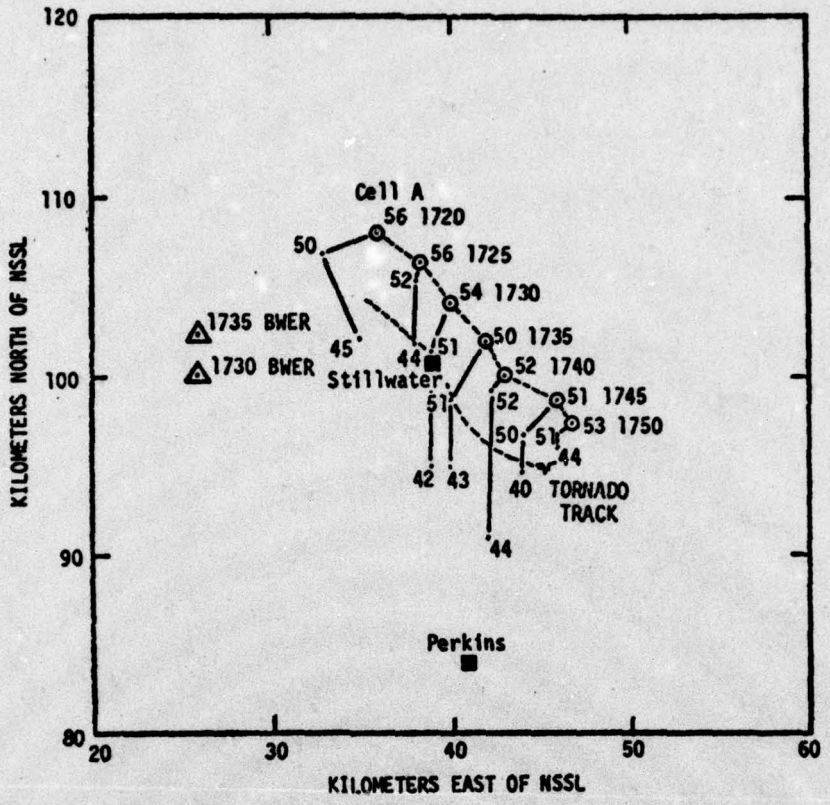

Fig. 37. PVSZ centers for the Stillwater storm on 13 June 1975.

Figure 38. The 4-km reflectivity gradient around the BWER was only 18 dbz (19 dbz in the BWER to 37 dbz). Figure 39 shows the BWER-Cell A relationship 5 min later (1735 CST) while the tornado is on the ground in Stillwater. By 1740 CST (3 min before the tornado lifted), the BWER had dissipated.

Evaluation

Although a BWER was present during the tornado, its positional relationship was unlike any other storm described previously (or any described by either Canipe [1973] or Greene [1971]). The classic

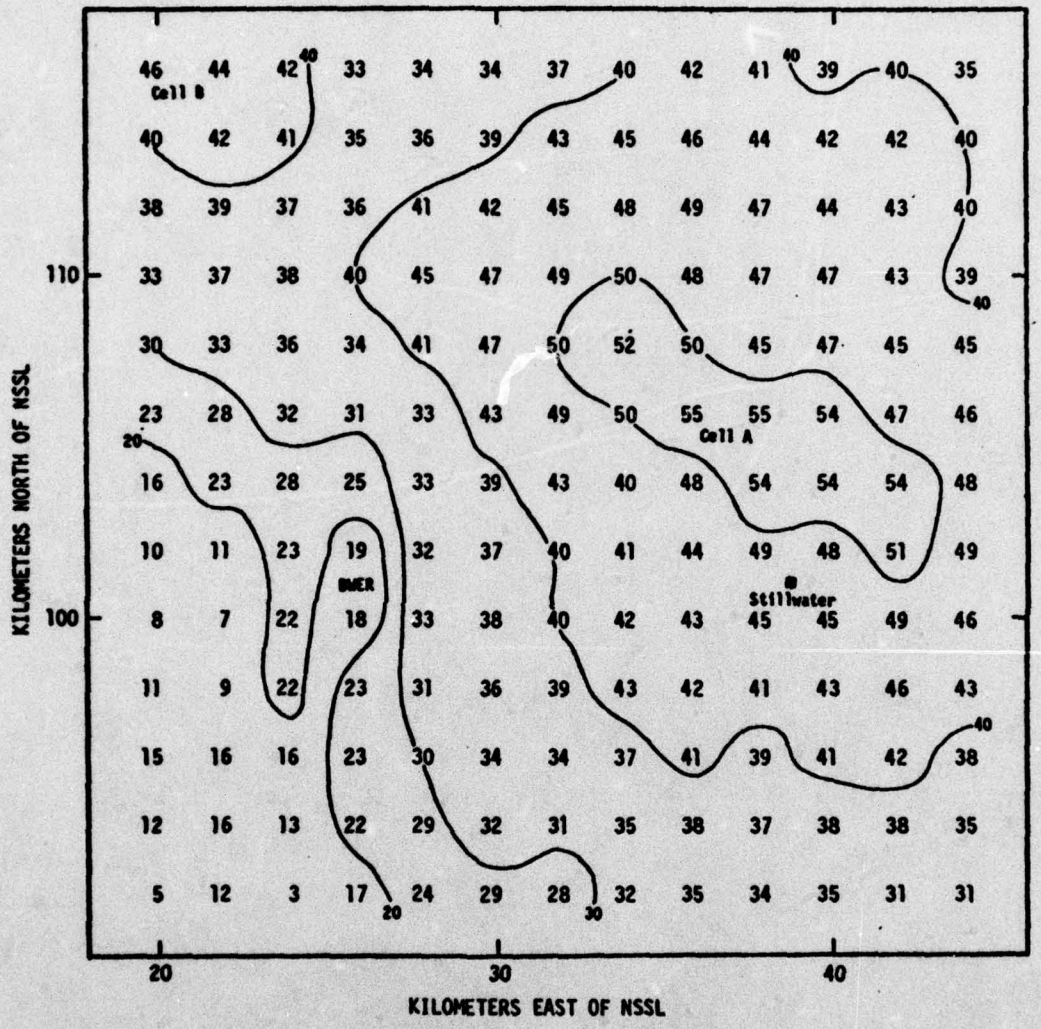

Fig. 38. Lower PVSZ map for 1730 CST, 13 June 1975. Isopleths of reflectivity in dbz.

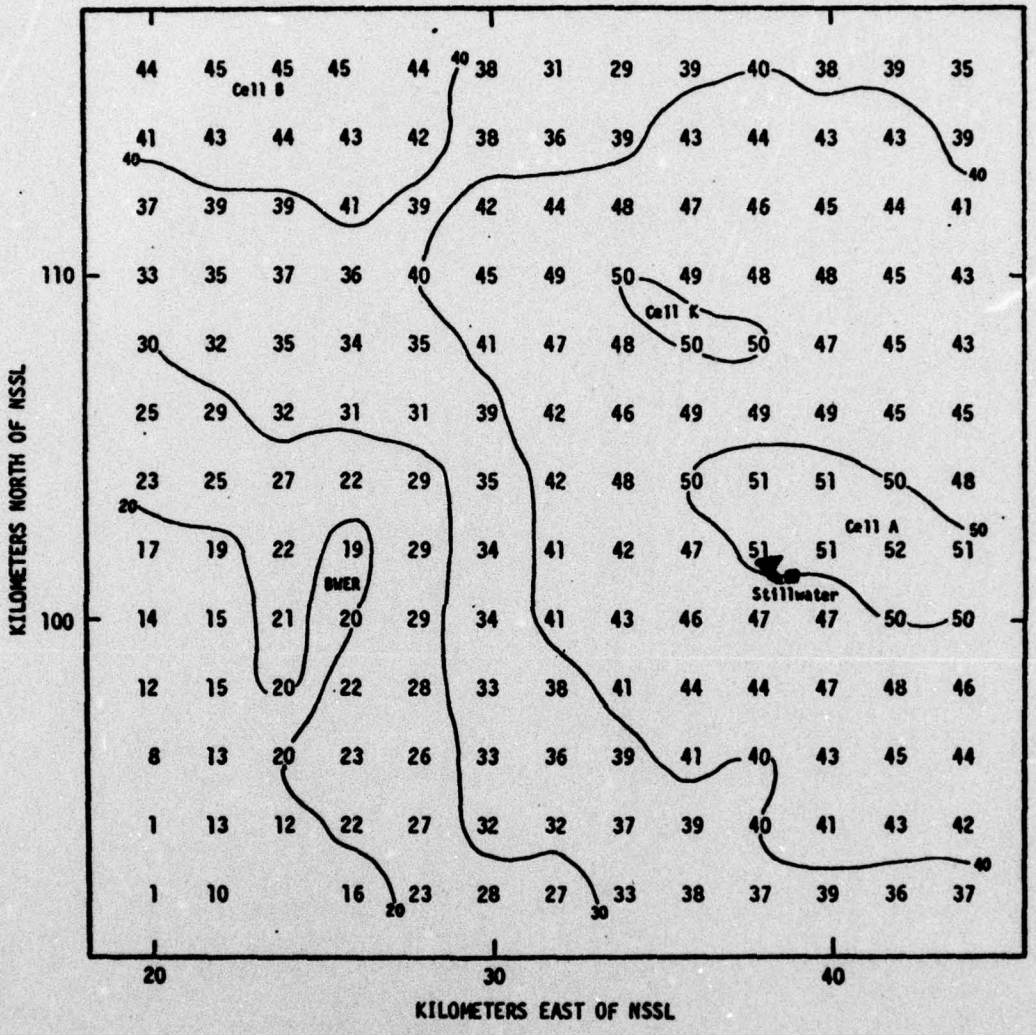

Fig. 39. Lower PVSZ map for 1735 CST, 13 June 1975. Isopleths of reflectivity in dbz.

eastward-moving cell, with the BWER to the southeast and the tornado to the southwest, was not present; instead, a super-cell of the type described by Marwitz [1972], with the tornado located very near the cell's center (see Figure 39), evolved. While the BWER was present, the tilt of Cell A was not toward the BWER but almost 90 deg to it, the closest point being 13 km to the east at 1730 CST (see Figure 37). Furthermore, the 4-km reflectivity gradient was 18 dbz, only 4 dbz less than that of the false BWER identifier near Cell E in the Drumright storm (see Figure 32). There were no noticeable changes in TVSZ values and the upper PVSZ values, reflecting changes in mass, showed no marked decrease at 1725 CST or 1730 CST, but rather a steady decline through 1730 CST and then a sudden decrease from 44 dbz to 40 dbz as the tornado dissipated. No other BWERs were present in any of the other cells in the system. It is apparent that Canipe's technique for the identification of tornadoes does not work well with this type of storm.

CHAPTER IV

CONCLUSIONS AND RECOMMENDATIONS

Conclusions

The objective of this investigation has been to determine the accuracy and operational usefulness of a proposed method for tornado identification from the use of analyses of digital radar data. Three cases involving several tornadoes were evaluated by using the identification techniques described by Canipe [1973]. The study led to the following conclusions.

1) Although Table 11 of Canipe's study shows his technique to be 100 per cent accurate in identifying tornadoes, results from this investigation show the method to be less than 100 per cent accurate. Some of the following specific conclusions concerning Canipe's technique are presented in support of this statement.

2) The BWER is always present when a tornado or funnel cloud is reported. It generally forms before the tornado touches ground and dissipates shortly before the tornado lifts. Although no BWER was found in the Harrah storm, the BWER may have been hidden in the ground clutter or inside the radar coverage.

3) BWERs are present not only during tornadoes but at other times also. Further, the 4-km reflectivity gradient surrounding the BWER, which may be used as a measure of the BWER intensity, frequently is the same for cells that produce tornadoes as for those that do not. Therefore, while neither the occurrence nor magnitude of the BWER is a

positive identifier of a tornado, the occurrence can be used as a high probability identifier.

4) The tilt of the core of reflectivity, if not vertical, is not always toward the BWER, as shown in the Stillwater storm. However, the Yukon and Drumright storms did have a tilt over or toward the BWER and, therefore, the tilt can be used as a high-probability identifier.

5) The values of TVSZ revealed only one occurrence of explosive development and, therefore, a poor correlation with tornado occurrences. This conclusion was just as anticipated by Vogel [1973].

6) In two out of three cases (Stillwater being the exception), the upper PVSZ values decreased as the tornado touched down, just as predicted by Canipe [1973]. Table 5 is a summary of the observed characteristics of each storm.

TABLE 5. Summary of Observed Characteristics

Storm	Date	Approx. Time(CST)	BWER w/ Parent	Satellite Present	BWER w/ Satellite	Tilt	Upper Level Mass Change	Explosive Development	Reported Event
Yukon	23 May 1974	1730	No	Yes	Yes	Toward BWER	---------	No	Tornado
Cell E	23 May 1974	1810	No	Yes	Yes	Downwind	Decreased	No	None
Cell H	23 May 1974	1810	Yes	No	No	Downwind	Constant	No	None
Drumright	8 June 1974	1530	Yes	No	No	Vertical	Decreased	Yes	Funnel
	8 June 1974	1555	Yes	No	No	Toward BWER	Decreased	No	Tornado
Cell E	8 June 1974	1600	Yes	No	No	Toward Shear	Decreased	No	None
Harrah	8 June 1974	1555	?	No	No	Downwind	---------	---	Tornado
Stillwater	13 June 1975	1730	Yes	No	No	45 deg right of wind	Constant	No	Tornado

Several conclusions also were reached concerning the use of Canipe's technique on an operational basis.

1) PVSZ analyses do provide a rapid, simple tool for evaluating the structure and relative intensity of cells in a storm system. The method of summing reflectivities in depth and then converting the total to dbz for display is superior to previous methods in that it retains small-scale features such as the BWER and hides few signatures present in the individual CAZMs. The method also takes less computer-processing time (and hence less money) than the liquid-water conversion method employed by Canipe [1973].

2) A computer analysis of storm tilt could be very difficult to achieve in complex storm situations. Middle- and upper-level PVSZ maxima frequently exhibit a pattern quite different from that found in the lower PVSZ map. Two or three lower PVSZ maxima appear to merge into one centrally-located mid-level maximum. This makes the correlation of a mid-level PVSZ maximum to its low-level counterpart a difficult task, particularly for a computer and its programmer.

3) Since all BWERs do not indicate the presence of a tornado, an attempt was made to ascertain whether those associated with tornadoes exhibited some unique characteristic. Possibilities, such as a limiting maximum value of the reflectivity in the BWER, a limiting minimum value of the reflectivity of the nearest cell, and a limiting minimum value of the reflectivity difference over a 4-km radius area around the BWER, were examined. No conclusion can be drawn due to the limited number of case studies; however, for informational purposes, the maximum value in the BWER appears to be no greater than 22 dbz, the maximum reflectivity value of the nearest cell appears to be at least 46 dbz, and the 4-km reflectivity gradient around the BWER appears to be at least

18 dbz. Further, extreme caution must be exercised when using these values, as BWERs not associated with tornadoes approached, or in one case exceeded, these limits.

Recommendations

The following recommendations are made concerning the tornado identification technique.

1) Additional storm cases in Oklahoma should be studied to determine statistically the accuracy of this identification technique and how its accuracy compares to other presently-used methods, including doppler radar.

2) The additional storm case studies also should be used to determine whether the limiting values placed on the BWER can be refined statistically.

3) Storm cases from southern areas such as Texas and the Gulf states should be examined to determine the applicability of this technique to those locations.

The following recommendations are made concerning the processing of digital radar data.

1) The mixed 6-bit and 8-bit word-length method for storing digital radar data on tape, presently employed by NSSL, should be abandoned in favor of the previously-used 8-bit method due to incurred increased cost of retrieval from the mixed word-length tapes (approximately three times that of the older system).

2) Action should be taken by NSSL to reduce excessive noise appearing in the tapes which would be difficult to handle in an automatic

computerized identification technique.

3) Radar range markers frequently appear in the digital data. They must be eliminated as the markers induce erroneously high values of reflectivity along their path.

4) A simpler program requiring less computer core space must be developed before a mini-computer can be used to provide real-time displays, either via a printer or a cathode ray tube.

Concluding Remarks

It has been the purpose of this investigation to determine whether tornadoes produce a unique signature in analyses of digital radar data. No unique identifying signature was found, but rather a combination of features which indicate the presence of a tornado with a high probability. Additional studies are required to determine the precise probability. The author believes that work should continue in this area and that techniques should be developed to make this type of identification technique an operational reality.

REFERENCES

Battan, L. J., Radar Meteorology, 161 pp., University of Chicago, 1959.

_____, Radar Observation of the Atmosphere, 324 pp., University of Chicago, 1973.

Bensch, R. R., The circulation of a tornado cyclone as revealed by single doppler radar and chaff, Proc. 9th Severe Local Storms Conf., pp. 91-95, Boston, 1975.

Bigler, S. G., An analysis of tornado and severe weather echoes, Proc. 5th Radar Meteorol. Conf., pp. 167-175, Boston, 1955.

Boyd, E. I., and D. J. Musil, Radar climatology of convective storms in western Nebraska, Proc. 14th Radar Meteorol. Conf., pp. 429-432, Boston, 1970.

Brandes, E. A., The use of digital radar data in severe storm detection and prediction, Proc. 15th Radar Meteorol. Conf., pp. 45-58, Boston, 1972.

_____, Severe thunderstorm flow characteristics revealed by dual-doppler observations: 6 June 1974, Proc. 9th Severe Local Storms Conf., pp. 85-90, Boston, 1975.

Browning, K. A., and F. H. Ludlam, Airflow in convective storms, Quart. J. Roy. Meteorol. Soc., 88, 117, 1962.

Burgess, D. B., Unpublished storm damage survey and analysis for the National Severe Storms Laboratory, 1976.

Canipe, Y. J., Temporal variability in intensity-height profiles of a severe storm using digital radar data, M. S. Thesis, Texas A&M University, College Station, 78 pp., 1972.

_____, On the structure and development of severe local storms as revealed by digital radar observations, Ph. D. Dissertation, Texas A&M University, College Station, 142 pp., 1973.

Chisholm, A. J., The radar and airflow structure of Alberta hailstorms, Proc. 14th Radar Meteorol. Conf., pp. 35-42, Boston, 1970.

Donaldson, R. J., Methods for identifying severe thunderstorms by radar: a guide and bibliography, Bull. Amer. Meteorol. Soc., 46, 174, 1965.

Foote, G. B., C. G. Wade, and K. A. Browning, Air motion and hail growth in supercell storms, Proc. 9th Severe Local Storms Conf., pp. 444-451, Boston, 1975.

Greene, D. R., Numerical techniques for the analysis of digital radar data with applications to meteorology and hydrology, Ph. D. Dissertation, Texas A&M University, College Station, 124 pp., 1971.

Lemon, L. R., D. W. Burgess, and R. A. Brown, Tornado production and storm sustenance, Proc. 9th Severe Local Storms Conf., pp. 100-104, Boston, 1975.

Marshall, J. S., The constant-altitude presentations of radar weather patterns, Proc. 6th Radar Meteorol. Conf., pp. 321-324, Boston, 1957.

Marwitz, J. D., The structure and motion of severe hailstorms. Part I: Supercell storms, J. Appl. Meteorol., 11, 166, 1972.

_____, and E. X. Berry, The airflow within the weak echo region of an Alberta hailstorm, J. Appl. Meteorol., 10, 487, 1971.

McCarthy, J., G. M. Heymfield, and L. G. Tidwell, Evolution of a tornadic cyclone as seen by dual-doppler, instrumented airplane and chaff, Proc. 9th Severe Local Storms Conf., pp. 389-395, 1975.

Muench, H. S., Use of digital radar data in severe weather forecasting, Bull. Amer. Meteorol. Soc., 57, 298, 1976.

Penn, S., C. Pierce, and J. K. McGuire, The squall line and Massachusetts tornadoes of June 9, 1953, Bull. Amer. Meteorol. Soc., 36, 109, 1955.

Phillips, J. F., Cloud structure from defense meteorological satellite data, M. S. Thesis, Texas A&M University, College Station, 142 pp., 1975.

Probert-Jones, J. R., The radar equation in meteorology, Quart. J. Roy. Meteorol. Soc., 88, 485, 1962.

Rinehart, R. E., D. Atlas, and P. J. Eccles, Meteorological interpretation of doppler radar data in a hailstorm, Proc. 16th Radar Meteorol. Conf., pp. 73-78, Boston, 1975.

Vogel, J. E., Applications of digital radar in the analysis of severe local storms, M. S. Thesis, Texas A&M University, College Station, 94 pp., 1973.

Wilk, D. E., W. L. Watts, D. W. Sirmans, R. M. Lhermitte, E. Kessler, and K. C. Gray, Weather radar data systems at the National Severe Storms Laboratory, Proc. 5th Radar Meteorol. Conf., pp. 14-23, Boston, 1967.

Wilk, D. E., and K. C. Gray, Processing and analysis techniques used with NSSL weather radar systems, Proc. 14th Radar Meteorol. Conf., pp. 369-374, Boston, 1970.

_____, and E. Kessler, Quantitative radar measurements of precipitation, Meteorol. Monographs, 11, Boston, 1970.

Wilson, J. W., Severe storm identification with the WSR-57, Proc. 14th Radar Meteorol. Conf., pp. 60-62, Boston, 1971.

APPENDIX A

This appendix contains the format used by NSSL for recording digital radar data during the years 1974 and 1975. Both Appendix A and Appendix B are provided as an aid to investigators who may choose to work at some future time with the type of NSSL data used in this thesis. It is hoped that by listing the actual program used in this investigation, other researchers will find this documentation adequate as a starting point for their work.

MASTER MAGNETIC TAPE
RADAR DIGITAL ENCODER
RECORD FORMAT
1974-1975

FIRST RECORD OF EACH PPI SECTOR

Characters	Fortran Specification	Legend
1-6	I6	Date (month-day-year)
7-12	I6	Time (CST)
13-15	F3.1	Tilt
16-21	F6.3	Delay in kilometers
22-27	F6.3	Gate length in kilometers
28-30	I3	Beginning azimuth
31-33	I3	Ending azimuth
34-37	I4	Normalization range in kilometers (zero entry indicates no normalization)
38	I1	Hardware normalization if one
39	I1	Anomalous propagation*
40	I1	Interference*
41	I1	Time constant
42-44	I3	Antenna rotation time in seconds
45-47	F3.1	Horn noise (dB)
51-306	64F4.1	Calibrations (dB)
307-309	I3	Number of missing radials
310-438	NI3	Azimuths of missing radials
Data records follow		* Zero entry indicates undetermined
Tapes are 7 track, 556 BPI, odd parity, binary		

DATA RECORDS OF EACH PPI SECTOR

Data records on the 1975 archived WSR-57 radar data tapes are 438 character long and contain two radials of information each. The format is:

First Radial

col	1-200	200 Data Gates (0-63) (6 binary bits/gate)
	201-203	Azimuth
	204-205	Elevation Angle
	206	STC 1=on 0=off
	207-209	Julian Day
	210-215	Time (CST) HHMMSS
	216-217	Delay Code
	218	Gate Length Code
	219	Time Constant Code

Second Radial

220-419	200 Data Gates
420-422	Azimuth
423-424	Elevation Angle
425	STC 1=on 0=off
426-428	Julian Day
429-434	Time (CST) HHMMSS
435-436	Delay Code
437	Gate Length Code
438	Time Constant Code

Immediately following the last radial in the PPI sector, a special flag radial will appear in either the "left" or "right half" of the current record. This radial consists of 200 gates of calibration information* and 19 columns of eight's where the housekeeping would normally appear. For example, if the last data radial appeared in column 220-438 (right half) then the next record would look like:

col	1-200	Calibration 64F3.1 **
	201-219	Eight's
	220-438	Nothing

If the last data radial appeared in columns 1-219 (left half), the record would look like:

col	1-200	Data
	201-219	Housekeeping
	220-419	Calibration 64F3.1 **
	420-438	Eight's

Immediately following the last record of the last PPI sector on the tape, there is a record containing 438 nines, and then an END-OF-FILE.

* Calibration adjusted according to Sirmans. See NSSL Tech Memo 64. Does not apply to 1974 tapes.

** Calibration values are recorded MOD 100; i.e., if actual value is 104.5, recorded value is 4.5.

APPENDIX B

This appendix contains the program used to read the tapes, produce the digital analysis, and print the resultant maps. The program is a highly modified version of that used by Phillips [1975] and is based on the algorithms developed by Greene [1971].

START MAIN PROGRAM
THIS PROGRAM USES NSSL DIGITAL DATA FROM MAGNETIC TAPES FOR YEARS 1974 AND 1975.
THE PROGRAM WILL COMPUTE THE FOLLOWING

1. CAZMS - CONSTANT ALTITUDE REFLECTIVITY MAPS - MAY BE DETERMINED FOR EVERY 5000 FT FROM SURFACE TO 50000 FT. COVERS 100x100 KM GRID, DATA PRINTED IN 2 KM INTERVALS. STATEMENT 156 CONTROLS THE CAZM PLOT SUBPROGRAM.
2. PVSZ - PARTIAL VERTICAL SUMMED REFLECTIVITY MAPS - MAY BE DETERMINED IN INCREMENTS OF 5000 FT. STATEMENT 160 CONTROLS THE LAYERS TO BE COMPUTED AND PLOTTED.
3. TVSZ - TOTAL VERTICAL SUMMED RELECTIVITY MAPS - PLOTTED AUTOMATICALLY.

THE FOLLOWING ARE PROGRAM LIMITATIONS DUE TO CORE AVAILABILITY.

1. HANDLES UP TO 160 DEGREES OF RAW DATA (ODD AZIMUTH DATA ONLY).
2. HANDLES UP TO 140 KM OF DATA (EVEN KM DATA ONLY).
3. HANDLES UP TO 12 ANTENNA ELEVATION ANGLES.

DEFINITIONS
ARRAYS
ZZ - CONTAINS REFLECTIVITY DATA VIA CODED AZIMUTH AND RANGE FOR FIRST TILT ANGLE AND SUBSEQUENT VERTICALLY INTERPOLATED CAZMS.
ZW - CONTAINS RAW RELECTIVITY DATA VIA CODED AZIMUTH, RANGE AND TILT.
Z - CONTAINS CAZM DATA IN X, Y COORDINATES. CONVERTED TO DBZ BEFORE PLOTTING.
VIZ - CONTAINS SUMMED REFLECTIVITY FOR PVSZ MAPS. CONVERTED TO DBZ BEFORE PLOTTING.
TVIZ - CONTAINS SUMMED DBZ FOR TVSZ.
CLASS - CONTAINS DECODED DATA FROM ONE DATA RECORD (FULL WORDS).
HWORD - CONTAINS RAW DATA FROM ONE RECORD (HALF WORDS).
CALIB - CONTAINS EQUIVALENT DBM VALVES FOR 64 DIGITAL INTEGERS NUMBERED 0 THRU 63.
TILT - CONTAINS THE ANGLE IN DEG FOR EACH TILT-ANGLE USED (12 MAX).
MSAZ - CONTAINS THE AZIMUTHS OF MISSING RADIALS OF INFORMATION.

FOR DATA CARDS
ILEFT - DISTANCE EAST OR WEST OF NSSL, IN EVEN KM, TO THE LOWER LEFT CORNER OF THE 100x100 KM GRID PLUS TWO. THEREFORE WEST - POSITIVE, EAST - NEGATIVE, (I.E. 80 WEST=+82, 80 EAST=-78).
JDOWN - DISTANCE NORTH OR SOUTH OF NSSL, IN EVEN KM, TO THE LOWER LEFT CORNER OF THE 100x100 KM GRID PLUS TWO. THEREFORE SOUTH - POSITIVE, NORTH - NEGATIVE, (I.E. 30 NORTH=-30+2=-28) GRID MUST BE LOCATED SO THAT NSSL IS NOT IN THE BOX.
KAZ - DESIRED STARTING DATA AZIMUTH TO LOAD GRID BOX (MOVING CLOCKWISE).
LASTAZ - LAST DATA AZIMUTH REQUIRED TO LOAD GRID BOX.
NTILT - NUMBER OF TILT-ANGLES TO BE READ.
KRANGE - DISTANCE, IN EVEN KM, TO THE NEAREST POINT OF THE GRID BOX MINUS 4 KM. REQUIRED AS ONLY 140 KM OF THE AVAILABLE 200 KM OF DATA CAN BE USED.
SKPBGN & SKPEND - NUMBER OF FIRST AND LAST RECORD TO BE SKIPPED ON DATA TAPE TO GET TO DESIRED DATA. IF NO RECORDS ARE TO BE SKIPPED, BOTH ARE LOADED WITH ZERO.

KII, KKII - CONSTANTS USED FOR CODING AZIMUTH PARAMETER FOR ZW ARRAY.
L - NUMERICAL COUNTER FOR TILT BEING USED. USED IN ZW ARRAY, INCREMENTS FROM 1 TO NTILT.
DATE, TIME, ANTILT, ETC. - DATA READ FROM HEADER. SEE APPENDIX A FOR EXPLANATION.

START MAIN PROGRAM
THIS PROGRAM USES NSSL DIGITAL DATA FROM MAGNETIC TAPES FOR YEARS 1974 AND 1975.
THE PROGRAM WILL COMPUTE THE FOLLOWING

1. CAZMS - CONSTANT ALTITUDE REFLECTIVITY MAPS - MAY BE DETERMINED FOR EVERY 5000 FT FROM SURFACE TO 50000 FT. COVERS 100x100 KM GRID, DATA PRINTED IN 2 KM INTERVALS. STATEMENT 156 CONTROLS THE CAZM PLOT SUBPROGRAM.
2. PVSZ - PARTIAL VERTICAL SUMMED REFLECTIVITY MAPS - MAY BE DETERMINED IN INCREMENTS OF 5000 FT. STATEMENT 160 CONTROLS THE LAYERS TO BE COMPUTED AND PLOTTED.
3. TVSZ - TOTAL VERTICAL SUMMED RELECTIVITY MAPS - PLOTTED AUTOMATICALLY.

THE FOLLOWING ARE PROGRAM LIMITATIONS DUE TO CORE AVAILABILITY.

1. HANDLES UP TO 160 DEGREES OF RAW DATA (ODD AZIMUTH DATA ONLY).
2. HANDLES UP TO 140 KM OF DATA (EVEN KM DATA ONLY).
3. HANDLES UP TO 12 ANTENNA ELEVATION ANGLES.

DEFINITIONS
ARRAYS
ZZ - CONTAINS REFLECTIVITY DATA VIA CODED AZIMUTH AND RANGE FOR FIRST TILT ANGLE AND SUBSEQUENT VERTICALLY INTERPOLATED CAZMS.
ZW - CONTAINS RAW RELECTIVITY DATA VIA CODED AZIMUTH, RANGE AND TILT.
Z - CONTAINS CAZM DATA IN X, Y COORDINATES. CONVERTED TO DBZ BEFORE PLOTTING.
VIZ - CONTAINS SUMMED REFLECTIVITY FOR PVSZ MAPS. CONVERTED TO DBZ BEFORE PLOTTING.
TVIZ - CONTAINS SUMMED DBZ FOR TVSZ.
CLASS - CONTAINS DECODED DATA FROM ONE DATA RECORD (FULL WORDS).
HWORD - CONTAINS RAW DATA FROM ONE RECORD (HALF WORDS).
CALIB - CONTAINS EQUIVALENT DBM VALVES FOR 64 DIGITAL INTEGERS NUMBERED 0 THRU 63.
TILT - CONTAINS THE ANGLE IN DEG FOR EACH TILT-ANGLE USED (12 MAX).
MSAZ - CONTAINS THE AZIMUTHS OF MISSING RADIALS OF INFORMATION.

FOR DATA CARDS
ILEFT - DISTANCE EAST OR WEST OF NSSL, IN EVEN KM, TO THE LOWER LEFT CORNER OF THE 100x100 KM GRID PLUS TWO. THEREFORE WEST - POSITIVE, EAST - NEGATIVE, (I.E. 80 WEST=+82, 80 EAST=-78).
JDOWN - DISTANCE NORTH OR SOUTH OF NSSL, IN EVEN KM, TO THE LOWER LEFT CORNER OF THE 100x100 KM GRID PLUS TWO. THEREFORE SOUTH - POSITIVE, NORTH - NEGATIVE, (I.E. 30 NORTH=-30+2=-28) GRID MUST BE LOCATED SO THAT NSSL IS NOT IN THE BOX.
KAZ - DESIRED STARTING DATA AZIMUTH TO LOAD GRID BOX (MOVING CLOCKWISE).
LASTAZ - LAST DATA AZIMUTH REQUIRED TO LOAD GRID BOX.
NTILT - NUMBER OF TILT-ANGLES TO BE READ.
KRANGE - DISTANCE, IN EVEN KM, TO THE NEAREST FOINT OF THE GRID BOX MINUS 4 KM. REQUIRED AS ONLY 140 KM OF THE AVAILABLE 200 KM OF DATA CAN BE USED.
SKPBGN & SKPEND - NUMBER OF FIRST AND LAST RECORD TO BE SKIPPED ON DATA TAPE TO GET TO DESIRED DATA. IF NO RECORDS ARE TO BE SKIPPED, BOTH ARE LOADED WITH ZERO.

KII, KKII - CONSTANTS USED FOR CODING AZIMUTH PARAMETER FOR ZW ARRAY.
L - NUMERICAL COUNTER FOR TILT BEING USED. USED IN ZW ARRAY, INCREMENTS FROM 1 TO NTILT.
DATE, TIME, ANTILT, ETC. - DATA READ FROM HEADER. SEE APPENDIX A FOR EXPLANATION.

```
ANTILT - ANENNA TILT ANGLE IN DEGREES
LVL - COUNTER USED FOR CAZM IDENTIFIER AND PLOT ROUTINE, INCREMENTS FROM 1 TO 10
LETTER LOCATIONS A THRU G USED TO DECODE 6-BIT BYTES
II - AZIMUTH PARAMETER FOR ZW ARRAY (IN CODED FORM)
INDEX - COUNTER USED FOR INDEXING THRU THE CLASS ARRAY. EQUALS RANGE IN KM FROM NSSL FOR FIRST RADIAL OF EACH DATA
        RECORD, USED AS RANGE PARAMETER FOR ZZ ARRAY
MNDECT - MINIMUM DETECTABLE REFLECTIVITY AFTER RANGE NORMALIZATION

III - AZIMUTH PARAMETER FOR ZZ ARRAY (IN CODED FORM)
INDEX2  - RANGE IN KM FROM NSSL FOR SECOND RADIAL OF EACH DATA RECORD, USED AS RANGE PARAMETER FOR ZZ ARRAY
MM - COUNTER USED TO PRODUCE PROPER MAP CAPTIONS IN PLOTZ SUBROUTINE
RP2 - EQUALS 2R' WHERE R' = 4/3RE, RE BEING THE RADIAS OF THE EARTH IN KM
TANTOP - TANGENT OF HIGHEST ELEVATION ANGLE USED .
H - HEIGHT OF CAZM IN KM

XK - CLOSEST DISTANCE TO NSSL (IN KM) THAT DIGITAL DATA ARE AVAILABLE AT HEIGHT, H. FUNCTION OF MAX ANTENNA TILT USED
IRM - INNER RANGE MARKER - NEAREST EVEN KM INSIDE DISTANCE XK
ORM - OUTER RANGE MARKER - OUTER LIMIT OF DATA TO BE CONVERTED TO CYLINDRICAL COORDINATES.
SR - SLANT RANGE TO DESIRED EVEN KM POINT ON SURFACE AT HEIGHT, H.
IR1 - CODED RANGE COUNTER FOR ZW ARRAY
IR2 - TOGETHER WITH IR1  THESE POINTS DEFINE THE NEAREST EVEN KM DATA POINTS IN THE ZW ARRAY WHICH BRACKET THE
      DESIRED EVEN KM POINT ON THE SURFACE AT HEIGHT, H.

PHIP - PHI PRIME, THE ANGLE BETWEEN THE GROUND AND THE DESIRED POINT ON THE SURFACE AT HEIGHT, H, CORRECTED FOR BEAM
       BENDING
PT1 - PT4 - CONTAINS REFLECTIVITY DATA FOR 4 POINTS SURROUNDING DESIRED POINT IN ZZ ARRAY
SUBTIL - DIFFERENCE IN DEGREES BETWEEN THE ELEVATION ANGLES USED TO BRACKET THE EVEN KM POINT ON THE SURFACE AT
         HEIGHT, H.

DS - PERCENTAGE DISTANCE BETWEEN LOWER DATA ELEVATION ANGLE USED (TILT (L)) AND DESIRED POINT IN ZZ ARRAY
DR - PERCENTAGE DISTANCE BETWEEN CLOSEST EVEN KM DATA POINT AND DESIRED POINT IN ZZ ARRAY
EE - REFLECTIVITY AT DISTANCE DS BETWEEN INNER DATA POINTS
FF - REFLECTIVITY AT DISTANCE DS BETWEEN OUTER DATA POINTS
ZT - REFLECTIVITY AT DISTANCE DR BETWEEN POINTS EG AND FF
```

```
0001          DIMENSION ZZ(181,200), ZW(80,70,12), VIZ(51,51), TVIZ(51,51),
              CZ(51,51)
0002          INTEGER*4 SKPBGN,SKPEND,CLASS(438),DATE,TIME,A(110),E,G,
              CAZMTH,BEGAZ,ENDAZ,STC,AP,TC,ROTIME,MSAZ(20),ORM
0003          INTERGER*2 HWORD(219),B
0004          REAL*4 MNDECT,CALIB(64),TILT(12),INDX,INDX2
```

```
0005          LOGICAL*1 C(438),D(4),F(4)
0006          EQUIVALENCE (A(110),B),(A,C),(D,E),(F,G,HWORD)
0007          COMMON ZZ,Z
      REWIND TAPE UNIT 10 AND READ FIRST DATA CARD, COMPUTE CONSTANTS, AND CLEAR ARRAYS
0008          REWIND 10
0009        1 READ(5,5000,ERR=995,END=999) ILEFT,JDOWN,KAZ,LASTAZ,NTILT,KRANGE,
             CSKPBGN,SKPEND
0010          KII=KAZ/2-1
0011          KKII=(360-KAZ)/2+2
0012          CALL CLEAR (ZZ,36200)
0013          CALL CLEAR (ZW,67200)
0014          CALL CLEAR (VIZ,2601)
0015          CALL CLEAR (TVIZ,2601)
0016          CALL CLEAR (CLASS,438)
      SKIP RECORDS TO BEGINNING OF FIRST DESIRED RECORD
0017          IF(SKPBGN.EQ.0) GO TO 13
0018          DO 12 K=SKPBGN,SKPEND
0019       11 READ(10,1002,ERR=998,END=999) (HWORD(I))
0020       12 CONTINUE
0021       13 L=0
      DO LOOP TO READ IN DATA FROM ALL DESIRED TILT ANGLES
0022          DO 100 LL=1,NTILT
      READS HEADER RECORD, STORE RAW DATA IN 219 HALF WORDS (HWORD), ADD HEX FOFO TO EACH HALF WORD, STORE RESULT BACK IN
      HWORD.  READ THE RESULT BY A CORE-TO-CORE READ SUBPROGRAM CALLED CORE, RESULT STORED IN LOCATIONS SPECIFIED IN READ
      (99) STATEMENT.  PRINTS DATA FOR COMPARISON TO DESIRED DATA.
0023       15 READ(10,1000,ERR=997,END=999) (HWORD(I), I=1,219)
0024          L=L+1
0025          DO 17 I=1,219
0026          HWORD(I)=HWORD(I)+61680
0027       17 CONTINUE
0028          CALL CORE (HWORD,438)
0029          READ(99,3000) DATE,TIME,ANTILT,DELAY,GATELN,BEGAZ,ENDAZ,NRANGE,
             CSTC,AP,INTERF,TC,ROTIME,NOISE,(CALIB(I),I=1,64),NOMSAZ,
             C(MSAZ(I),I=1,20)
0030          TILT(L)=ANTILT
0031          WRITE(6,6000) DATE,TIME,ANTILT,NOMSAZ,(MSAZ(I),I=1,20)
0032          LVL=0
      READS DATA RECORD, STORES RAW DATA IN 109 FULL WORDS (A) AND ONE HALF WORD (B).  SINCE A AND C EQUIVALENCED, READS BACK
      DATA ONE BYTE AT A TIME AND STORES EACH BYTE IN LAST BYTE OF D.  SINCE D EQUIVALENCED TO E, E CONTAINS ONE BYTE OF DATA
      AS A FULL WORD.  THIS RESULT STORED IN CLASS ARRAY.  OVERALL RESULT:  438 BYTES OF DATA STORED IN C CONVERTED TO 438
      WORDS OF DATA STORED IN CLASS.
0033       26 E=0
```

```
0034      27  READ(10,1001,ERR=996,END=999) (A(I),I=1,109),8
0035          DO 31 I=1,438
0036          D(4)=C(I)
0037          CLASS(I)=E
0038      31  CONTINUE
      TO READ THE AZIMUTH CONTAINED IN BYTES 201-203, EACH BYTE IS READ INTO F(2),F(3) and F(4).  AS F IS EQUIVALENCED
      WITH HWORD, THE STORED AZIMUTH IS CORRECTED BY ADDING HEX FOFO TO  THE RESULT.  READ BY SUBPROGRAM CORE, THE RESULTANT
      AZIMUTH IS STORED IN AZMTH.
0039          G=0
0040          J=2
0041          DO 37 I=201,203
0042          F(J)=C(I)
0043          J=J+1
0044      37  CONTINUE
0045          DO 40 I=1,2
0046          HWORD(I)=HWORD(I)+61680
0047      40  CONTINUE
0048          CALL CORE (HWORD,4)
0049          READ(99,3001) AZMTH
      AZIMUTH CHECKED.  IF 888 IS READ, ALL DATA FROM SECTOR HAS BEEN READ IN.  IF NOT 888, CHECKED TO SEE IF AZIMUTH LIES BETWEEN
      KAZ AND LASTAZ.  IF DATA IS DESIRED, ZW AZIMUTH ARRAY PARAMETER(II) IS COMPUTED.  USES STMT 49 IF AZMTH LESS THAN 180
      DEG, STMT 51 IF AZMTH GREATER THAN OR EQUAL TO 180 DEGREES.
0050          IF(AZMTH.EQ.888) GO TO 85
0051          IF(KAZ.LT.LASTAZ) GO TO 48
0052          IF(AZMTH.LT.KAZ.AND.AZMTH.GT.LASTAZ) GO TO 58
0053          IF(AZMTH.LT.180) GO TO 51
0054          GO TO 49
0055      48  IF(AZMTH.LT.KAZ.OR.AZMTH.GT.LASTAZ) GO TO 58
0056      49  II=AZMTH/2-KII
0057          GO TO 53
0058      51  II=AZMTH/2+KKII
      FIRST RADIAL OF INFORMATION ON DATA RECORD IS READ.  EVEN KM DATA COVERING 140 KM OF RANGE ARE READ BEGINNING AT KRANGE
      +2.  DATA STORED IN CLASS ARRAY IS IN DIGITAL INTEGER FORM (0-63).  BEFORE LOADING IN ZW ARRAY, DATA IS CONVERTED TO DBM,
      RANGE NORMALIZED, AND CONVERTED TO REFLECTIVITY IN MM**6 PER M**3.  DATA WHICH APPROACHES MINIMUM DETECTABLE SIGNAL
      STRENGTH (MNLDECT) IS SET EQUAL TO ZERO.
0059      53  DO 57 I=2,140,2
0060          INDEX=I+KRANGE
0061          INDX=FLOAT(INDEX)
0062          ZW(II,I/2,L)=10.0**(-0.1*CALIB(CLASS(INDEX))+2*(ALOG10(INDX))+
             C6.9)
0063          MNDECT=10.0**(-0.1*CALIB(1)+2*(ALOG10(INDX))+6.9)
0064          IF(ZW(II,I/2,L).LE.MNDECT.OR.ZW(II,I/2,L).LE.1.0) ZW(II,I/2,L)=0.0
```

```
0065          IF(L.GT.1) GO TO 57
0066          III=AZMTH/2+1
0067          ZZ(III, INDEX)=ZW(II,I/2,L)
0068       57 CONTINUE
      SECOND RADIAL OF INFORMATION ON DATA RECORD IS READ, AZMTH CHECKED AND ZW AND ZZ ARRAYS LOADED IF DATA IS DESIRED
0069       58 G=0
0070          J=2
0071          DO 63 I=420,422
0072          F(J)=C(I)
0073          J=J+1
0074       63 CONTINUE
0075          DO 66 I=1,2
0076          HWORD(I)=HWORD(I)+61680
0077       66 CONTINUE
0078          CALL CORE (HWORD,4)
0079          READ(99,3001) AZMTH
0080          IF(AZMTH.EQ.888) GO TO 85
0081          IF(KAZ.LT.LASTAZ) GO TO 75
0082          IF(AZMTH.LT.KAZ.AND.AZMTH.GT.LASTAZ) GO TO 26
0083          IF(AZMTH.LT.180) GO TO 77
0084          GO TO 76
0085       75 IF(AZMTH.LT.KAZ.OR.AZMTH.GT.LASTAZ) GO TO 26
0086       76 II=AZMTH/2-KII
0087          GO TO 79
0088       77 II=AZMTH/2+KKII
0089       79 DO 83 I=2,140,2
0090          INDEX=I+KRANGE+219
0091          INDEX2=I+KRANGE
0092          INDX2=FLOAT(INDEX2)
0093          ZW(II,I/2,L)=10.0**(-0.1*CALIB(CLASS(INDEX))+2*(ALOG10(INDX2))+
             C6.9)
0094          MNDECT=10.0**(-0.1*CALIB(1)+2*(ALOG10(INDX))+6.9)
0095          IF(ZW(II,I/2,L).LE.MNDECT.OR.ZW(II,I/2,L).LE.1.0) ZW(II,I/2,L)=0.0
0096          IF(L.GT.1) GO TO 83
0097          III=AZMTH/2+1
0098          ZZ(III,INDEX2)=ZW(II I/2,L)
0099       83 CONTINUE
      DATA READ PROCESS CONTINUES TILL 888 AZMTH ENCOUNTERED WHICH COMPLETES DATA READ FOR FIRST ELEVATION ANGLE
0100          GO TO 26
      TWO-DIMENSIONAL POLAR ARRAY (ZZ) IS CARRIED TO THE QUADRATIC INTERPOLATING SUBROUTINE QD2 ALONG WITH THE GRID SYSTEM
      COORDINATES.  A TWO-DIMENSIONAL RECTANGULAR ARRAY IS RETURNED CONTAINING AN X-Y PLOT OF THE FIRST TILT ANGLE, NORMALLY
      ZERO DEGREES
```

```
0101      85  IF(L.GT.1) GO TO 100
0102          CALL QD2 (ILEFT,JDOWN)
      REFLECTIVITY VALUES IN THE Z ARRAY ARE PREPARED FOR CONVERSION TO DBZ, THEN CONVERTED, AND THE ARRAY TAKEN TO THE PLOT Z
      SUBROUTINE
0103          DO 91 I=1,51
0104          DO 91 J=1,51
0105          IF(Z(I,J).LT.1.0) Z(I,J)=0.0
0106          IF(Z(I,J).EQ.0.0) GO TO 91
0107          Z(I,J)=10.0*ALOG10(Z(I,J))
0108      91  CONTINUE
0109          MM=1
0110          CALL PLOTZ (DATE,TIME,LVL,ILEFT,JDOWN,MM)
      ALL REMAINING TILT DATA IS READ INTO THE ZW ARRAY
0111     100  CONTINUE
      COMPUTES CONSTANTS TO BE USED IN VERTICAL INTERPOLATION OF SPHERICAL DATA INTO CYLINDRICAL COORDINATES AT A CONSTANT
      HEIGHT
0112     101  RP2=16990.173
0113          TANTOP=TAN(.0174533*ANTILT)
0114          IF(TANTOP.EQ.0.0) TANTOP=.0174550
      VERTICALLY INTERPOLATES SPHERICAL DATA OF ZW ARRAY TO YIELD CONSTANT ALTITUDE CYLINDRICAL ARRAY ZZ, COMPUTES THE
      CLOSEST DISTANCE TO NSSL THAT DIGITAL DATA ARE AVAILABLE AT HEIGHT,H
0115          DO 168 M=1,10
0116          CALL CLEAR (ZZ,36200)
0117          LVL=5000*M
0118          H=FLOAT(LVL)/3280.8399
0119          HSQ=H**2
0120          XK=H/TANTOP
0121          IRM=(IFIX((XK+1.0)/2))*2
0122          IF(IRM.LT.KRANGE) IRM=KRANGE+2
0123          IF(IRM.LT.2) IRM=2
0124          ORM=IRM+136
0125          IF(ORM.GT.198) ORM=198
      COMPUTES THE NEAREST EVEN KM POINTS IN THE DATA ARRAY ZW, THAT BRACKET THE DESIRED EVEN KM POINT ON THE SURFACE AT
      HEIGHT,H
0126          DO 145 II=1,80
0127          DO 145 IR=IRM,ORM,2
0128          X=FLOAT(IR)
0129          SR=SQRT(HSQ+X**2)
0130          IR1=(IFIX(SR)-KRANGE)/2
0131          IR2=IR1+1
0132          PHIP=H/X-X/RP2
0133          IF(PHIP.LT.0.0) PHIP=0.0
```

```
0134          PHIP=57.2958*ATAN(PHIP)
0135          IF(PHIP.GE.ANTILT) GO TO 145
      COMPUTES THE ELEVATION ANGLES IN THE DATA ARRAY ZW, WHICH BRACKET THE DESIRED EVEN KM POINT ON THE SURFACE AT HEIGHT,H
0136          DO 126 I=2,NTILT
0137          L=I-1
0138          IF(PHIP.LT.TILT(I)) GO TO 127
0139       126  CONTINUE
      EXTRACTS DATA FROM ZW ARRAY FOR THE 4 POINTS ON A GIVEN RADIAL IN THE SPHERICAL ARRAY WHICH BRACKET A CONSTANT LEVEL
      POINT ON THE SAME RADIAL IN THE CYLINDRICAL ARRAY, ZZ.  INTERPOLATES LINEARLY THE DATA TO FIND REFLECTIVITY VALUE FOR
      POINT IN ZZ ARRAY.
0140       127  PT1=ZW(II,IR1 L)
0141          PT2=ZW(II,IR1,L+1)
0142          PT3=ZW(II,IR2,L)
0143          PT4=ZW(II,IR2,L+1)
0144          IF(PT1.NE.0.0.OR.PT2.NE.0.0.OR.PT3.NE.0.0.OR.PT4.NE.0.0) GO TO 133
0145          GO TO 145
0146       133  SUBTIL=TILT(L+1)-TILT(L)
0147          IF(SUBTIL.EQ.0.0) SUBTIL=1.0
0148          DS=(PHIP-TILT(L))/SUBTIL
0149          DR=(SR-FLOAT((IFIX(SR/2.0))*2))/2
0150          EE=PT1+(PT2-PT1)*DS
0151          FF=PT3+(PT4-PT3)*DS
0152          ZT=EE+(FF-EE)*DR
0153          III=II+KAZ/2
0154          IF(II.GE.KKII) III=II-KKII+1
0155          ZZ(III,IR)=ZT
0156       145  CONTINUE
      CONVERTS CYLINDRICAL ARRAY ZZ AT HEIGHT, H, INTO RECTANGULAR ARRAY Z VIA SUBROUTINE QD2.  DATA LOADED ALSO INTO ARRAY
      VIZ.  DATA THEN CONVERTED TO DBZ AND LOADED INTO TVIZ ARRAY.
0157          CALL QD2 (ILEFT,JDOWN)
0158          DO 155 I=1,51
0159          DO 155 J=1,51
0160          VIZ(I,J)=VIZ(I,J)+Z(I,J)
0161          IF(Z(I,J).LT.1.0) Z(I,J)=0.0
0162          IF(Z(I,J).EQ.0.0) GO TO 155
0163          Z(I,J)=10.0*ALOG10(Z(I,J))
0164          TVIZ(I,J)=TVIZ(I,J)+Z(I,J)
0165       155  CONTINUE
      STATEMENT CONTROLS WHICH CAZMS, IF ANY, ARE TO BE PRINTED.  STMT 158 USED IN COMPUTED "GO TO" TO PRINT CAZM
0166       156  GO TO (159,159,159,159,159,159,159,159,159,159),M
0167       157  MM=MM+1
0168          CALL PLOTZ (DATE,TIME,LVL,ILEFT,JDOWN,MM)
```

```
0168          CALL PLOTZ (DATE,TIME,LVL,ILEFT,JDOWN,MM)
0169      159 CALL CLEAR (Z,2601)
      STATEMENT CONTROLS SUMMATION AND PRINT  OF PVSZ MAPS.  EACH COMPUTED "GO TO" STATEMENT WILL PRINT IN 5000 FT INCREMENTS.
      FOR CANIPE'S TECHNIQUE, 3RD, 7TH AND 10TH ARE PRINTED YIELDING 15,000, 35,000, AND 50,000 FT DIVISION POINTS BETWEEN
      LAYERS.  SUMMED REFLECTIVITY CONVERTED TO DBZ BEFORE PRINTING.  NOTE:  A CHANGE IN STMTS 156 OR 160 REQUIRES A CHANGE
      IN STMT 342 IN THE PLOTZ SUBROUTINE
0170      160 GO TO (168,168,161,168,168,168,161,168,168,161),M
0171      161 DO 165 I=1,51
0172          DO 165 J=1,51
0173          IF(VIZ(I,J).LT.1.0) GO TO 165
0174          Z(I,J)=10.0*ALOG10(VIZ(I,J))
0175      165 CONTINUE
0176          MM=MM+1
0177          CALL PLOTZ (DATE,TIME,LVL,ILEFT,JDOWN,MM)
0178          CALL CLEAR (VIZ,2601)
0179      168 CONTINUE
      COMPUTES TVSZ VALUES BY DIVIDING SUM BY 10.  PRINTS TVSZ MAPS
0180          DO 174 I=1,51
0181          DO 174 J=1,51
0182          Z(I,J)=TVIZ(I,J)/10.0
0183      174 CONTINUE
0184          MM=MM+1
0185          CALL PLOTZ (DATE,TIME,LVL,ILEFT,JDOWN,MM)
0186          GO TO 1
      CONTROLLS PRINTING OF ERROR STATEMENTS SHOULD ERROR BE ENCOUNTERED IN TAPE READ.
0187      995 WRITE(6,6001)
0188          GO TO 999
0189      996 WRITE(6,6002)
0190          GO TO 999
0191      997 WRITE(6,6003)
0192          GO TO 999
0193      998 WRITE(6,6004)
0194          GO TO 11
0195      999 STOP
0196     1000 FORMAT(219A2)
0197     1001 FORMAT(109A4,A2)
0198     1002 FORMAT(A2)
0199     3000 FORMAT(2I6,F3.1,2F6.3,2I3,I4,4I1,I3,F3.1,3X,64F4.1,I3,20I3)
0200     3001 FORMAT(I4)
0201     5000 FORMAT(4I3,I2,I3,2I5)
0202     6000 FORMAT('0',I6,2X,I6,2X,F4.1,3X,I3,2X,20(I3,1X))
0203     6001 FORMAT('1',10X,'ERROR OCCURRED ON CARD READ SN 1')
```

AD-A047 816 AIR FORCE INST OF TECH WRIGHT-PATTERSON AFB OHIO F/G 17/9
TORNADO IDENTIFICATION FROM ANALYSES OF DIGITAL RADAR DATA.(U)
DEC 76 D W PITTMAN
UNCLASSIFIED AFIT-CI-78-9 NL

2 OF 2
AD
AD047816

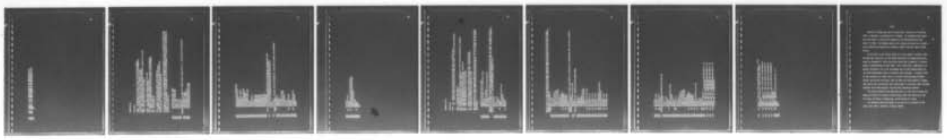

END
DATE
FILMED
1-78
DDC

```
0204      6002  FORMAT('1',10X,'ERROR OCCURRED ON TAPE AZMTH READ SN 27')
0205      6003  FORMAT('1',10X,'ERROR OCCURRED ON TAPE HEADER READ SN 16')
0206      6004  FORMAT('1',10X,'ERROR OCCURRED ON TAPE SKIP READ SN 11',16)
0207            END
```

SUBROUTINE QD2

DEFINITIONS

FLOATI - DISTANCE WEST(+) OR EAST(-) OF NSSL IN KM TO THE GRID COORDINATE.
FLOATJ - DISTANCE NORTH(+) OR SOUTH(-) OF NSSL IN KM TO THE GRID COORDINATE.
R - DIRECT DISTANCE FROM NSSL TO THE GRID COORDINATE (IN KM).
THETA - ANGLE, IN DEGREES FROM TRUE NORTH, OF GRID COORDINATE.
AZONE - NEAREST ODD AZIMUTH TO THETA, IN CODED FORM TO BE USED AS PARAMETER FOR ZP ARRAY.
AZTWO - NEXT CODED AZIMUTH CLOCKWISE FROM AZONE.

AZTHRE - NEXT CODED AZIMUTH COUNTER-CLOCKWISE FROM AZONE.
REALI - NEAREST ODD AZIMUTH TO THETA (IN DEG).
X - PERCENTAGE OF DISTANCE FROM NEAREST ODD ANGLE TO ANGLE OF GRID COORDINATE.
IR1 - NEAREST EVEN KILOMETER DISTANCE TO R, THE DISTANCE TO THE GRID COORDINATE.
IR2 - TWO KM BEYOND IR1.
IR3 - TWO KM INSIDE IR1.

REALJ - NEAREST EVEN KILOMETER DISTANCE TO GRID COORDINATE.
Y - PERCENTAGE OF DISTANCE FROM NEAREST EVEN KM TO GRID COORDINATE.
AAA THRU III - 9 NEAREST DATA POINTS CHOSEN, TO BE USED IN INTERPOLATION.
B THRU F AND FONE - INTERPOLATED VALUES OR REFECTIVITY.

THIS SUBROUTINE STEPS THROUGH THE RECTANGULAR GRID COORDINATES AND COMPUTES A VALUE OF REFLECTIVITY FOR EACH USING AN INTERPOLATION SCHEME WHICH SELECTS DATA FROM THE 9 NEAREST CYLINDRICAL COORDINATE DATA POINTS, CONTAINED IN THE ZP ARRAY (ZZ IN MAIN PROGRAM). THE OUTPUT ARRAY, ZEE (Z IN THE MAIN RPOGRAM), IS RETURNED TO THE MAIN PROGRAM FOR PLOTTING OR FURTHER USE.

```
0001          SUBROUTINE QD2 (ILEFT, JDOWN)
0002          REAL ZP(181,200),ZEE(51,51)
0003          INTEGER AZONE, AZTWO,AZTHRE
0004          COMMON ZP,ZEE
0005          DO 260 I=1,51
0006          DO 260 J=1,51
0007          ZEE(I,J)=0.0
      COMPUTES PARAMETERS OF ZP ARRAY FOR 9 NEAREST POINTS, CALLED AAA TO III.  SEE DEFINITIONS FOR EXPLANATION.
0008          FLOATI=FLOAT(2*I-ILEFT)
0009          FLOATJ=FLOAT(2*J-JDOWN)
0010          R=SQRT(FLOATI**2+FLOATJ**2)
0011          IF(R.LT2.0.OR.R.GT.200.0) GO TO 260
0012          THETA=(ATAN2(FLOATI,FLOATJ))*57.2958
```

```
0013          IF(THETA.LT.0.0) THETA=THETA+360
0014          AZONE=IFIX(THETA/2.0+1.0)
0015          AZTWO=AZONE+1
0016          IF(AZTWO.GT.180) AZTWO=1
0017          AZTHRE=AZONE-1
0018          IF(AZTHRE.LE.0) AZTHRE=180
0019          REALI=FLOAT(2*AZONE-1)
0020          X=(THETA-REALI)/2.0
0021          IR1=(IFIX((R+1.0)/2.0))**2
0022          IR2=IR1+2
0023          IR3=IR1-2
0024          REALJ=FLOAT(IR1)
0025          Y=R-REALJ
0026          AAA=ZP(AZONE,IR1)
0027          BBB=ZP(AZONE,IR2)
0028          CCC=ZP(AZONE,IR3)
0029          DDD=ZP(AZTWO,IR1)
0030          EEE=ZP(AZTWO,IR2)
0031          FFF=ZP(AZTWO,IR3)
0032          GGG=ZP(AZTHRE,IR1)
0033          HHH=ZP(AZTHRE,IR2)
0034          III=ZP(AZTHRE,IR3)
      IF ALL 9 DATA VALUES ARE 0, LEAVES GRID SET TO 0 AND GOES ON TO THE NEXT GRID POINT.
0035          IF(AAA.NE.0.0.OR.BBB.NE.0.0.OR.CCC.NE.0.0.OR.DDD.NE.0.0.OR.EEE.NE.
             C0.0.OR.FFF.NE.0.0.OR.GGG.NE.0.0.OR.HHH.NE.0.0.OR.III.NE.0.0) GO
             CTO 236
0036          GO TO 260
      INTERPOLATION SCHEME.  SEE VOGEL (1973) FOR EXPLANATION.  FINAL VALUE ZZ STORED IN GRID COORDINATE
0037    236   B=(DDD-GGG)/2.0
0038          C=(BBB-CCC)/2.0
0039          D=DDD-AAA-B
0040          E=CCC-AAA+C
0041          IF(X.GE.0.0) GO TO 248
0042          IF(Y.GE.0.0) GO TO 245
0043          F=III-AAA+B+C-D-E
0044          FONE=III
0045          GO TO 254
0046    245   F=AAA-B+C+D+E-HHH
0047          FONE=HHH
0048          GO TO 254
0049    248   IF(Y.GE.0.0) GO TO 252
0050          F=AAA+B-C+D+E-FFF
0051          FONE=FFF
```

```
0052          GO TO 254
0053      252 F=EEE-AAA-B-C-D-E
0054          FONE=EEE
0055      254 ZZ=AAA+(B*X)+(C*Y)+D*X**2)+E*Y**2)+F*X*Y)
0056          ZZ=AMAZI(ZZ,AMINI(AAA,DDD,GGG,BBB,CCC,FONE))
0057          IF(ZZ.LT.0.0) GO TO 260
0058          ZEE(I,J)=ZZ
0059      290 CONTINUE
0060          RETURN
0061          END
```

SUBROUTINE PLOTZ

DEFINITIONS

ARRAY: BUF - STORAGE LOCATION OF DATA TO BE PRINTED ON EACH LINE, 126 CHARACTERS LONG
DIG - CONTAINS CHARACTER REPRESENTATION FOR INTEGER VALUES 0 THRU 9. SEE DATA STATEMENT NUMBER 0005.

BLNK - A HOLLERITH BLANK CHARACTER
PLUS - A HOLLERITH PLUS SIGN (+)
NN - COUNTER WHICH STEPS ACROSS THE PAGE IN INCREMENTS OF 5 PRINT LOCATIONS REPRESENTING 2 KM INTERVALS.
NUM - INTERGER VALUE OF DBZ FOR GIVEN GRID COORDINATE
ND1 - CODED VALUE REPRESENTING 100'S DIGIT OF DBZ VALUE (SHOULD BE 0)
ND2 - CODED VALUE REPRESENTING 10'S DIGIT OF DBZ VALUE
ND3 - CODED VALUE REPRESENTING UNIT'S DIGIT OF DBZ VALUE

IW - DISTANCE IN KM EAST OR WEST TO LOWER LEFT CORNER OF GRID - USED FOR CAPTIONS
NS - DISTANCE IN KM NORTH OR SOUTH TO LOWER LEFT CORNER OF GRID - USED FOR CAPTIONS
INN - COUNTER USED TO COMPUTE NN FOR RIGHT HALF OF MAP.

THIS SUBROUTINE TALES A 50x50 RECTANGULAR ARRAY AND PLOTS FIRST THE LEFT HALF AND THEN THE RIGHT HALF OF THE ARRAY. THE RESULTANT PLOT IS 25 INCHES SQUARE WHEN BOTH HALVES ARE PIECED TOGETHER. AT A 2 KM INTERVAL, THE MAP COVERS A 100 KM SQUARE.

```
0001          SUBROUTINE PLOTZ (ND,NT,LVL,IL,JD,MM)
0002          DIMENSION ZP(181,200), X(51,51), BUF(126), DIG(10)
0003          COMMON ZP,Z
0004          DATA BLNK/1H /,PLUS/1H+/
0005          DATA DIG/1H0,1H1,1H2,1H3,1H4,1H5,1H6,1H7,1H8,1H9/
0006          WRITE(6,4000)
```

STARTING WITH THE UPPER LEFT HAND CORNER OF THE RECTANGULAR GRID, DBZ VALUES FROM THE ZP ARRAY ARE LOADED A LINE AT A TIME INTO THE BUF ARRAY. FIRST, THE 126 CHARACTERS OF THE BUF ARRAY ARE SET EQUAL TO A BLANK. THEN EVERY 25 CHARACTERS ARE SET EQUAL TO A PLUS (+). THESE GRID MARKS REPRESENT A DISTANCE OF 10 KM.

```
0007          DO 330 JJ=1,51
0008          J=52-JJ
0009          DO 310 I=1,126
0010          BUF(I)=BLNK
0011      310 CONTINUE
0012          IF(MOD((J-1),5).NE.0) GO TO 315
0013          DO 314 I=1,126,25
0014          BUF(I)=PLUS
0015      314 CONTINUE
```

```
      DBZ DATA FROM THE ZP ARRAY ARE ROUNDED TO THE NEAREST INTEGER AND LOADED INTO THE PROPER LOCATION IN THE BUF ARRAY.
      DECIMAL NUMBERS ARE BROKEN INTO 10'S AND UNIT'S DIGITS WHICH ARE LOADED AS CHARACTERS INTO THE BUF ARRAY AT LOCATIONS
      DETERMINED BY THE NN COUNTER.
0016     315  DO 327 I=2,26
0017          NN=5*(I-1)+1
0018          NUM=IFIX(Z(I,J)+0.5)
0019          IF(NUM.LE.0) GO TO 327
0020          IF(NUM.LT.10) GO TO 325
0021          IF(NUM.ST.100) GO TO 323
0022          ND1=NUM/100+1
0023          BUF(NN-2)=DIG(ND1)
0024     323  ND2=MOD(NUM,100)/10+1
0025          BUF(NN-1)=DIG(ND2)
0026     325  ND3=MOD(NUM,10)+1
0027          BUF(NN)=DIG(ND3)
0028     327  CONTINUE
      AFTER ENTIRE LINE OF DATA IS LOADED, WHICH COVERS 50 KM EAST-WEST AT A GIVEN DISTANCE NORTH, THE LINE IS PRINTED BY
      PRINTING THE BUF ARRAY.
0029          WRITE(6,401) (BUF(III),III=1,126)
0030          CONTINUE
      PRINTS CAPTIONS FOR MAPS.  DEPENDS ON ILEFT AND JDOWN ENTERED.
0031          IWEST=IL-2
0032          IW=IABS(IWEST)
0033          JSOUTH=JD-2
0034          JS=IABS(JSOUTH)
0035          IF(IWEST.GE.0) GO TO 336
0036          IF(JSOUTH.GE.0) GO TO 340
0037          GO TO 341
0038     336  IF(JSOUTH.GE.0) GO TO 338
0039          GO TO 339
0040     338  WRITE(6,402) IW,JS
0041          GO TO 342
0042     339  WRITE(6,403) IW,JS
0043          GO TO 342
0044     340  WRITE(6,404) IW,JS
0045          GO TO 342
0046     341  WRITE(6,405) IW,JS
0047     342  GO TO (343,345,346,347,349,351),MM
0048     343  WRITE(6,406) ND,MT,LVL
0049          GO TO 352
0050     345  WRITE(6,407) ND,MT
0051          GO TO 352
0052     347  WRITE(6,408) ND,MT
```

```
0053          GO TO 352
0054      349 WRITE(6,409) ND,NT
0055          GO TO 352
0056      351 WRITE(6,410) ND,NT
0057      352 WRITE(6,400)
      RIGHT HALF OF MAP LOADED AND PRINTED JUST AS LEFT HALF.
0058          DO 377 JJ=1,51
0059          J=52-JJ
0060          DO 357 I=1,126
0061          BUF(I)=BLNK
0062      357 CONTINUE
0063          IF(DOD((J-1),5).NE.0) GO TO 362
0064          DO 361 I=1,126,25
0065          BUF(I)=PLUS
0066      361 CONTINUE
0067      362 DO 375 I=27,51
0068          INN=I-25
0069          NN=5*(INN-1)+1
0070          NUM=IFIX(Z(I,J)+05)
0071          IF(NUM.LE.0) GO TO 375
0072          IF(NUM.LT.10) GO TO 373
0073          IF(NUM.LT.100) GO TO 371
0074          ND1=NUM/100+1
0075          NUF(NN-2)=DIG(ND1)
0076      371 ND2=MOD(NUM,100)/10+1
0077          BUF(NN-1)=KIG(ND2)
0078      373 ND3=MOD(NUM,10)+1
0079          BUF(NN)=DIG(ND3)
0080      375 CONTINUE
0081          WRITE(6,4010 (BUF(III),III=1,126)
0082      377 CONTINUE
0083          WRITE(6,411)
0084          WRITE(6,412)
0085      400 FORMAT(1H1)
0086      401 FORMAT(1H ,126A1,///)
0087      402 FORMAT(' ','LE',///' ','THE LOWER LEFT HAND GRID MARK IS ',I3,
          C' KM WEST AND ',I3,' KM SOUTH OF NSSL')
0088      403 FORMAT(' ','LE',///' ','THE LOWER LEFT HAND GRID MARK IS ',I3,
          C' KM WEST AND ',I3,' KM NORTH OF NSSL')
0089      404 FORMAT(' ','LE',///' ','THE LOWER LEFT HAND GRID MARK IS ',I3,
          C' KM EAST AND ',I3,' KM SOUTH OF NSSL')
0090      405 FORMAT(' ','LE',///' ','THE LOWER LEFT HAND GRID MARK IS ',I3,
          C' KM EAST AND ',I3,' KM NORTH OF NSSL')
```

```
0091      406  FORMAT(' ','DATE',I7,' TIME',I7,4X,'REFLECTIVITY VALUES,  Z = 10**
          C(MAP VALUE/10), AT THE',I6,' FT LEVEL.',3X,'2KM X 2KM GRID
          CINTERVAL.')
0092      407  FORMAT(' ','DATE',I7,' TIME',I7,4X,'PARTIAL VIZ FROM SURFACE TO
          C15000 FT (INDBZ).')
0093      408  FORMAT(' ','DATE',I7,' TIME',I7,4X,'PARTIAL VIZ FROM 15000 TO
          C35000 FT (IN DBZ).')
0094      409  FORMAT(' ','DATE',I7,' TIME',I7,4X,'PARTIAL VIZ FROM 35000 TO
          C50000 FT (INDBZ).')
0095      410  FORMAT(' ','DATE',I7,' TIME',I7,4X,'TOTAL VIZ FROM SURFACE TO
          C50000 FT (IN DBZ/10).')
0096      411  FORMAT(1H ,124X,1HRE)
0097      412  FORMAT(' ','DATE',I7,' TIME',I7,4X,'LEVEL',I6,' FT.')
0098           RETURN
0099           END
```

VITA

Donald W. Pittman was born in Evansville, Indiana on 21 February 1944, to Kenneth P. and Marjorie B. Pittman. He attended grade school and high school in Evansville graduating from Benjamin Bosse High School in 1962. He attended Evansville College and worked as a cooperative electronics engineering student at NASA's Marshall Space Flight Center.

He enlisted in the United States Air Force (USAF) in October 1964. Selected for schooling via the Airman Education and Commissioning Program, he attended St. Louis University receiving a Bachelor of Science degree in Meteorology in June 1968. After receiving a commission as a Second Lieutenant, his first assignment was as Staff Meteorologist to the 379th Bombardment Wing at Wurtsmith AFB, Michigan. In August 1970, he was selected for flight duty as an Aerial Reconnaissance Weather Officer and served five years with the USAF Hurricane Hunters at Ramey AFB, Puerto Rico and Keesler AFB, Mississippi in positions that included Squadron Staff Meteorologist and Assistant Operations Officer.

The author entered Texas A&M University in June 1976 to pusue the degree of Master of Science in Meteorology under the auspices of the Air Force Institute of Technology, United States Air Force.

His permanent mailing address is in care of his parents at 105 Aztec Lane, RR# 2, Chandler, Indiana, 47610.